University of Iceland
Faculty of Science
Department of Chemistry
August 2008

Conformational behaviour of substituted silacyclohexanes

Rannsóknir á stellingajafnvægi setinna silacyclohexan afleiða

M.sc. thesis

Sunna Ólafsdóttir Wallevik

Supervisor: Prof. Ingvar Helgi Árnason
Co-supervisor: Prof. Ágúst Kvaran

Academic Dissertation

Submitted to the Department of Chemistry, Faculty of Science, University of Iceland

This work was carried out at the Science Institute, University of Iceland

M.Sc. Committee

Prof. Ingvar Árnason (supervisor),

Department of Chemistry, University of Iceland

Prof. Ágúst Kvaran (co-supervisor),

Department of Chemistry, University of Iceland

Prof. Már Másson (external examiner),

Department of Pharmacy, University of Iceland

I hereby declare that this thesis is based on my own observations, is written by me and has neither in part nor as whole been submitted for a higher degree.

Sunna Ólafsdóttir Wallevik

Hér með lýsi ég því yfir að ritgerð þessi er samin af mér og að hún hefur hvorki að hluta né í heild verið lögð fram áður til hærri prófgráðu.

Sunna Ólafsdóttir Wallevik

Abstract

The monosubstituted silacyclohexanes; $C_5H_{10}SiHX$ with X = F, Cl, Br, I, SiH_3, OMe, $N(Me)_2$, ^tBu, CN and N_3 (**3-12**) were synthesized with the main aim of investigating the molecular structure of their axial and equatorial chair conformers as well as the thermodynamic equilibrium between these species. These derivatives were intended for investigations by means of gas electron diffraction (GED), dynamic nuclear magnetic resonance (DNMR) and temperature dependent Raman spectroscopy. This work is an ongoing project and has as of yet not been completed for all the derivatives. When possible these experimental results in the gas and liquid phase were compared to the quantum chemical calculations available (MP2, DFT and composite methods) and to results for analogous cyclohexane derivatives. The *A* values for the monosubstituted silacyclohexanes were found to be substantially lower than for the corresponding cyclohexane analogues and in all cases except for one, they show a preference of the axial conformation.

The following 1,1-disubstituted silacyclohexane rings, $C_5H_{10}SiXY$ with X = Me and Y = F, X = Me and Y = CF_3 as well as X = SiF_3 and Y = F (**13**, **14** and **16**) were also synthesized, so as to be investigated with respect to their conformational properties, using the same methods as described above. $C_5H_{10}SiXY$ with X = Me and Y = D (**15**) was synthesized in order to be investigated by Raman spectroscopy to complete the investigation of $C_5H_{10}SiHMe$ (**1**). The available results indicate that a simple additive model, which assumes that the conformational properties derived from the relevant monosubstituted rings are either complementary or competitive, cannot be applied and more sophisticated model is required.

$CF_3Me_2SiSiMe_2CF_3$ (**17**) was synthesized and its seemingly unusual conformational properties were investigated by gas electron diffraction (GED), temperature dependent Raman spectroscopy and quantum chemical calculations (QC). The results indicate that there is only one conformer in the gaseous phase, while three rotamers were observed in the liquid phase. The novel compounds $(C_5H_{10}SiH)_2NMe$ (**19**) and $(C_5H_{10}SiH)_2NH$ (**24**) were also synthesized and the process of conformational analysis was initiated by performing preliminary QC calculations.

Ágrip

Einsetnar afleiður silacyclohexans; $C_5H_{10}SiHX$ með X = F, Cl, Br, I, SiH_3, OMe, $N(Me)_2$, ^tBu, CN og N_3 (**3**-**12**) voru smíðaðar, með áherslu á að rannsaka sameindarbyggingu áslægra og þverlægra stólforma þeirra og jafnframt ákvarða varmafræðilegt jafnvægi þeirra á milli. Lagt var upp með að rannsaka þessar afleiður með beygju rafeindageisla í gasham (GED), hitastigsháðri Raman titringsrófagreiningu og lághita kjarnarófs mælingum (DNMR). Þetta verkefni stendur enn yfir og sumar afleiðurnar hafa enn ekki verið rannsakaðar með öllum tiltækum aðferðum. Þegar möguleiki var á, voru niðurstöður tilrauna bornar saman við spágildi skammtafræðilegra reikninga (MP2, DFT og sambærilegar aðferðir) og við samsvarandi cyclohexan afleiður. Niðurstöðurnar kveða á um að *A* gildi einsetnra silacyclohexan afleiða séu töluvert lægri en fyrir samsvarandi cyclohexan afleiður og allar þær afleiður sem rannsakaðar voru í verkefninu, með einni undantekningu, hafa tilhneigingu til þess að vera á því formi þar sem að meira er af sameindinni með sethópinn í áslægri stöðu.

Eftirtaldar 1,1-tvísetnar silacyclohexan afleiður, $C_5H_{10}SiXY$ með X = Me og Y = F, X = Me og Y = CF_3 og jafnframt X = SiF_3 og Y = F (**13**, **14** og **16**) voru smíðaðar, í þeim tilgangi að vera rannsakaðar með sömu aðferðum og var lýst hér að ofan. Afleiðan $C_5H_{10}SiXY$ með X = Me og Y = D (**15**) var einnig smíðuð og rannsökuð með Raman titringsrófagreiningu, til þess að gera fyllri rannsókn á $C_5H_{10}SiHMe$ (**1**). Þær niðurstöður sem liggja fyrir benda til þess að einfalt líkan, þar sem gert er ráð fyrir að hægt sé að leggja saman stellingajafnvægis eiginleika hverjar einsetinnar afleiðu fyrir sig, gildi ekki, heldur þurfi flóknara líkan til.

CF_3Me_2Si-$SiMe_2CF_3$ (**17**) var smíðað og óhefðbundnir stellingajafnvægis eiginleikar þess voru rannsakaðir með beygju rafeindageisla í gasham (GED), hitastigsháðri Raman litrófsgreiningu og skammtafræðilegum reikningum. Niðurstöðurnar benda til þess, að einungis ein rúmhverfa sé til staðar í gasfasa **17**, á meðan þrjár rúmhverfur fundust í vökvafasa þess. Einnig voru nýstárlegu efnasamböndin $(C_5H_{10}SiH)_2NMe$ (**19**) og $(C_5H_{10}SiH)_2NH$ (**24**) smíðuð og rannsókn stellingajafnvægis þeirra hafin með skammtafræðilegum reikningum.

Acknowledgements

I am very grateful to Prof. Ingvar Árnason for all his guidance and supervision during my work on this project. It has been a pleasure working with him.

I would also like to thank following people at the University of Iceland for their assistance:

- Prof. Ágúst Kvaran my co-supervisor for his guidance and DNMR analysis.
- Dr. Sigríður Jónsdóttir for all the help provided during NMR spectroscopy measurements and for DNMR measurements.
- Svana H. Stefánsdóttir for providing some starting materials and solvents.
- Haraldur Þórðarson and Sverrir Guðmundsson for providing glassware and glassblowing.
- Dr. Sigurður V. Smárason for MS measurements.
- Dr. Andras Bodi and Rangar Björnsson for quantum chemical calculations

I am very grateful for having had the opportunity to travel to Austria and work with Karl Hasslers research group in Graz and to have had the privilege of working at the Institute of Inorganic Chemistry, Graz University of Technology. I would like to thank Prof. Karl Hassler for all his help concerning Raman spectroscopy and for the invitation.

I would also like thank the following people at other Universities for their contribution:

- Dr. Ana Dzambaski and Dr. Margit Hölbling at Graz University of Technology for all the help provided during Raman spectroscopy measurements. For teaching me how to operate the Raman Instrument and how to fit and analyse the Raman data and for measuring other samples for me before and after my residence in Graz.
- Other co-workers in Hasslers group: Pierre-Marie Noblet and Ute Laky.

- Dr. Alexander V. Belyakov and Mr. Alexander A. Baskakov at Saint-Petersburg State Technological Institute for GED measurements.
- Prof. Georgiy V. Girichev and Prof. Nina I. Giricheva at the Ivanovo State University of Chemistry and Technology for GED measurements.
- Dr. Sarah Masters (née Hinchley) at the School of Chemistry, University of Edinburgh for her collaboration concerning 1,2-Bis(trifluoromethyl)-1,1,2,2-tetramethyl-disilane.
- Mr. Dieter Müller at the Universität Karlsruhe for MS measurements.
- Prof. Heinz Oberhammer, Tübingen, for GED consultation and overall assistance.
- Prof. Lodovico Lunazzi at the University of Bologna for supplying the DNMR simulation program QCPE no. 633.

I would also like to thank:

- The Icelandic Research Fund and the University of Iceland Research Fund, for financial support.
- My group co-workers Ester I. Eyjólfsdóttir, Rangar Björnsson and Dr. Andras Bodi for their collaboration and discussion.
- All my colleagues at the University of Iceland, Science Institute, who provided a friendly working atmosphere and helpful assistance.
- Kristján F. Alexandersson for proofreading this work and for all his love and patience.

Table of Contents

List of Figures

List of Tables

1 Introduction

Silicon, the eighth most common element in the universe, is traditionally known as the less reactive chemical analogue of carbon. Carbon and silicon occupy the first two seats of group 14 and over the last decades it has been standard practice in organosilicon chemistry to illustrate the similarities and differences between analogous carbon and silicon compounds. By now the chemistry of organosilicon compounds is well known and over a hundred thousand different substances have been synthesized and studied [1,2]. Thermodynamic stability and chemical inertness are typical characteristics for many of those substances, as a consequence of the relatively strong Si-C bond (both these elements are tetravalent and are able to form strong covalent bonds). Siliconcarbide (SiC) is an example of the strength of the Si-C bond, as it is nearly as hard as diamond and has many useful properties [1].

The structural similarities associated with carbon and silicon counterparts are especially pronounced when looking at the structural configuration of saturated chain and ring systems. There are many examples of this, take for instance Si_4H_{10} and C_4H_{10} which both exist as mixtures of anti and gauche conformers at ambient temperature and the analogues; Si_6Me_{12}/C_6Me_{12}, C_6H_{12}/C_5SiH_{12} and Si_6H_{12}/C_6H_{12} which all have chair-conformation as the global minimum [3-12]. However, when replacing a carbon atom with a silicon atom in a system under investigation, there are some notable effects which must be considered. The bonds associated with the substituted silicon will be longer than they are for the carbon congener, along with being somewhat weaker. The torsional force constants will also be lower, giving overall lower barriers for associated rotations.

Knowledge of the conformational preferences and the rates of the ring inversion processes of saturated six-membered rings are important for determining the chemistry of such systems. The potential energy barriers of chair-chair or chair-twist interconversions in a large number of saturated rings containing nitrogen, oxygen, sulphur and selenium have usually been found to be similar and in some cases even greater than for the corresponding cyclohexane derivatives [13-23]. However, there exists considerably less information regarding the conformational dynamics of the

analogous silicon rings and even less for germanium, tin and lead six-membered rings.

Six-membered cyclic Si-containing systems (analogues to cyclohexanes having either 1, 2, 3 or 6 silicon atoms replacing the same amount of carbon atoms) are expected to exhibit chair conformations that are more flexible and coplanar than the corresponding cyclohexane derivatives. This has been shown in comprehensive conformational investigation of these system over the last decades [8,9,24-38]. This can be attributed to the longer C-Si bond lengths in the rings in comparison to the C-C bond length, which effectively distorts the overall bond distances of the rings making the ground state conformation already close to a possible transition state of the ring reversal. Another possible factor for this conformational flexibility could be lower torsional force constants than in the analogous cyclohexane systems. This is supported by the comparison of the rotational barriers of methylsilane and ethane. Ethane has a rotational barrier of 2.9 kcal/mol while methylsilane has substantially lower barrier of l.7 kcal/mol [39,40].

The impetus for the work leading to this thesis came from a comprehensive investigation of silacyclohexanes $C_5H_{10}SiH_2$ and two of its derivatives $C_5H_{10}SiHMe$ and $C_5H_{10}SiHCF_3$, performed during the last decade by Arnason and his group at the Science Institute, University of Iceland [8,9,32,34,35]. This work provided very interesting results, different to previous expectations which will be discussed further in the respective chapter. This created a good foundation for further studies of different derivatives and also generated interest into whether analogous germanium systems would behave in similar way. Studies of these systems may provide important clues to what mechanisms are causing the observed behaviour.

Thus, at the beginning of this project, the intention was to synthesize selected derivatives of monosubstituted 1-silacyclohexanes and 1-germacyclohexanes and to investigate their conformational properties with suitable methods available. As the project developed, the emphasis of the work changed and further collaboration projects with Universities abroad became feasible. Furthermore the synthesis of monosubstituted silacyclohexanes generated increased interest for the investigation on various 1,1-disubstituted silacyclohexanes. Time restrictions therefore required

that the studies of the germanium derivates had to be placed on hold (although some synthesis attempts were made), while efforts were concentrated on the investigations of the silacyclohexane systems. Nevertheless, studies of the germanium systems are still thought to be worthwhile and future studies of them would without a doubt provide very interesting information that would add to the understanding of the conformational behaviour of saturated six membered ring systems. This project is therefore focused on silicon containing systems, predominantly silacyclohexane derivatives. The systems examined in the present work are outlined here below.

Monosubstituted and 1,1-disubstituted silacyclohexanes were synthesized with the main aim of investigating the molecular structure of their chair conformers. These derivatives were intended for investigations by means of gas electron diffraction (GED), dynamic nuclear magnetic resonance (DNMR) and temperature dependent Raman spectroscopy. When possible these experimental results in the gas and liquid phase were compared to the quantum chemical calculations available (MP2, DFT and composite methods) and to results for analogous cyclohexane derivatives, to examine the effect that such a substitution has on the conformation properties of these systems.

During the progression of this work, collaboration projects were launched, as mentioned before. One of these projects, involving the synthesis and conformational analysis of a highly substituted disilane, will be discussed in detail herein. Furthermore, during synthesis required for this thesis, interesting results were encountered that led to the attempt of some noteworthy experimental work concerning the synthesis of series of silacyclohexanes linked by nitrogen and phosphorous. These attempts and their results will also be discussed.

The GED measurements in the present work were performed by collaborators at Saint-Petersburg State Technological Institute and at the Ivanovo State University of Chemistry and Technology. DNMR measurements were performed at the Science Institute, University of Iceland. Raman measurements were performed at the Institute of Inorganic Chemistry, Graz University of Technology and the author had the opportunity to go there and perform a great deal of these measurements herself.

The general structure of this thesis is as follows: First the main concept used in this thesis will be discussed, namely “Conformational analysis”. The general methodology behind it will be outlined along with the specific methods used to investigate it. Then the synthetic methods will be described and the conformational analysis results will be introduced. As of yet, not all results are available for each derivative, however, the results that have been obtained will be presented herein. These results will be discussed and attempts will be made to identify any general trends of intrinsic behaviour.

2 Conformational analysis

2.1 General information

The term “conformation” refers to the spatial arrangements of atoms within a molecule, i.e. the movement of the atoms relative to each other, without changing the chemical bonding of that particular system. The term “conformer” refers to a stable molecular structure, which corresponds to a local minimum on the potential energy hypersurface of a given molecule. Conformational isomers or conformers are therefore phenomena that belong to a molecule and have the same structural formula, but these conformers are distinguishable as having relatively different energies. It is possible, however, that a molecule has two or more conformers of the same energy (cyclohexane has for example two equivalent chair conformers and six equivalent twist conformers of higher energy). Conformers of the same energy are related by rotation or pseudorotation within the molecule. The most common path between two conformers is via the rotation around a single bond. These kinds of stable rotational conformers are named rotamers and are separated by rotational barriers. A rotational barrier is the activation energy required to jump from one conformer to another [11,41,42].

Conformational analysis is therefore the study and documentation of the structure of the various conformers of a molecule, along with the determination of the energy difference and the rotational barriers between them [11,41,42].

The first considerations of this matter were published by Sachse and Bischoff in the end of the 19th century. Bischoff was the first to investigate ethane derivatives and tried to rationalise the staggered conformation of ethane derivatives from some of their reactions [43]. Meanwhile Sache was the first person to predict the chair shape of cyclohexane and he also realised that such a prediction would lead to the two chemically different axial and equatorial conformers [44,45]. Unfortunately Sache also predicted that observation of these distinguished chair forms should be possible at ambient conditions. His ideas were not accepted mainly because all attempts to experimentally detect these different chair forms failed. The general misconception

that cyclohexane was geometrically flat continued for the next sixty years as no one realised that ring inversion between the axial and equatorial conformers would be a very rapid process, difficult to detect at room temperature. In the year 1918 Mohr revisited the subject and amongst other things, speculated that the interconversion of cyclohexane would occur via boat and twist configuration [46]. However, it wasn't until 1950 that Derek Barton brilliantly explained the connection between conformation and reactivity for the first time, which earned him, along with Odd Hassel, the Nobel prize in chemistry in the year 1969 for his contribution to the field of conformational chemistry [47-49]. After Bartons publication this field attracted enormous interest, both from the world of chemistry and physics and their work is still today the foundation for all the extensive work that has been performed concerning various organic and inorganic system, extending to various more complicated systems [47].

Since then conformational analysis has been widely applied throughout chemistry. Linear alkanes and cyclohexane are the two systems with the most conformational analysis results published to date. Linear alkanes with their eclipsed and gauche conformers and cyclohexane with its chair and boat conformers. Atropisomers have also been under the microscope recently, with many interesting results coming to the surface [50-52]. Another example of conformational isomerism that has received a lot of interest of late is the folding of proteins, where some shapes are stable and functional, but others are not.

2.1.1 The science behind conformational analysis

When examining a conformer, the interactions within the molecule that affect the stability of the conformer usually fall within three groups:

1. Interactions of orbitals belonging to adjacent atoms.
2. Steric repulsion.
3. Electrostatic effects, mainly due to polar bonds.

In a large collection of molecules, the number of molecules possessing conformers of a certain energy can be calculated using statistical mechanics. The population distribution of particles between energy levels can be described using the Boltzmann distribution,

$$\frac{N_i}{N} = \frac{g_i \exp\left(\frac{-E_i}{k_B \cdot T}\right)}{q} \qquad (2.1.1.1)$$

where N_i is then number of particles occupying energy state E_i (having the degeneracy g_i), N is the total number of particles, k_B is the Boltzmann constant and q is the partition function. The Boltzmann distribution can be modified into equation 2.1.1.2, which calculates the ratio of two conformers, i and j.

$$\frac{N_i}{N_j} K = \exp\left(\frac{-\Delta G}{R \cdot T}\right) \qquad (2.1.1.2)$$

Here ΔG is the free energy difference between i and j. K is a constant that incorporates amongst other things entropy and degeneracy.

An interesting aspect of conformational analysis that often has to be considered is how the lifetime of the conformers affects the measurements made by the various spectroscopic methods. This can be illustrated by examining a system possessing two conformers, A and B. The average lifetime of these conformers is the average time that the system exists as either A or B, before interconverting into the other conformer. The energy barriers between conformers control the corresponding reaction rate, the higher the barrier is, the higher the average lifetime of the two conformers. If the average lifetime of conformers is larger than the timescale of the spectroscopic method, then two separate signals will be observed, whereas if the average lifetime is smaller, an averaged out spectrum will be observed. The

broadening of the signals for fast decaying conformers can also be predicted by the energy-time uncertainty principle (equation 2.1.1.3).

$$\Delta E \Delta \tau \geq \hbar \quad \text{or} \quad \Delta \nu \Delta \tau \geq \frac{1}{2\pi} \tag{2.1.1.3}$$

The shorter the lifetime of the conformer, the more uncertainty there is regarding its energy, hence the broadening of its signal. When the lifetime is of similar magnitude as the timescale of the spectroscopic method, an energy "blur" is measured. This phenomenon is called the coalescence of the spectral bands.

2.1.2 Conformational analysis methods

The spectroscopic methods used in this work span a large timescale range. NMR spectroscopy is generally considered the slowest method, with a typical time scale in the range of 10^{-3} to 10^{-4} s. Microwave spectroscopy and Raman spectroscopy fall into the mid range with timescales of 10^{-9} and 10^{-13} s respectively. The fastest method used was gas electron diffraction, which is among the fastest methods available, with a time scale of 10^{-20} s.

Quantum chemical calculations (QC) play a key role in modern day conformational analysis. They are used both as a tool to aid experimental conformational analysis and also to verify experimental results. With the increased computational power available today, especially due to the computer clusters that have been set up, quantum chemical calculations are becoming more accurate and accessible for all those who wish to use them.

In the following subchapters, these experimental and theoretical methods will be discussed in more detail.

2.2 Dynamic nuclear magnetic spectroscopy (DNMR)

NMR spectroscopy is one of the most valuable tools for diagnosing structure and stereochemistry of molecules and has been found to be especially useful for both thermodynamic and kinetic studies.

NMR analysis of the characteristic time dependent phenomena at or near the „coalescence“ point for chemical exchange processes, is traditionally referred to as „dynamic nuclear magnetic resonance“ (DNMR). The method concerns itself with environmental changes of magnetic nuclei, due to exchange between different sites with different chemical shifts and/or different coupling constants [53]. Energy differences between conformations of substituted cyclohexanes as well as their site exchange processes have for instance been extensively measured by this technique, since it is a very convenient method for studies of conformational equilibrium of rotational barriers which lie between 5 and 25 kcal/mol [47,53].

One of the main benefits of the DNMR method is that it allows the determination of the characteristic rate constant k for interconversional processes (stereomutation), usually brought about by measurements at variated temperatures. When these rate constants fall in the range of the NMR timescale, rate constants of first order or pseudo-first-order in the range 10^{-1} - 10^{6} s^{-1}, can be measured [54]. Thus a single averaged out spectrum (i.e. statistically weighted average with respect to chemical shifts and coupling constants) will be obtained if the magnitude of the rate constant is large with respect to the NMR time scale. Conversely if the rate constant of an exchange process of species in equilibrium, is small with respect to the NMR time scale, two signals will be shown for the individual entities in the NMR spectrum. Broadened spectra will, however, be observed for intermediate rates of exchange [2,53-55].

The desired thermodynamic and kinetic information is usually obtained by analysis of exchange broadened spectra using the band shape method, although other methods are also available [53,56]. The rate constant k for exchange processes due to two conformers is dependent on temperature and can be described as a single rate

constant at the coalescence temperature by the Eyrings equation 2.2.1, also named the activated complex theory;

$$k = \kappa(k_B T/h) \exp(-\Delta G^{\ddagger}/RT) \qquad (2.2.1)$$

where κ is the transmission coefficient, k_B is the Boltzmann's constant, h is the Planck's constant, R is the universal gas constant, T is the temperature and $\Delta G^{\ddagger}$ is the free activation energy. Here k is the measured quantity used to calculate the Gibbs free energy of activation ($\Delta G^{\ddagger}$) for each temperature value. $\Delta H^{\ddagger}$ and $\Delta S^{\ddagger}$ can now be further calculated by plotting equation 2.2.2 for various temperature values [53].

$$\Delta G^{\ddagger} = \Delta H^{\ddagger} - T\Delta S^{\ddagger} \qquad (2.2.2)$$

By using this approximation for the thermodynamic NMR analysis, the $\Delta S^{\ddagger}$ values unfortunately tend to be a bit inaccurate due to the restricted temperature range approachable in NMR spectroscopy. However, the $\Delta G^{\ddagger}$ values are not affected by this limitation and are found to be fairly accurate [47].

DNMR spectroscopy can also be used to calculate the conformational populations of a given system and therefore the free energy difference (ΔG) of its conformers, using equation 2.2.3. It must be kept in mind that both ΔG and K are temperature dependent.

$$\Delta G = -RT\ln(K) \qquad (2.2.3)$$

$$K = n_{ax}/n_{eq}; \quad n = \text{molar fraction}$$

Several magnetically active nuclei can be affected at the same time in many exchange processes, for example ^{1}H, ^{13}C, ^{19}F and ^{31}P. The analysis of an exchange process can be made much simpler by choosing the appropriate type of nucleus to be studied [2]. In the work leading to this thesis, low temperature ^{13}C-DNMR measurements were performed to investigate site exchange processes between the

axial and equatorial conformers of mono- and 1,1-disubstituted silacyclohexanes. Whenever F-atoms were part of the substituent, ^{19}F-DNMR measurements were preferred.

The energy transition threshold for flipping one chair to another in silicon containing ring systems is considerably lower than for analogous carbon systems. For silacyclohexanes this barriers is typically 5-6 kcal/mol vs. 10-12 kcal/mol for cyclohexanes [10]. It is therefore necessary to slow down the conformational equilibrium sufficiently by extensive cooling, when DNMR is used for conformational analysis (often down to at least 113 K and even further) in order to observe distinguished conformers. However, many problems can arise when measuring at such extremely low temperatures. The number of suitable solvents at such low temperatures is limited. A suitable solvent should have a low viscosity, even at very low temperatures and the solubility of the sample must be sufficient. Special solvent mixtures have therefore been developed based on Freon substances, which have the ability of being liquids at very low temperatures, as well as keeping the substance under investigation solvated.

One of the Freon mixtures that has been developed consists of CD_2Cl_2 (for locking purpose) and the gaseous solvents; $CHFCl_2$ and CHF_2Cl, in the respective 1:1:3 ratio. That mixture was for example used in the ^{13}C-DNMR measurements of 1,1-dimethyl-1-silacyclohexane, dodecamethylcyclohexasilane and 1,1,4,4-tetramethyl-1,4-disilacyclohexane at temperatures down to 103 K in order to investigate the conformational properties of these species [26-28].

In some cases, for example when systems have even lower inversion barriers than mentioned above, the Freon mixture becomes insufficient in keeping the substance under investigation in solution. In the work leading to this thesis such a situation was encountered in one case. This problem was tackled by repeating the ^{13}C-DNMR measurement by using the gaseous pyrophoric SiD_4, as the solvent. We reasoned that SiD_4 could possibly keep the substance under investigation dissolved at the low temperatures required for the analysis as well as acting as the locking agent. This attempt was found to be very successful and could be an interesting alternative for other research groups when facing similar problems.

2.3 Gas Electron diffraction (GED)

GED has been found to be very effective method for determining the gaseous phase structure of molecules. It can also be used to examine the structure of one or more conformers of a given molecule, as long as one of the conformers does not dominate the population distribution.

Molecules in the solid state are affected by intermolecular interactions (so called packing effects). Using X-ray diffraction to investigate solid state structures has some noted drawbacks. Not only is the information obtained relevant to the solid phase of the substance which is not always of primary interest, but also the distances measured are not between nuclei, as X-ray diffraction measures the distances between areas of high electron density. By utilizing GED, however, internuclear distances which define the molecular structure are accurately measured. These results can relatively easily be compared to theoretical results, as the gas phase structure of the species under investigation is readily simulated by quantum chemical calculations [57].

GED is based on the dualism of the electron. An incoming electronic beam with a wavelength similar to the scale of the internuclear distances will be diffracted as it passes between two atomic cores. The diffracted electrons of all the pairs of cores interfere and the sum of the interference pattern over all molecules in the gas area will be displayed as a pattern on a photographic plate in the detector, consisting of concentric rings. With the knowledge of the wavelength of the incoming electrons as well as the classification of the distances of the diffraction maxima obtained from the experiment, one can determine the internuclear distances.

During the evaluation of the data, one must also consider that the core pairs are not stationary, the relative distance between them is constantly changing due to molecular vibration. The average intramolecular distance over one vibration will therefore be measured, which is smaller than the actual distance. This effect is known as the shrinkage effect and disturbs the spectra of low frequency torsional vibrations with large amplitudes [57]. In the present work the shrinkage effect was corrected by

use of a program called SHRINK [58,59]. The least squares refinement of the structural parameters and analysis of the experimental data was done by use of the SARACEN (Structure Analysis Restrained by Ab initio Calculations for Electronic diffractioN) method, with ab initio calculations supplying the initial values for the optimizing parameters along with the associated swings and vibrations [58,60-63].

The molecular scattering intensity is higher for heavy cores and for internuclear distances in the region of the bond lengths. This is evident from equation 2.3.1, where Z_i and Z_j are the nuclear charge numbers of the atom, with r_{ij} as the momentary bond length between atoms i and j, n_{ij} is the multiplicity of r_{ij}. The radial distribution function, *P(r)/r*, corresponds to the surface area A under the peak of the respective diffraction and is expressed as;

$$A \propto \frac{n_{ij} \cdot Z_i \cdot Z_j}{r_{ij}} \qquad (2.3.1)$$

An overall scheme depicting how the radial distribution function is obtained is shown in figure 2.3.1.

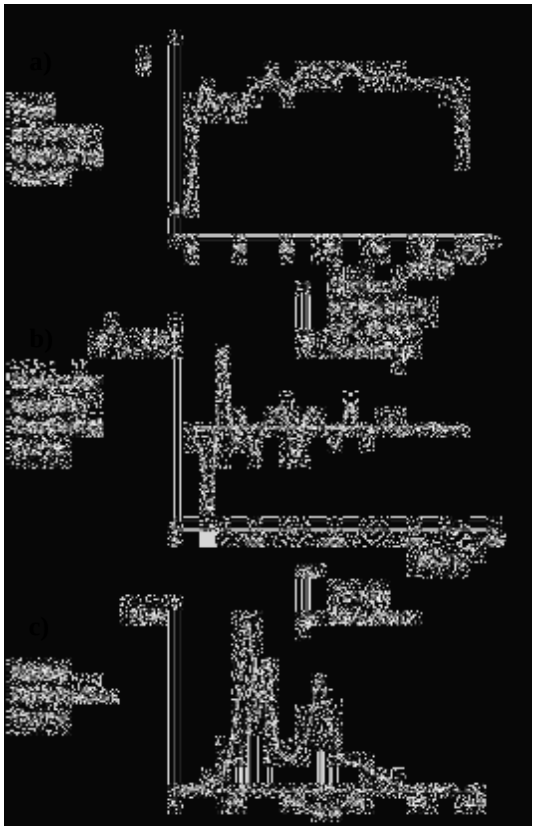

Figure 2.3.1: a) shows the raw scattering data (the total intensity scattering curve) which is converted into the molecular intensity scattering curve. b) shows the molecular intensity scattering curve after the background and the atomic scattering has been subtracted from the total intensity scattering curve. c) the radial distribution curve obtained by Fourier transformation of the Molecular Intensity curve [57].

When studying a system with multiple conformers separated by sufficiently large energy barriers, the diffraction intensities will be determined by a weighted average of all the conformers. This means that it is possible to calculate the ratio of the conformers along with the associated free energy difference, by means of calculating theoretically the radial distribution curves for the individual conformers, then fitting them to the experimental result. However, this is only possible if the calculated curves are sufficiently different for the fitting process to be viable.

2.4 Raman spectroscopy

Raman spectroscopy is a technique used to study vibrational, rotational and other low-frequency modes in a system and is often seen as an alternative to IR spectroscopy. When the frequency of the scattered monochromatic radiation is analysed, most of the incident radiation is elastically scattered (i.e. Rayleigh scattering), but a relatively small amount of the radiation (approximately only $1*10^{-7}$ of the scattered photons) is inelastically scattered, namely the Raman scattering. The source of this monochromatic light is normally a laser which is used to illuminate samples. The process leading to this inelastic scattering is the so called Raman effect, which occurs when photons bump into a molecule and interact with the electron cloud of its chemical bonds. This kind of a scattering can occur with a change in vibrational, rotational or electronic energy of a molecule. The shift in wavelength of the inelastically scattered photons supplies the chemical and structural information of the molecule which is being radiated. The vibrational state of the molecule which is being studied, causes the Raman scattered photons to be either higher or lower in energy, referred to as Stokes or anti-Stokes Raman scattering (see figure 2.4.1 below).

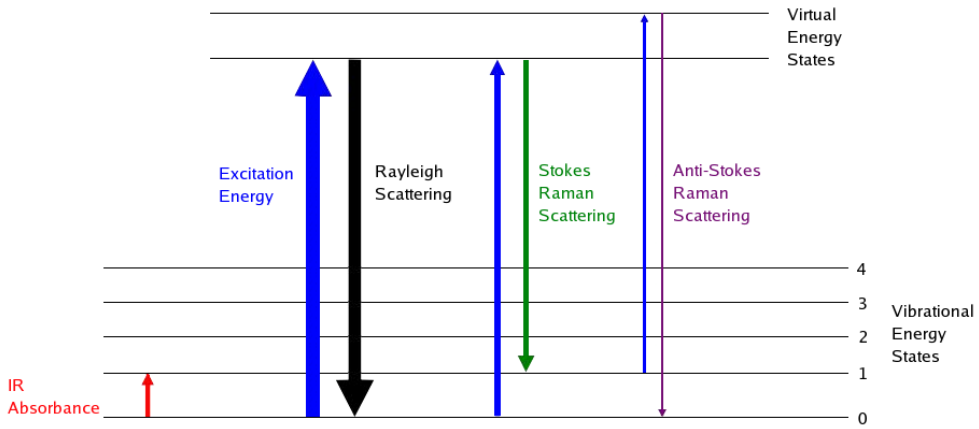

Figure 2.4.1: Energy level diagram demonstrating the elastic- and inelastic scattering of photons. The different signal strengths of the transitions are shown in an approximate manner.

Stokes radiation occurs at a longer wavelength and therefore has lower energy than the Rayleigh radiation and anti-Stokes radiation has higher energy. The energy difference between the incident photon and the Raman scattered photon is due to the

vibrational energy levels in the ground electronic state of the molecule and therefore the wavenumber of the Stokes and anti-Stokes lines are a direct measure of the vibrational energies of the molecule.

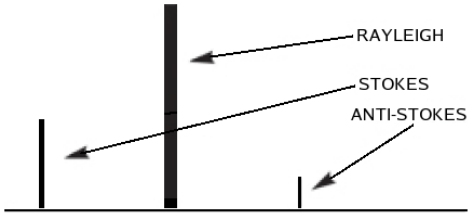

Figure 2.4.2: One can see that the Stokes and anti-Stokes lines are equidistant from the Rayleigh line. That is because one vibrational quantum of energy is gained or lost for the both of them.

The anti-Stokes line is considerably smaller than the Stokes line (see figure 2.4.2), as a consequence of the fact that only molecules that are vibrationally excited prior to irradiation can give rise to the anti-Stokes lines. Hence, in Raman spectroscopy, usually only the more intense Stokes line is measured as the Raman scattering is a relatively weak process and the number of photons Raman scattered is quite small, making detection of anti-Stoke lines difficult. However, there are several processes which can be used to enhance the sensitivity of a Raman measurement [64].

2.4.1 Raman Selection Rules and Intensities

Many of the factors of Raman band intensities can be explained by simple formulas for the classical electromagnetic field. The dipole moment, P, induced in a molecule by an external electric field E, is proportional to the field as shown in equation 2.4.1.1.

$$P = \alpha E \qquad (2.4.1.1)$$

The proportionality constant α is the polarizability of the molecule, i.e. a measurement of how easily the electron cloud can be distorted. Molecular vibration can change the polarizability of a molecule and this accounts for the occurrence of a Raman scattering. The change is described by the polarizability derivative $\frac{\partial \alpha}{\partial q_k}$, where q_k is the normal coordinate of the vibration. The selection rule for a Raman-

active vibration is given in equation 2.4.1.2. It states that for a vibration to be Raman active, the polarizability must change during the vibration.

$$\partial\alpha/\partial q_k \neq 0 \qquad (2.4.1.2)$$

The square of the polarizability derivative is proportional to the scattering intensity of the vibration and therefore the square of the induced dipole. Vibrations of bonds with a highly distributed electron cloud are the typically the strongest Raman scatterers, as the electron cloud is easily distorted by an external electric field. Bending or stretching of the bond associated with the vibration changes the distribution of electron density substantially and causes a large change in induced dipole moment.

The Raman selection rule is comparable to the one for an infrared-active vibration, which states that during the vibration there must be a net change in the permanent dipole moment for the vibration to be IR active. Group theory concludes that if a molecule has a centre of symmetry, then IR active vibrations will not show up in Raman and vice versa.

2.4.2 The history of Raman spectroscopy

The first spectra occurring in the visible range of the electromagnetically spectra were discovered by Sir William Herschel around 1800. Nevertheless it wasn't until the early days of quantum chemistry that it became possible to explain the exact cause and the theoretical background of UV, Vis and IR spectra. It was in the year 1928 that Raman and Krishnan discovered the inelastic scattering of photons (the Raman effect), at which time they were only able to investigate vibrational spectra using vis-sources of light. Raman spectroscopy, however, only became widely utilised around 1960 due to the development of lasers as ideal sources of light, in combination with D.H. Rank's development of photomultipliers as detectors [64,65]. It soon became obvious that IR-absorption intensities and Raman-emission

intensities were very different and all symmetrical diatomic molecules gave strong signals in Raman spectra but gave no signals in IR spectrum.

2.4.3 Infrared vs. Raman

An advantage of Raman spectroscopy in comparison to IR spectroscopy is the fact that the samples are relatively simple in preparation, as laboratory cuvette glassware can normally be used. Another advantage is that humidity and oxidation-sensitive substances are not as problematic. Polar solvents such as water can be used, which would disturb IR measurements due to strong self-absorption. This is of interest when examining the stability of individual conformers of a substance in different solvents and also as it may allow more accurate allocation of individual spectral bands. If one of the conformers has a higher dipole moment than the others, then it is better stabilized in polar solvents than in non polar solvents. Intensive spectral bands in a spectrum for a polar solvent can be assigned to the conformer with the higher dipole moment [66].

2.4.4 Experimental determinations of enthalpies and energy barriers between different conformers with Raman spectroscopy

Raman spectroscopy has been found to be a very valuable method for determining the conformational composition of either neat liquids or solutions in a wide temperature range. If an enthalpy difference exists between two (or more) conformers, then the intensities of their respective spectral bands will vary with temperature. The timescale of the method is much shorter than in NMR spectroscopy. This is beneficial from a dynamic point of view, as the mean life-times of the conformers need to be larger than the time scale of the method. If the molecule which is being examined, possesses two conformers (1 and 2), each corresponding to a local minima on the potential energy hypersurface and an energy barrier exists between them, which is larger than 0.60 kcal/mol (at 298 K), then conformers 1 and 2 will demonstrate distinguishable signals in the vibrational Raman spectrum. A wavenumber difference of about 10-20 cm^{-1} is usually enough to achieve

distinguishable signals. A smaller wavenumber difference between the conformers will result in overlapping of the signals, leading to an averaged out spectrum. Quantum chemical calculations are used in order to assign signals to conformers and also in the search for a suitable solvent when solutions are being measured (to make sure that observed signals for the solvents do not interfere with Raman signals that are being studied). Quantum chemical calculations are also used to select a suitable vibrational mode for the investigation by van't Hoff analysis and to make sure that no overlapping bands are associated with that particular vibrational mode. It must be noted that the calculated wavenumber values are usually a little bit lower than the measured wavenumber values.

The population of the two conformational states 1 and 2 varies with temperature according to Boltzmann statistics. The quantitative determination of the enthalpy difference ΔH, between conformer 1 and 2, is calculated using the van't Hoff equation:

$$\Delta H = -R \cdot T \cdot \ln\left(\frac{A_1}{A_2}\right) + C \qquad (2.4.4.1)$$

Where ΔH and the scattering coefficients α_1 and α_2 are assumed to be temperature independent (α_1, α_2 and S are part of the constant term C). A_1 and A_2 are the intensities of the vibrational bands for conformers 1 and 2. Either the deconvolutionised heights or areas of the bands can be used for the A_1/A_2 ratio. The analysis of the deconvolutionised spectral bands in this work was accomplished using the software Labspec [67].

By measuring the intensity difference of these terms at various temperatures the value of the enthalpy difference ΔH can be obtained from the slope of the plot $\ln(A_1/A_2)$ against T^{-1}. Raman spectroscopy is, however, limited to only obtaining ΔH values, since simple integration of the spectral peaks does not determine the molar

fraction of distinguished conformers. Raman spectroscopy does therefore not provide as much thermodynamic information as DNMR and GED.

2.5 Quantum chemical (QC) calculations

The execution of the quantum chemical calculations (QC) is not within the scope of the work leading to this thesis, except for some frequency calculations required for the Raman analysis. It is, however, extremely useful to compare the experimental results with the QC calculations using various levels of theory, as this both helps to identify anomalous experimental result and to rationalise experimental conclusions. Herein the QC calculations results being referred to were performed by other members of the Arnason group or otherwise available results. However, derivations and explanations of the methods will not be covered here.

3 Conformational investigation of silacyclohexane systems

3.1 Introduction and purpose of the investigation

The conformational behaviour of saturated six-membered ring systems is considerably well understood and plays an important role in organic stereochemistry, making it widely utilized in the pharmaceutical and polymer industry. Cyclohexane is an example of such a system and has often been considered as the cornerstone of cyclic conformational analysis, as it has been extensively studied along with its derivatives. Considerably less data has until now been available on the conformational properties of one of its closest analogues, silacyclohexane, of which only a few representative derivatives have been conformationally studied in recent years in the Arnason group at the Science Institute, University of Iceland [32-36].

The main stereochemical analysis performed on cyclohexane is the examination of the ring inversion process. The global minimum of cyclohexane is well known to be the chair conformation and a ring inversion is said to have occurred when each hydrogen atom goes from being in the equatorial or the axial position to the respective opposite. The reaction path of this site exchange process has to pass through a transition state of half-chair or sofa-like conformation, which then relaxes into a twist conformer. From there the molecule passes again through a second equivalent transition state before it ends up in the inverted chair. A boat conformation, a saddle point between two twist conformers, can but must not, be a part of the inversion pathway for cyclohexane [12,41,42]. This is demonstrated in figure 3.1.1. Ring interconversion for other saturated six-membered ring systems follow a similar process to this, although the number and types of stable conformers encountered between the chair conformations can vary from the ones mentioned above. This has also been found to be the case for the interconversional process for silacyclohexane systems which have been studied by Arnason and his group [8-10]. The intermediate conformers encountered for silacyclohexane were the boat and the twist conformers and the ring flipping process was found to be the following; chair → half-chair → twist → boat → twist → boat → twist → half-chair → chair [8-10].

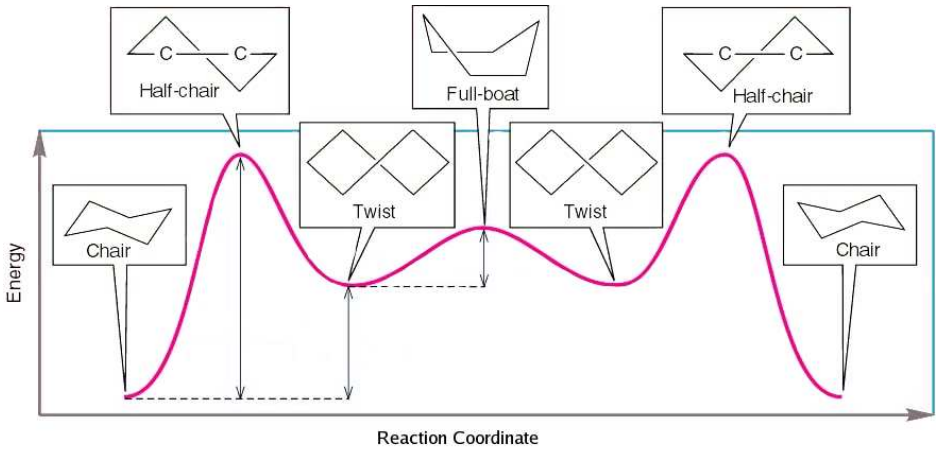

Figure 3.1.1: An energy profile for the ring interconversion of cyclohexane, showing the stable intermediate conformers.

As mentioned in the introduction, saturated six membered carbon rings become more flexible with the substitution of C by Si atoms. This increased flexibility is a sign that the barrier for the site exchange reaction is appreciably lower than for the analogous carbon systems. This phenomenon is very well illustrated when comparing the ring inversion barriers of ring systems containing an increasing number of silicon atoms (see scheme 3.1.1). Scheme 3.1.1 clearly shows how the inversion barriers decrease as a function of the number of silicon atoms. It also shows that the largest decrease per substituted silicon atom occurs when only one carbon atom is replaced.

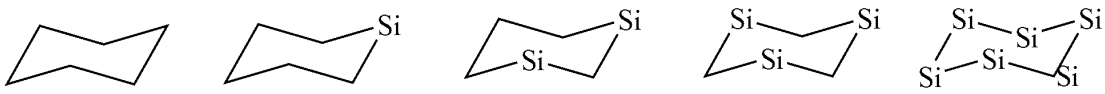

i) 10.8 kcal/mol ii) 5.7 kcal/mol iii) 4.6 kcal/mol iv) 5.5 kcal/mol v) 3.6 kcal/mol

Scheme 3.1.1: The ring inversion barriers of various silicon containing six-membered ring systems in comparison to cyclohexane. Quantum chemical calculation methods used; i) DFT [47], ii) RI-DFT (SV(P)) [8], iii) mPW1PW91 **(***6-311G(2df,p)***)** [68], iv)MM3[29] and v) MP2 (6-31G*) [69].

When investigating the ring inversion of monosubstituted six membered rings, new terminology for the conformers of the ring has to be introduced, as the two chair conformers are no longer equivalent. The substituent will either posses the equatorial

or the axial position. Therefore the two chair conformers are termed the equatorial conformer (**e**) or the axial conformer (**a**). Determination of the free energy difference of these two conformers and therefore the energy difference associated with the ring inversion, allows the calculation of the relative conformer populations of the two conformers (see scheme 3.1.2).

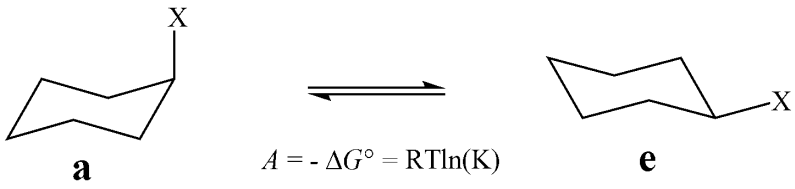

Scheme 3.1.2: Representative ring flipping process showing the equilibrium between the axial (**a**) and the equatorial (**e**) conformers and definition of the *A* value. It should be noted that in this thesis, $\Delta G_{e\rightarrow a}$ and *A* will both be used to denote the same value.

For cyclohexanes a general preference for the equatorial conformer is found, resulting in a positive *A* value (see Scheme 3.1.2 for the definition of *A*), with the rare exception of having mercury or alkali metals as the substituent (where the *A* value is close to zero or even negative) [47]. Bulkier and heavier substitutents generally result in higher *A* values.

In monosubstituted silacyclohexanes, this general trend does not seem to apply, as the Arnasons group have previously shown in studies of 1-methyl-1-silacyclohexane (**1)** and 1-trifluoromethyl-1-silacyclohexane (**2**) [32,34,35,68].

Compound **1** was shown to have equatorial preference (by GED, ^{13}C-DNMR, MW and supported by QC calculation), thereby disproving earlier investigations using MM2 and older force field methods and room temperature ^{1}H-NMR spectroscopy studies [70-72]. These two methods predicted preference of the axial conformation of **1**. However, the studies performed by Arnason et al. concluded *A* values of; 0.45 kcal/mol (GED), 0.23 kcal/mol (^{13}C-DNMR at 110 K) and values ranging from 0.46-0.6 kcal/mol (QC depending on the level of theory). A microwave spectroscopy study resulted in a ΔE value of 0.0 ± 0.2 kcal/mol. The *A* values on the other hand for the analogous cyclohexane, namely methylcyclohexane, have been reported to be

considerably higher in the range of 1.8-2.0 kcal/mol [73]. Arnasons group therefore showed that **1** in fact has a positive *A* value albeit a much lower one than its cyclohexane analogue.

Having the methyl group replaced by a trifluoromethyl group (**2**), gave the following experimental *A* values; –0.19 kcal/mol (GED at 293 K) and 0.4 kcal/mol (^{19}F-DNMR at 113 K). QC calculations supported these seemingly inconsistent findings by modelling both the gaseous and the solvent phase [35]. Compound **2** therefore seems to prefer the axial position **2a** in the gaseous phase while the equatorial conformation **2e** is favoured in the liquid phase at low temperatures. This is very unusual behaviour and opposite to what is known for the cyclohexane analogue trifluoromethylcyclohexane where the *A* value was found to be substantially higher, or 2.5 kcal/mol (by ^{19}F-DNMR at 300 K) [74].

The above examples show that monosubstituted silacyclohexanes do not necessarily follow the trend set by the corresponding cyclohexane derivatives. The *A* values from the results above were found to be substantially lower and it can be seen that going from the gaseous phase to the liquid phase can have an effect on the conformational properties. However, a general trend cannot be deduced from these two examples so further investigation was deemed necessary. We therefore set out to investigate a number of monosubstituted silacyclohexane systems with the overall aim of determining the general trends which these systems follow, along with finding out some of their intrinsic conformational properties.

1,1-Disubstituted saturated ring systems share many of the properties described above. They also follow a similar ring inversion processes and the global energy minimum of the systems is expected to be a chair like configuration. 1,1-Disubstituted cyclohexane rings have previously been investigated, therefore making studies of the analogous silicon systems interesting along with presumptively being the first conformational analysis of such systems [75-78]. Investigations of disubstituted silacyclohexanes may also provide helpful insights into the general conformational behaviour of substituted silacyclohexanes.

3.2 Synthesis of starting materials for silacyclohexane derivatives

Chlorosilacyclohexanes and chloromethylsilacyclohexanes (prepared as described by West), were in most cases used as the starting material for the synthesis of the mono- and 1,1-disubstituted silacyclohexanes in the present work [79]. Their syntheses are shown in schemes 3.2.1 and 3.2.2. It should be pointed out that a mixture of chlorinated and brominated derivatives is obtained by this method. Thus typically up to 30% of the bromo derivative is formed because of halogen exchange between the di-Grignard $BrMg(CH_2)_5MgBr$ (or the MgBrCl reaction salt) and the halogenated-silane reactant during the reaction.

Chlorosilacyclohexane was prepared as a starting material for most of the synthesis of the monosubstituted silacyclohexanes in this work. A di-Grignard (after being prepared in a traditional way by the reaction of 1,5-dibromopentane and magnesium shavings in diethyl ether) was reacted with trichlorosilane as described in scheme 3.2.1.

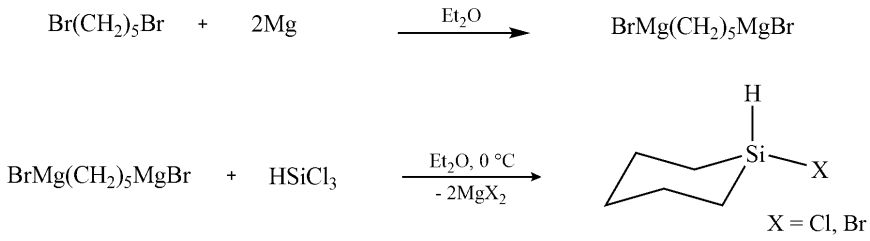

Scheme 3.2.1

Chloromethylsilacyclohexane was prepared as a starting material for the synthesis of all but one of the 1,1-disubstituted silacyclohexanes, by the reaction of a di-Grignard and trichloromethylsilane (see scheme 3.2.2).

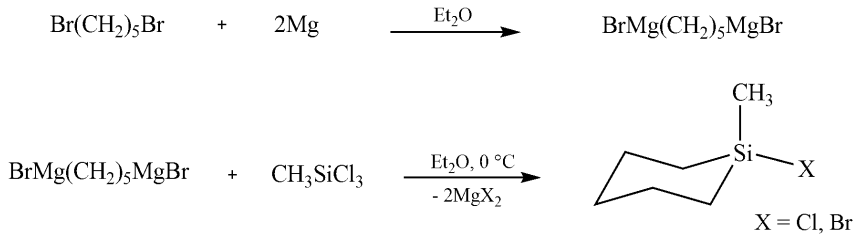

Scheme 3.2.2

In the following chapters when referring to chlorosilacyclohexanes and chloromethylsilacyclohexanes as reactants, they will always consist of the halogenated mixture described above.

Descriptions for typical runs of these starting materials are given in the experimental chapter.

3.3 Conformational properties of monosubstituted silacyclohexanes

3.3.1 Synthesis of monosubstituted halosilacyclohexanes

1-Fluoro-1-silacyclohexane (**3**) was prepared according to a general procedure described by Schott et al., by the reaction of chlorosilacyclohexane and hydrofluoric acid at –30 C° (see scheme 3.3.1.1) [80].

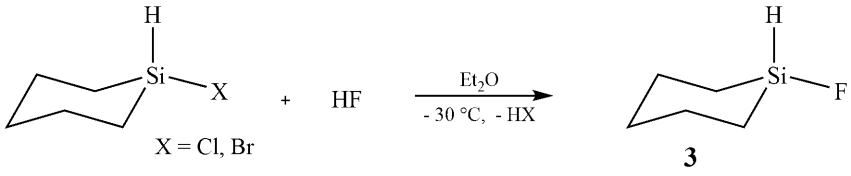

Scheme 3.3.1.1

Two different methods (both found to be successful) will be introduced herein for the synthesis of analytically pure 1-chloro-1-silacyclohexane (**4**). The former involves a gas condensation reaction of hydrogen chloride and 1-phenyl-1-silacyclohexane in vacuo at –78 °C (as can be seen in scheme 3.3.1.2 below), based on a similar description by Fritz [81]. 1-Phenyl-1-silacyclohexane was formed by the reaction of chlorosilacyclohexane and a phenylgrignard. The phenylgrignard was prepared in a traditional way, by the reaction of phenylbromide and magnesium shavings dissolved in diethyl ether.

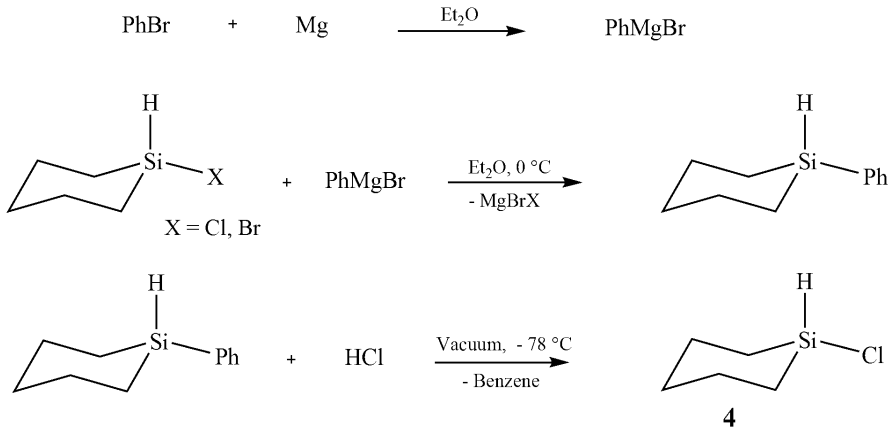

Scheme 3.3.1.2

The latter method of preparing analytically pure **4** is technically easier since it does not involve a gas condensation reaction nor a five step overall synthesis. 1,5-dichloropentane was now used as the starting material for the synthesis of $ClMg(CH_2)_5MgCl$, instead of 1,5-dibromopentane to avoid obtaining any 1-bromo-1-silacyclohexane as a by-product due to the halogen-halogen interchange. The di-Grignard was reacted with trichlorosilane obtaining pure 1-chloro-1-silacyclohexane (**4**) (see scheme 3.3.1.3).

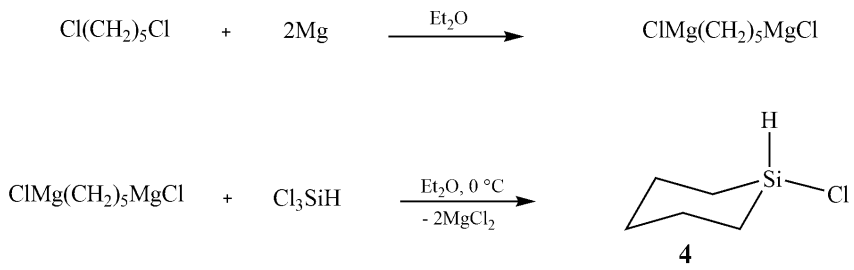

Scheme 3.3.1.3

The drawback of this synthesis was that it gave a very low total yield in comparison to the former method (16% vs. 58%). However, this procedure has not yet been repeated to see if something went awry during the reaction process or whether using 1,5-dichloropentane (instead of the conventionally used 1,5-dibromopentane as described by West) reduces the yield, due to it being less reactive in the di-Grignard reaction.

Analytically pure 1-bromo-1-silacyclohexane (**5**) was prepared according to the former method of synthesizing **4** as a five step synthesis, again having the gas condensation reaction of hydrogen bromide and 1-phenyl-1-silacyclohexane in vacuo at –78 °C as the critical step. This process can be seen in scheme 3.3.1.4.

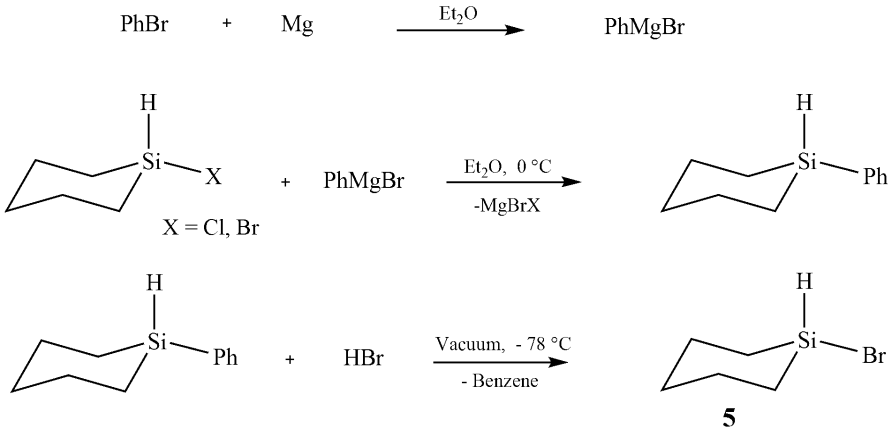

Scheme 3.3.1.4

1-Iodo-1-silacyclohexane (**6**) was prepared according to similar procedures described by Metz et al. and by Negrebetsky et al., by the reaction of chlorosilacyclohexane and iodomethylsilane in dichloromethane (see scheme 3.3.1.5) [82,83].

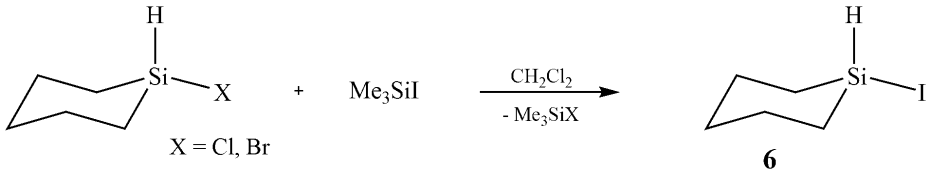

Scheme 3.3.1.5

3.3.2 Synthesis of monosubstituted silacyclohexanes having X = SiH_3, OMe, $N(Me)_2$, ^tBu, CN and N_3

The 1-chloro-1-trichlorosilyl-1-silacyclohexane used as the starting material for the synthesis of 1-silyl-1-silacyclohexane (**7**), was prepared in slight variation to the general preparation of silacyclohexanes described by West [79]. First the di-Grignard was prepared (in the traditional way described before) which was then reacted with hexachlorodisilane dissolved in diethyl ether. Again a mixture of chlorinated and brominated derivatives is obtained by that method due to halogen exchange between the di-Grignard $BrMg(CH_2)_5MgBr$ (or the MgBrCl reaction salt) and $Cl_3Si\text{-}SiCl_3$, during the reaction. The resulting 1-chloro-1-trichlorosilyl-1-silacyclohexane from that step, which contained ~ 25-30% impurities of partly brominated products, was now reacted further with lithiumaluminiumhydride obtaining the hydrogenated species **7**.

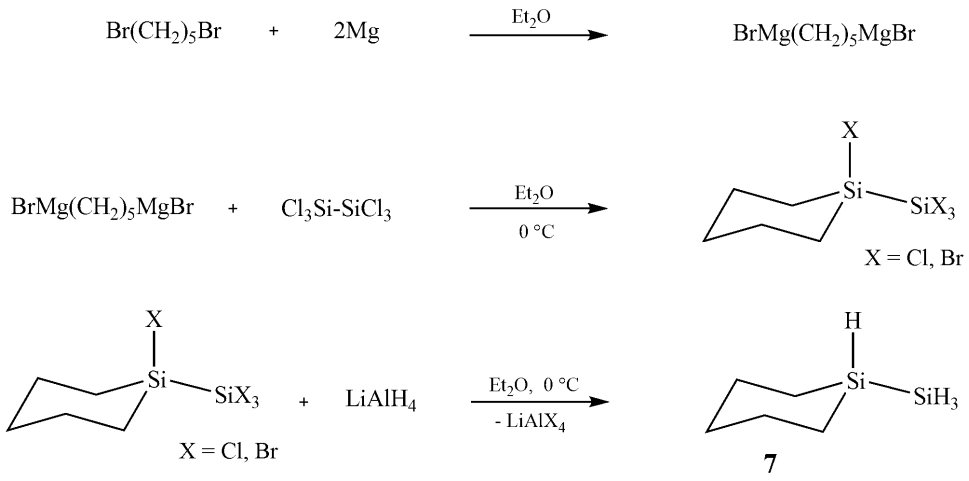

Scheme 3.3.2.1

1-Methoxy-1-silacyclohexane (**8**) was prepared according to a general procedure described by Welsh et al. (the synthesis of $(t\text{-}Bu)_2HSiOMe$) [84]. Chlorosilacyclohexane was reacted with two equivalents of triethylamine and methanol using diethyl ether as a solvent (see scheme 3.3.2.2).

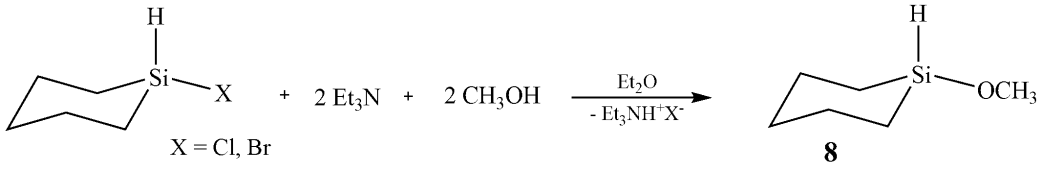

Scheme 3.3.2.2

1-Dimethylamine-1-silacyclohexane (**9**) was prepared in slight variation to a standard preparation of $Et_2SiN(Me)_2$ and similar silanes [85]. This synthesis again involves a gas condensation reaction since dimethylamine was condensed under vacuum into a reaction flask containing cyclohexane, which was used as a solvent during the reaction. Chlorosilacyclohexane was then reacted with two equivalents of dimethylamine using a cooler maintained at –78 °C for 12 hours. This reaction can be seen in scheme 3.3.2.3.

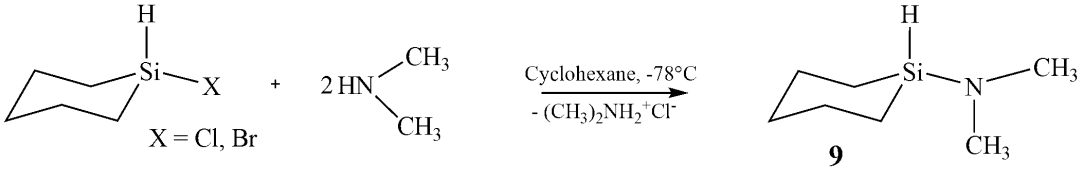

Scheme 3.3.2.3

1-Tertbuthyl-1-silacyclohexane (**10**) was prepared according to a general procedure described by Gompper [86]. A Pentane solution of tertbuthyllithium (1.5 M) was slowly reacted with chlorosilacyclohexane dissolved in diethylether at –78 °C. This reaction can be seen in scheme 3.3.2.4.

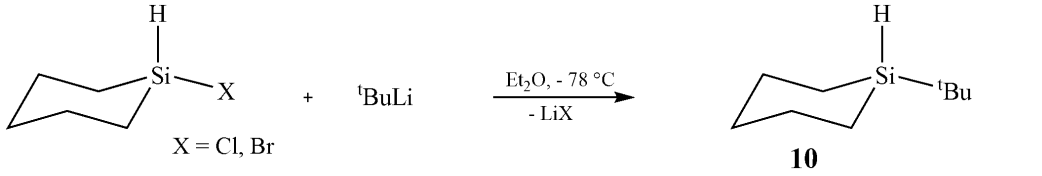

Scheme 3.3.2.4

1-Cyano-1-silacyclohexane (**11**) was prepared according to a novel approach of heterogeneous reactions of trialkylsilyl chlorides with inorganic salts catalysed by PEG400 (polyethylene glycol) and zinc iodide [87]. The reaction product **11** was formed by vigorously stirring a solution of anhydrous sodium cyanide, chlorosilacyclohexane, PEG400, zinc iodide and dichloromethane, for 24 hours. This reaction is shown in scheme 3.3.2.5.

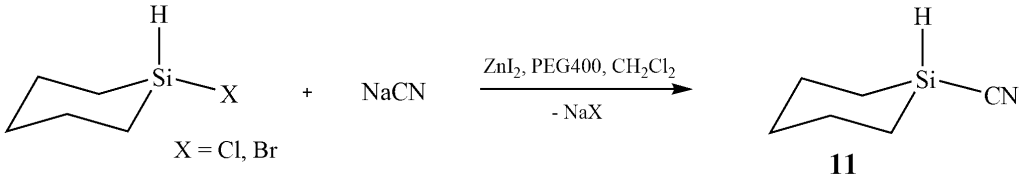

Scheme 3.3.2.5

1-Azide-1-silacyclohexane (**12**) was prepared by means of the same reaction conditions as **11**, by vigorous stirring of a solution of anhydrous sodium azide, chlorosilacyclohexane, PEG400, zinc iodide and dichloromethane for 1 week. This reaction is shown in scheme 3.3.2.6. Since this procedure did not yield sufficiently pure **12**, the synthesis will have to be repeated with a shorter stirring time to hopefully attain purer **12**.

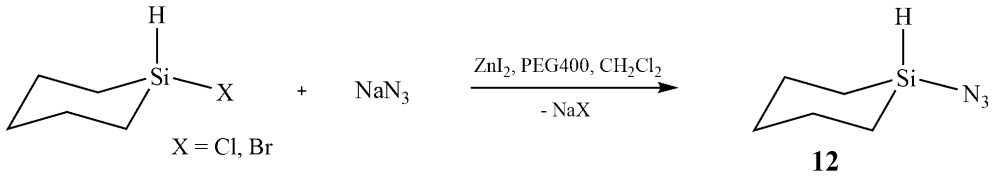

Scheme 3.3.2.6

In the next subchapters the conformational analysis of **3**-**5** and **7**-**9** by various methods will be covered. To illustrate the experimental conformational analysis of the monosubstituted silacyclohexane systems, **3** was chosen, as the most extensive data from each experimental method exists at this point for **3**. Data which has very recently been published by our group [33,36]. However, no experimental data exists yet for **6** and **10**-**12**, as these compounds have only very recently been prepared.

3.3.3 Low temperature ^{19}F- and ^{13}C-NMR spectroscopy.

3.3.3.1 ^{19}F-DNMR measurements

The low temperature ^{19}F-NMR spectra for **3** were recorded at regular intervals from room temperature down to 112 K. At temperatures down to about 135 K the equilibrium between the axial and equatorial conformer (**3a** and **3e**) was still relatively fast compared to the NMR timescale giving only an averaged spectrum for the two conformers. At temperatures below 135 K the equilibrium is obviously slowing down and considerable broadening of the signal can clearly be seen as the temperature drops. At 126 K it becomes evident that two sets of peaks corresponding to the Si-F signal are forming, indicating the existence of a major and a minor conformer of **3**. According to a trend which appears to generally apply for cyclohexanes, the resonance signal appearing at lower frequency (lower ∂ value), when studying chemical exchange, can be assigned to the axial conformer [88-90]. Based on this trend as well as the results for the calculated geometric parameters (using the B3LYP/6-31G(d,p) and the MP2/6-31G(d,p)), the more intense signal was assigned to the axial conformer **3a**, while the smaller signal was assigned to the equatorial conformer **3e** [36]. At 112 K the peaks have become well separated and an obvious intensity difference can be seen between the two signals. At this stage it can therefore be estimated that at 112 K more molecules of **3** possesses the axial chair conformer **3a** than the equatorial chair form **3e**.

Through DNMR-simulation of the spectra, the free energy of activation ($\Delta G^{\ddagger}$) and the total free energy change (ΔG) of the interconversion process of **3**, can be determined via calculations of the rate constant and the equilibrium constant respectively, as a function of temperature. Both the experimental and simulated spectra at various temperatures are depicted in figure 3.3.1. At 112 K it was found that $\Delta G^{\ddagger}_{e\rightarrow a}$ = 5.0 kcal/mol, $K_{e\rightarrow a}$ = 1.79 and $\Delta G_{e\rightarrow a}$ = –0.13 (2) kcal/mol, giving 64% (2) preference of the axial conformer. Determination of $\Delta H^{\ddagger}$ and $\Delta S^{\ddagger}$ of **3** using equation 2.2.2 can be seen in figure 3.3.2.

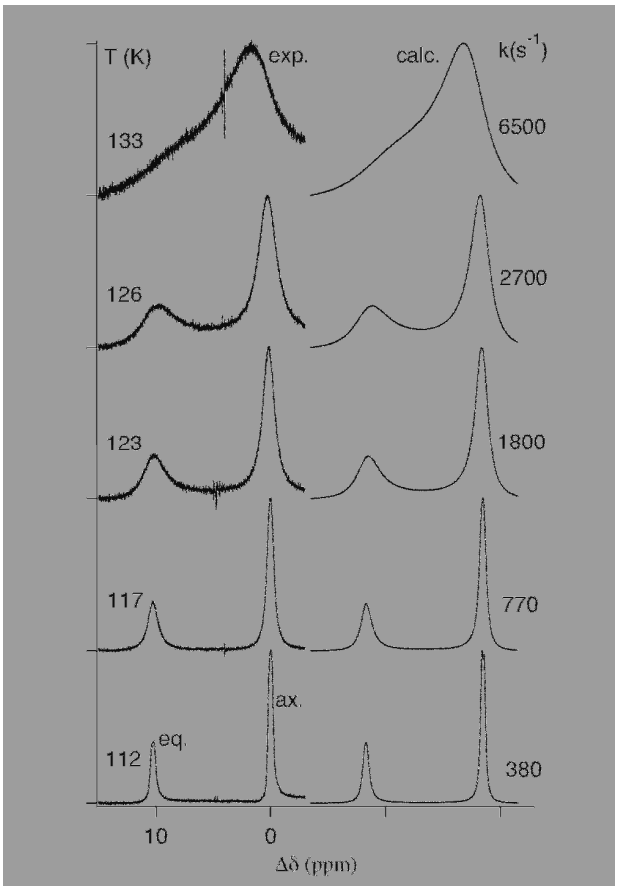

Figure 3.3.1: Experimental (on the left) and simulated (on the right) ^{19}F NMR spectra of **3** in a 1:1:3 mixture of CD_2Cl_2, $CHFCl_2$ and CHF_2Cl at various temperatures.

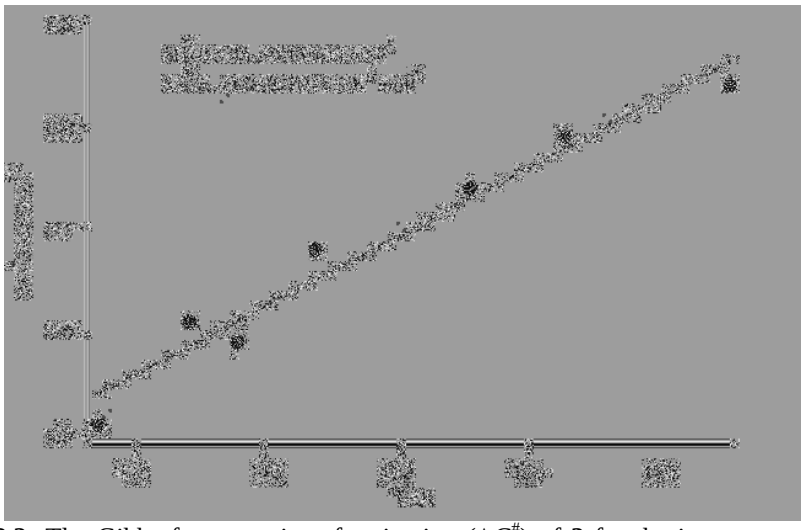

Figure 3.3.2: The Gibbs free energies of activation ($\Delta G^{\#}$) of **3** for the interconversion between the equatorial and axial conformation. Averaged $\Delta H^{\#}$ and $\Delta S^{\#}$ values were calculated from the linear fit of the expression $\Delta G^{\#} = \Delta H^{\#} - T\Delta S^{\#}$ for the temperature range 110 – 130 K.

3.3.3.2 ^{13}C-DNMR measurements

^{13}C- DNMR measurements of **7** were first performed using the Freon solvent mixture, which was used for all other DNMR measurements in the work leading to this thesis. Unfortunately **7** crystallized out of the solvent mixture before reaching the coalescence temperature of any of the carbon signals of **7**, making the DNMR analysis of **7** impossible in Freon solvents. Another solvent was then chosen, namely the pyrophoric SiD_4, which could possibly keep **7** dissolved at the sufficiently low temperatures required for the analysis as well as acting as the locking agent. This proved to be correct and successful low temperature ^{13}C-NMR measurements of **7** using SiD_4 as the solvent were made. At 100 K it was found that $\Delta G_{e\rightarrow a}$ = 0.12(3) kcal/mol, giving 35% (3) preference of the axial conformer. At this point $\Delta G^{\ddagger}_{e\rightarrow a}$ and *k* have not yet been evaluated.

Attempts were made to measure low temperature ^{13}C-NMR spectra of **8** and **9** using the Freon solvent mixture, but to little avail since both these derivatives crystallized out of the solvent mixture before reaching the coalescence temperature of any of the carbon signals, making the ^{13}C-DNMR analysis impossible. No further attempt have been made at this point, however, using the pyrophoric SiD_4 as the solvent for the DNMR measurements may lead to positive results as was seen for **7**.

Samples for low temperature ^{13}C- DNMR measurements of **4** and **5** have been prepared in the Freon mixture, but not yet been measured. They will hopefully be measured as soon as possible.

3.3.4 Gas electron diffraction (GED) analysis

Gas electron diffraction was performed for **3** by shooting a beam of electrons at a molecular stream of **3**. After analysis of these measurements the "radial distribution function" (RDF) of **3** was obtained. This function describes the interaction between atoms within a molecule as a function of the distance between them (see figure 3.3.3). The measured function obtained shows a weighted average of the axial and the equatorial chair forms.

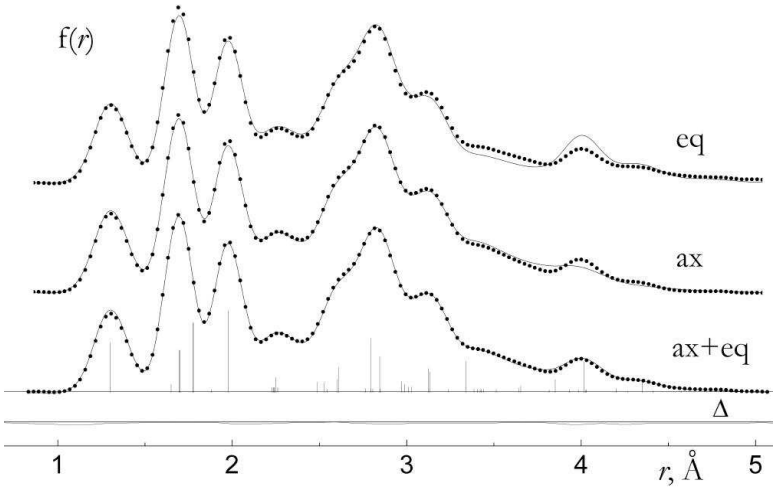

Figure 3.3.3: Theoretical and experimental radial distribution functions for **3**. The experimental curve is indicated by dots while the calculated curve is shown by solid lines.

Figure 3.3.3 also shows the calculated RDF curves for both the axial and the equatorial chair forms. It can be seen that the biggest difference between the curves is in the region $r > 3$ Å, due to the nonbonded interaction between the fluorine atom and carbon atoms within the ring. By fitting these calculated functions in various ratios with the experimentally obtained function, until the least square method gave the lowest R value possible, the percentage of each chair form was obtained. These simulations predicted the population of the axial conformer **3a** to be 63 (8) % abundant in the vapour of **3** at 293 K corresponding to an *A* value of -0.31(20) kcal/mol.

The GED measurement and analysis for **7** was performed in a similar way as described for **3**. According to the GED data the axial conformer **7a** has 57(7)% abundance in the vapour of **7** at 321 K and therefore the equatorial conformer **7e** was 43(7)% abundant for the same conditions. This value corresponds to an *A* value of -0.17(15) kcal/mol.

GED measurements of **4** and **5** have been performed, but their GED data has not yet been fully evaluated. Samples of **8** and **9** have been prepared for GED measurements, but unfortunately not yet been measured.

3.3.5 Low temperature Raman measurements

Temperature-dependent Raman measurements were performed for **3** in the temperature range of 300-210 K (neat liquid), 300–120 K (pentane solution) and 293 – 200 K (dichloromethane solution). The room temperature spectrum of pure **3** in the range of 100-2450 cm^{-1} can be seen in figure 3.3.4.

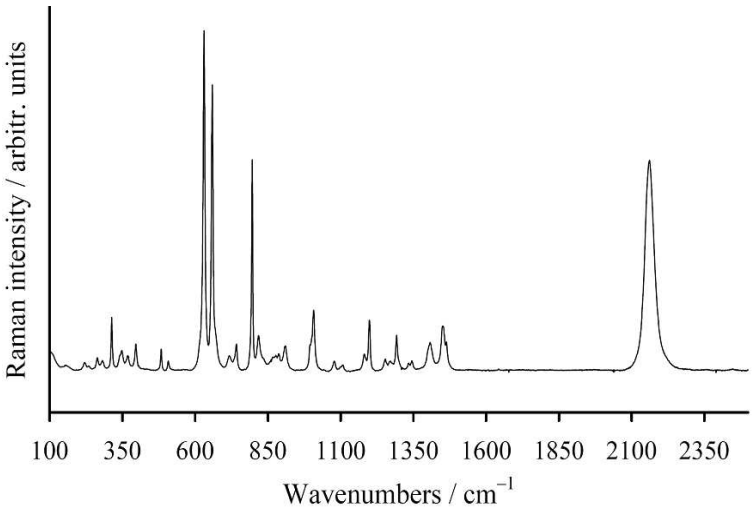

Figure 3.3.4: Raman spectrum of pure liquid **3** at room temperature.

Quantum chemical frequency calculations (B3LYP/6-31G(d,p)) were performed for the axial and equatorial conformers of **3** (**3a** and **3e** respectively). They revealed that the symmetrical SiC_2-vibration (ν_sSiC_2) was the most useful vibration for the low temperature Raman analysis of **3**. The calculated ν_sSiC_2-vibrations values for **3** were; 620 cm^{-1} for **3a** and 652 cm^{-1} for **3e**. Figure 3.3.5 shows the actual experimental values for the symmetrical SiC_2-vibrations (ν_sSiC_2) of **3**, appearing at 630 cm^{-1} and 658 cm^{-1} for the axial and equatorial conformers respectively. As expected, the calculated values turned out to be a bit lower than the experimental values but nevertheless gave a correct overall picture of the vibrational Raman spectra and made the spectral interpretation possible.

From the low-temperature Raman spectra it became clear that the intensity of the ν_sSiC_2 equatorial chair conformer (appearing at the higher wavenumber) decreases with a decrease in temperature (see figure 3.3.5).

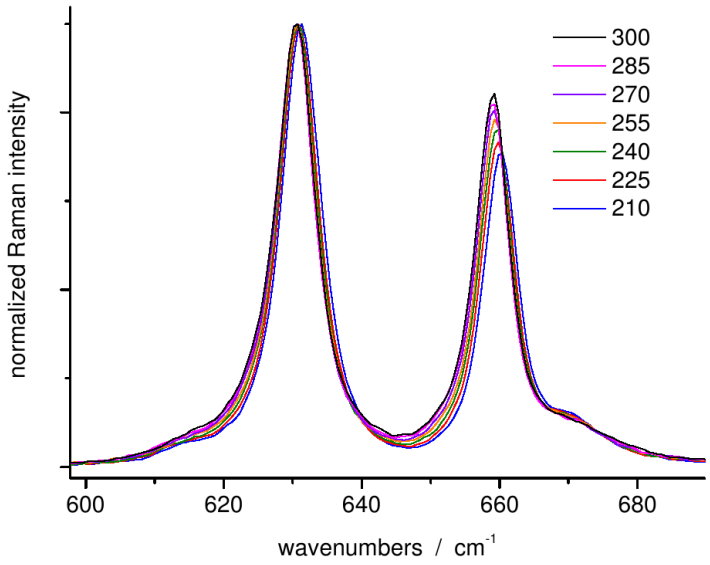

Figure 3.3.5: Raman spectra for the axial (630 cm^{-1}) and equatorial (658 cm^{-1}) conformers corresponding to the symmetrical SiC_2-vibrations of pure liquid **3** at different temperatures.

The experimental enthalpy difference (ΔH) was determined by the van't Hoff plot of **3** (see figure 3.3.7) from equation 2.4.4.1, using the deconvolutionized peak heights and peak areas of the Raman spectra of the band pair 630/658 cm^{-1}. The band deconvolution is shown in figure 3.3.6.

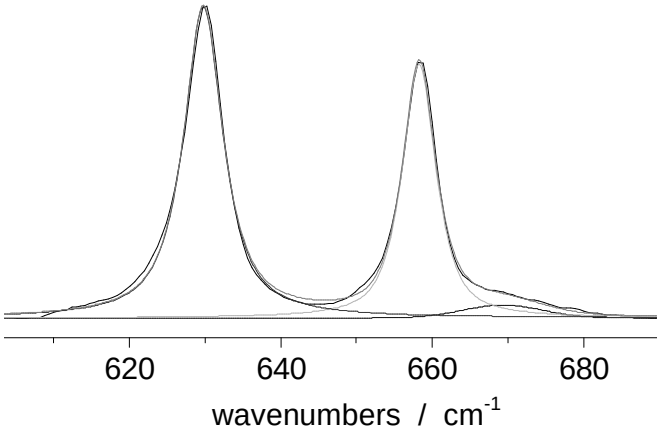

Figure 3.3.6: Band deconvolution of the symmetrical SiC_2-vibration of **3**.

The enthalpy of the ring inversion process of **3** was found to be: $\Delta H_{e\rightarrow a}$ = -0.26 kcal/mol (peak areas) and $\Delta H_{e\rightarrow a}$ = -0.25 kcal/mol (peak heights).

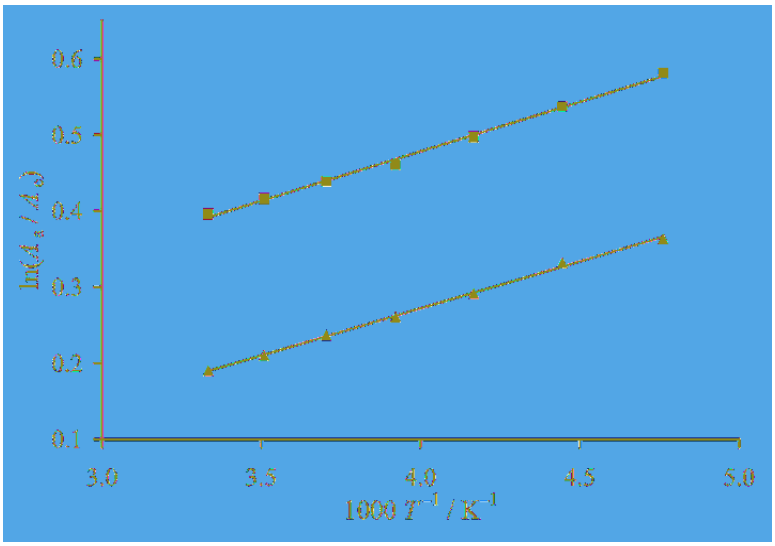

Figure 3.3.7: Van't Hoff plots of the band pair 630/658 cm^{-1} of pure **3** using peak areas (above) and peak heights (below).

The same behaviour was observed at decreasing temperatures for **3** in pentane (see figure 3.3.8) and CH_2Cl_2 solutions.

The evaluated enthalpy values for **3** in pentane solution were found to be $\Delta H_{e\rightarrow a,\ heights}$ = -0.21 kcal/mol and $\Delta H_{e\rightarrow a,\ areas}$ = -0.24 kcal/mol by using deconvolutionised peak heights and peak areas, respectively.

The evaluated enthalpy values for **3** in CH_2Cl_2 solution were on the other hand found to be $\Delta H_{e\rightarrow a,\ heights}$ = -0.30 kcal/mol and $\Delta H_{e\rightarrow a,\ areas}$ = -0.25 kcal/mol by using deconvolutionised peak heights and peak areas, respectively.

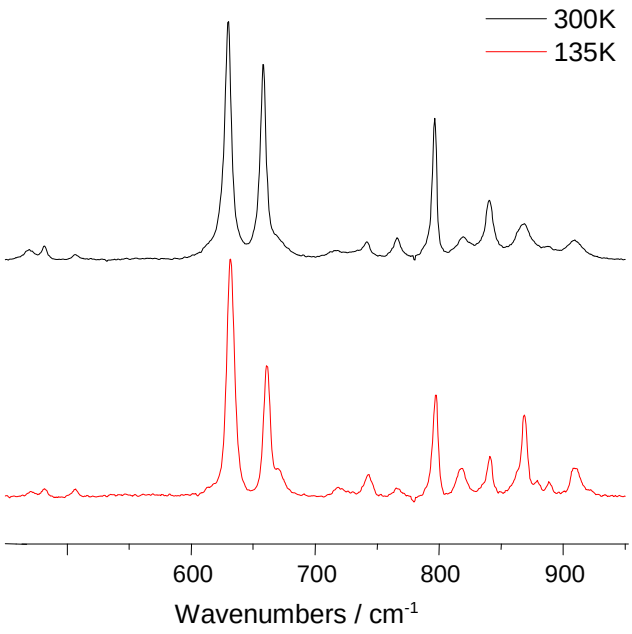

Figure 3.3.8: Temperature-dependent Raman spectra at 300K (above) and 135K (below) of **3** in pentane solution showing the $\nu_s SiC_2$ vibrations at 600 – 700 cm^{-1}.

Temperature-dependent Raman measurements have also been performed for **3-5** and **7-9** in the temperature range of 300–210 K (neat liquid), 300–210 K (heptane solution) and 293–210 K (THF solution).

The analysis of low temperature Raman measurements for **3-5** and **7-9** are summarized in table 3.3.1. It can be seen that different polarities of the medium do not massively affect the ΔH values. This is to be expected as the dipole moment of the equatorial and axial conformers should not vary greatly for the compounds being studied (see the Raman chapter).

Table 3.3.1: Summary of obtained enthalpy (ΔH) values from low temperature Raman analysis of the monosubstituted silacyclohexanes; **3-5** and **7-9**, using both deconvolutionised peak heights and peak areas. In all cases Δ*H* is the enthalpy difference between the axial and equatorial conformers i.e. $\Delta H_{e \rightarrow a}$.

	Vibrational mode	**Method of deconvolution**	**Neat liquid (ΔH) [kcal/mol]**	**Pentane solution (ΔH) [kcal/mol]**	**Heptane solution (ΔH) [kcal/mol]**	**CH_2Cl_2 solution (ΔH) [kcal/mol]**	**THF solution (ΔH) [kcal/mol]**
3 (-F)	$\nu_s SiC_2$	Peak heights	-0.25	-0.21	-	-0.25	-
		Peak areas	-0.26	-0.24	-	-0.30	-
4 (-Cl)	$\nu_s SiCl$	Peak heights	-0.48	-	-0.35	-	-0.58
		Peak areas	-0.69	-	-0.46	-	-0.62
5 (-Br)	$\nu_s SiBr$	Peak heights	-0.69	-	-0.33	-	-0.31
		Peak areas	-0.57	-	-0.47	-	-0.89
7 (-SiH3)	$\nu_{as} SiSi$	Peak heights	-0.19	-	-0.22	-	-0.19
		Peak areas	-0.29	-	-0.09	-	-0.10
8 (-OMe)	$\nu_s SiC_2$	Peak heights	-0.08	-	-0.06	-	-0.06
		Peak areas	-0.15	-	-0.11	-	-0.10
9 (-$N(Me)_2$)	$\nu_s SiC_2$	Peak heights	0.27	-	0.31	-	0.29
		Peak areas	0.30	-	0.27	-	0.28

3.3.6 Quantum chemical Calculations

The minimum energy path for the chair to chair interconversion of **3** has been reported [36]. It was calculated in redundant internal coordinates using the STQN-path method available in Gaussian 03 [91]. The level of theory used was B3LYP/6-311+G(d,p).

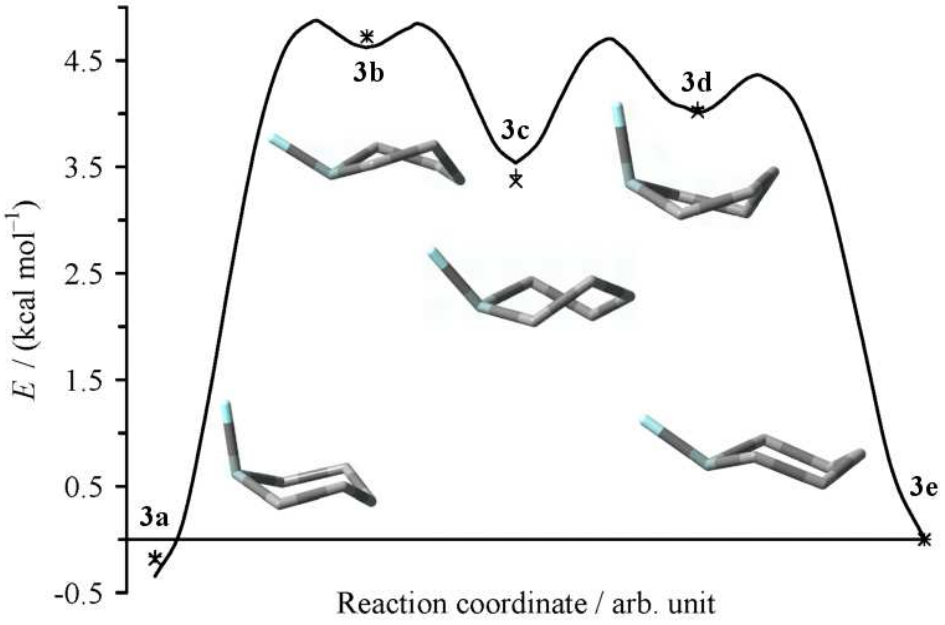

Figure 3.3.9: The chair-to-chair interconversion of **3**. This minimum-energy path was calculated by B3LYP/6-311+G(d,p). The crosses and pluses in the figure correspond to the CBS-QB3 and G3B3 ZPE-corrected 0 K relative energies, respectively (see table 3.3.2).

In figure 3.3.9 can be seen that the path goes through three intermediate conformations during the ring inversion of **3**. When starting in the axial conformation **3a**, the first one encountered is the **3b** twist form and from there it goes to a relatively more stable twist form **3c**, which marks the half way point in the ring inversion. The last conformer encountered before reaching the stable equatorial chair conformation **3e** is a third twist conformer **3d**. The calculated energies and the abundances for the five conformers can be seen in table 3.3.2.

Table 3.3.2: Relative energies at 0 K, free energies at 298 K and partial abundances **3a–e** in the gaseous phase of **3** [36].

	ΔE_{0K} / (kcal mol^{-1})		ΔG_{298K} / (kcal mol^{-1})		Partial abundance (%)	
	CBS-QB3	G3B3	CBS-QB3	G3B3	CBS-QB3	G3B3
3a	–0.18	–0.16	–0.18	–0.16	57	56
3b	4.72	4.73	4.30	4.32	0.03	0.03
3c	3.36	3.42	3.20	3.29	0.19	0.17
3d	4.02	4.05	3.58	3.63	0.10	0.09
3e	0.00	0.00	0.00	0.00	42	43

From the same QC calculations of **3** it was found that $\Delta G^{\ddagger}_{a\rightarrow e}$ = 4.86 kcal/mol. This is in fairly good agreement with the $\Delta G^{\ddagger}_{a\rightarrow e}$ = 5.13 kcal/mol derived from the ^{19}F-DNMR analysis.

The MP2/6-31G(d,p) level of theory gave A = -0.15 kcal/mol indicating a 56% abundance of the axial conformer **3a** in the vapour phase of **3** at 298 K, while B3LYP/6-31G(d,p) gave A value of -0.27 kcal/mol, indicating 61% abundance of the axial conformer **3a** in the vapour of **3** at 298 K.

Only some QC-calculations are available to date for **7**. These results can be seen in table 3.3.3 in the next subchapter. QC calculations for **4**, **5**, **8** and **9** are either currently being performed or will soon be performed.

3.3.7 Discussion

The monosubstituted silacyclohexanes **3**-**12** were prepared with the intention of being conformationally investigated by means of DNMR (either ^{19}F- or ^{13}C-DNMR), GED and variable Raman spectroscopy. In the case of **3**, investigation by microwave spectroscopy was also performed [33]. At present not all the experimental measurements have been completed, but the available results to date will be outlined here below. The most extensive data exist for **3**-**5** and **7**-**9**. However, no experimental data exists yet for **6** and **10**-**12**, as these compounds have only very recently been prepared.

First let us look at the results for the halosilacyclohexanes **3**-**6**. The *A* values for the corresponding monosubstituted halocyclohexanes derivatives have been found to be; 0.25-0.38 kcal/mol for fluorocyclohexane, 0.51-0.64 kcal/mol for chlorocyclohexane, 0.48-0.61 kcal/mol for bromocyclohexane and 0.47-0.59 kcal/mol for iodocyclohexane [92-99]. The *A* value of compounds **3**, **4** and **5**, however, were found, as expected from previous findings, to be substantially lower. The most striking trend is that they all have negative *A* values indicating that their equilibrium lies toward their axial conformation. When these results are compared to the cyclohexasilanes $Si_6H_{11}X$ (X = F, Cl, Br and I), the silicon analogue of cyclohexane where all the carbon atoms have been replaced by silicon, it is interesting to see that only in the case of $Si_6H_{11}F$ is the axial conformation favoured over the equatorial conformation [37]. All the other systems $Si_6H_{11}X$ (X = Cl, Br and I) favoured the equatorial conformation. The same pattern was seen for the undecamethylcyclohexasilane derivatives; $Si_6Me_{11}X$ (X = F, Cl, Br and I), studied by the same authors. The authors explained this by an effect similar to the gauche effect which causes elongation of the Si-F bond which stabilises the axial chair form [37]. Our findings for the monosubstituted halosilacyclohexanes **3**, **4** and **5** (having X= F, Cl and Br) are therefore in vast contrast to both their cyclohexane and cyclohexasilane analogues, as the axial conformer of the halosilacyclohexanes **3**-**5** is in all cases favoured over the equatorial conformer. Unfortunately no data exists yet for **6**, but it will be interesting to see whether it follows the same trend. The halosilacyclohexanes are currently being investigated, in collaboration with the

Tormena group at the state University of Campinas in Brazil, with respect to both coupling constants and solvation effects.

The conformational study of **7** (which represents a Si-Si system) predicted the equilibrium to be slightly towards the axial conformation, estimated to have 57% population of **7a** by GED giving *A* = -0.17 kcal/mol, supported by M06-2X calculations which gave 53% (-0.08 kcal/mol) population of **7a** (see table 3.3.3 for the complete summary of the results). Silylcyclohexane on the other hand gave *A* values of 1.45 and 1.44 kcal/mol found by ^{1}H- and ^{13}C-NMR (at 188 K) respectively, while ab initio calculations and MM3 calculations predicted 1.90 and 1.16 kcal/mol respectively [100,101]. GED on the other hand predicts 90% of the equatorial conformer at 75 °C (A value of 1.52 kcal/mol at 348K) [102]. It is interesting to see how the equilibrium progressively changes and how the *A* value is steadily decreasing when going from methylcyclohexane to silylcyclohexane and continues to decrease further when moving to the silacyclohexanes congeners **1** and **7**. With this decreasing *A* value the axial population of the substituent is clearly increasing accordingly. This is demonstrated in scheme 3.3.7.1. This behaviour could be explained in an over simplified way, by the increasing bond length between the substituents and the ring (going from C-C to Si-C to Si-Si bonds), stabilizing the axial position.

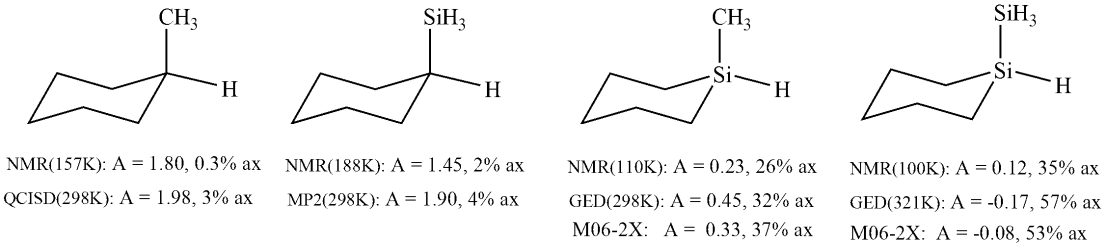

Scheme 3.3.7.1: *A* values and conformational populations for; methylcyclohexane, silylcyclohexane, methylsilacyclohexane (**1**) and silylsilacyclohexane (**7**). Values for **1** and **7** are taken from table 3.3.3, values for methylsilacyclohexane were taken from Wiberg et al. [73].

Another point of interest is that the two experiments for the liquid phase of **7** (DNMR and Raman) seem to give contrasting results. The *A* value from the DNMR indicates a preference of the equatorial position of **7**, whereas the Δ*H* values from the

Raman experiment indicate that the axial conformer is energetically favoured, behaviour that was also seen for **2**. For **2** it has been hypothesised that the polarisation of the Freon solvent mixture used in its DNMR measurements might have been an important factor for this observed behaviour. However, as **7** also exhibits the same propensity in a non polar SiD_4 solvent, the polarisation of the DNMR solvent does not seem to be the dominant factor. This apparent discrepancy could be rationalized by extracting entropy values from the DNMR analysis of **7**, to see how large a part entropy plays in this system. A conformational characteristic that **7** also shares with the previously studied **2**, is that they both display a change in conformational behaviour when going from the liquid phase to the gaseous phase. Both prefer the equatorial conformation in the liquid phase, while the axial conformation is preferred in the gaseous phase. This can be seen from the GED and DNMR results in table 3.3.3.

Compounds **8** and **9** have at present, only been investigated by means of low temperature Raman spectroscopy.

For **8** the low temperature Raman analysis gives $\Delta H_{e\rightarrow a}$ = -0.11 kcal/mol (neat liquid, average of heights and areas), i.e. the axial conformer is energetically more stable by 0.11 kcal/mol. This is in agreement with recently published QC results predicting a ΔE value of -0.15 kcal/mol for **8** [103]. The *A* value of the cyclohexane analogue of **8**, metoxycyclohexane, has been found to be 0.75 kcal/mol at 180 K accounting for only 11 % population of the axial conformer, which seems to be at odds with the results for **8**, although free energy values are needed for **8** to confirm this [75].

The same analysis for **9**, however, predicted that the equatorial conformer was more stable, with $\Delta H_{e\rightarrow a}$ = 0.28 kcal/mol (neat liquid, average of heights and areas). Compound **9** is therefore the only monosubstituted silacyclohexane system studied in this work which seems to display an equatorial preference, although again free energy calculations are needed to confirm this. The *A* value of the cyclohexane analogue of **9**, dimethylaminecyclohexane, was found to be 1.53 kcal/mol (in $CF_3Cl_3/CDCl_3$) and 1.31 kcal/mol (in both cases at 183 K), accounting for only 1.5% and 2.7% of the axial conformation, respectively [104]. The indicated equatorial

preference of **9** should therefore not be surprising if its carbon analogue, dimethylaminecyclohexane, is considered. Dimethylaminecyclohexane has a very strong equatorial preference (around 98%). Therefore it is not unusual for this preference to be replicated by **9**, especially considering the bulk of the substituent.

Samples of **8** and **9** have been prepared for GED- and ^{13}C-DNMR measurements and will be measured very soon. High level QC calculation will also be performed. It will be very interesting to see whether the first results for **8** and **9** will be supported, or whether contrary values will be seen like in the case of **2** and **7**.

In table 3.3.3 a summary of all available results for **3**-**5** and **7**-**9** to date is given. QC results seen there were recently performed by Ragnar Björnsson [105]

Table 3.3.3: Compilation of measured conformational properties of **3-5** and **7-9**, along with theoretical results (experimental results for **1** and **2** are from previous work). In all cases ΔH is the enthalpy difference between the axial and equatorial conformers i.e. $\Delta H_{e \rightarrow a}$. Raman values are the averages of the values obtained from peak heights and peak areas.

	DNMR (*A*[kcal/mol] / % axial)	**GED (*A*[kcal/mol] / % axial)**	**Raman (ΔH) [kcal/mol]**	**MW (ΔE) [kcal/mol]**	**QC (*A*[kcal/mol] / % axial)**	**QC (ΔE) [kcal/mol]**	**QC (ΔH) [kcal/mol]**
1 (-CH_3)	0.23(2) / 26(1)% T=113K	0.45(14) / 32(7)% T=298K	-	0.0 (2)	M06-2X: 0.33 / 37 % G3B3: 0.38 / 34 %	B3LYP: 0.52 MP2: 0.21	M06-2X: 0.19 G3B3: 0.24
2 (-CF_3)	0.4(1) / 17(2)% T=110K	-0.19(29) / 58(12)% T=293K	-0.53 (neat) -0.51 (pentane) - 0.62 (CH_2Cl_2)	-	M06-2X: -0.23 / 60 % G3MP2B3: -0.06 / 53 %	-	M06-2X: -0.48 G3MP2B3: -0.62
3 (-F)	-0.13(2) / 64(2)% T=112K	-0.31(20) / 63(8)% T=295K	-0.25 (neat) -0.22 (pentane) -0.28 (CH_2Cl_2)	-0.12 (7)	M06-2X: -0.06 / 53 % G3B3: -0.16 / 57 %	B3LYP: - 0.31 MP2: -0.23	M06-2X: -0.14 G3B3: -0.16
4 (-Cl)	-	-	-0.58 (neat) -0.40 (heptane) -0.60 (THF)	-	-	-	-
5 (-Br)	-	-	-0.63 (neat) -0.40 (heptane) -0.60 (THF)	-	-	-	-
7 (-SiH_3)	0.12(3) / 35(3) % T=100K	-0.17(15) / 57(7)% T=321K	-0.24 (neat) -0.15 (heptane) -0.15 (THF)	-	M06-2X: -0.08 / 53 % G3B3: 0.34 / 36 %	-	M06-2X: -0.14 G3B3: 0.12
8 (-OCH_3)	-	-	-0.11 (neat) -0.08 (heptane) -0.08 (THF)	-	-	-	-
9 (-$N(CH_3)_2$)	-	-	0.28 (neat) 0.29 (heptane) 0.28 (THF)	-	-	-	-

3.4 Conformational properties of 1,1-disubstituted silacyclohexanes

3.4.1 Synthesis of 1,1-disubstituted silacyclohexanes

1-Fluoro-1-methyl-1-silacyclohexane (**13**) was prepared in variation to the general preparation of $(Me)_XSiF_{4-X}$ (described by Hagen et al.) [106]. Chloromethylsilacyclohexane was reacted at 0 °C with an excess of antomonytrifluoride as demonstrated in scheme 3.4.1.1 below.

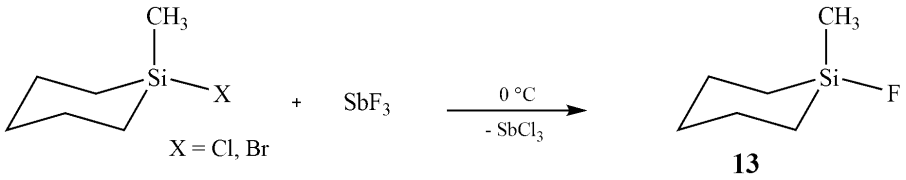

Scheme 3.4.1.1

The main purpose of synthesizing **13** was to compare it to well documented conformational properties of **1** and the recently published properties of **3** [32-34,36,68]. The methyl group has a moderate preference for the equatorial position **1e**, whereas the fluorine prefers the axial position **3a** (see scheme 3.4.1.2). It was therefore very interesting to see whether these effects were additive in compound **13**, in such a way that these conformational preferences complement each other. If that would be the case then the **13e** conformer should have over 90% population.

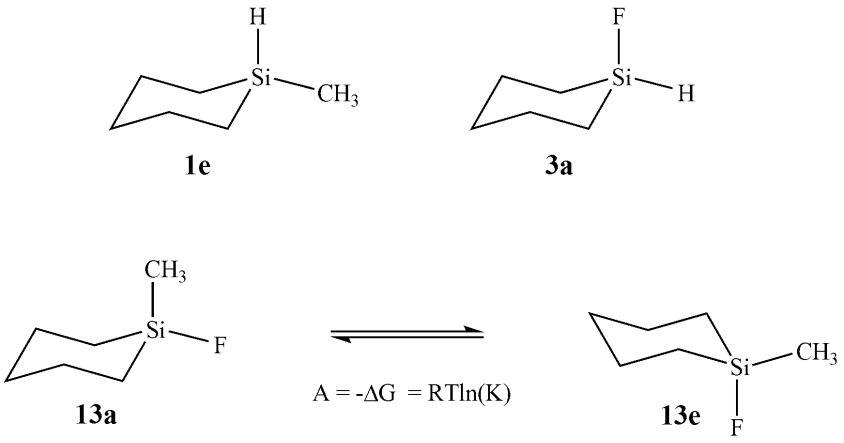

Scheme 3.4.1.2

1-Trifluoromethyl-1-methyl-1-silacyclohexane (**14**) was prepared in slight variation to the standard preparation of F_3CSiCl_3 [107]. Its synthesis involves a gas condensation reaction of excess CF_3Br in vacuo into a reaction flask containing partly brominated chloromethylsilacyclohexane, which was then reacted with equimolar $P(NEt_2)_3$ dissolved in CH_2Cl_2, at –78 °C (see scheme 3.4.1.3).

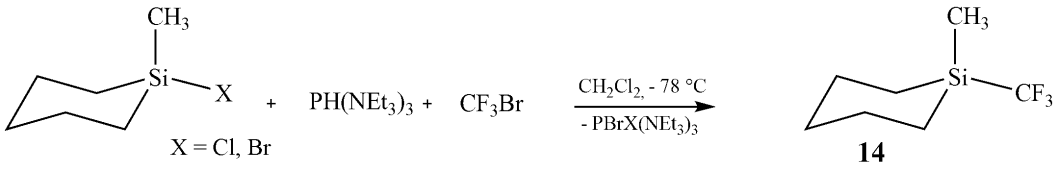

Scheme 3.4.1.3

Again knowing well the conformational behaviour of **1** as well as the conformational properties of **2**, we were eager to compare these results with the ones for **14** [35]. As established earlier the methyl group has a preference for the equatorial position **1e**, however, the trifluoromethyl group was found to slightly prefer the axial position **2a** in, the gaseous phase, while in solution at very low temperatures the equatorial position **2e** was found to be more favourable (see scheme 3.4.1.4). If the effects of these groups were additive in compound **14**, then conformer **14e** (i.e. where the methyl group possesses the equatorial position) should have over 90% population in the gaseous phase, while **14a** should be slightly preferred in solution at low temperatures, due to the competing conformational preferences of the two substituents.

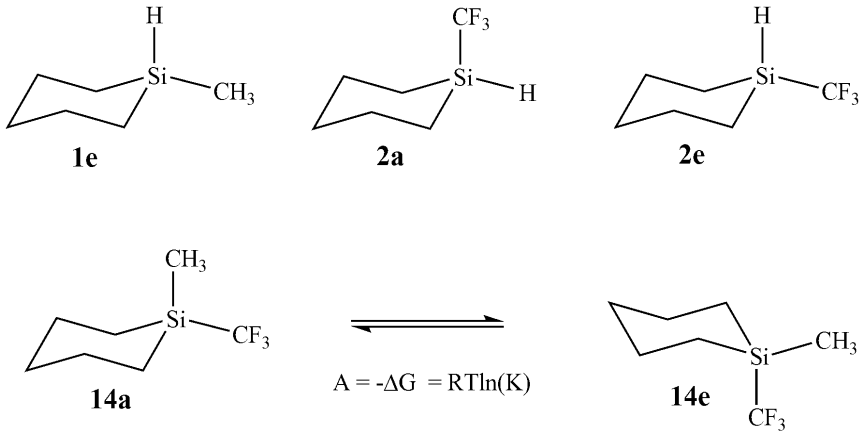

Scheme 3.4.1.4

1-Deuterium-1-methyl-silacyclohexane (**15**) was synthesized by reacting chloromethylsilacyclohexane and lithiumaluminumdeuteride at 0 °C using diethyl ether as the reaction solvent (see scheme 3.4.1.5).

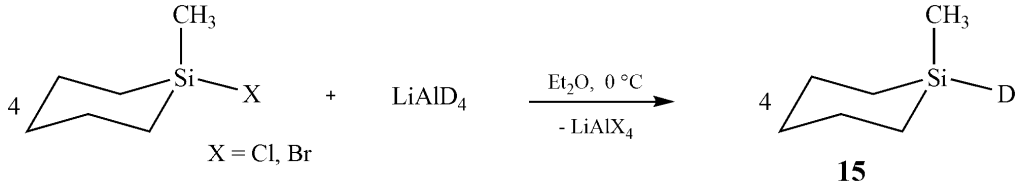

Scheme 3.4.1.5

The main purpose of synthesizing **15** was to measure its temperature dependent Raman spectra, since the analogous spectra for the well studied **1** was found to be problematic.

Like mentioned in the introduction of this chapter, **1** had previously been studied by means of ^{13}C-DNMR, GED and MW spectroscopy and supported by QC calculations. Low temperature Raman analysis of **1** would present the opportunity to compare its results in both polar and non-polar solvents to newly performed solvent calculations of **1**.

Unfortunately, when attempted, the Raman measurements of **1** did not give any usable information since the wavenumber difference obtained was not sufficient to attain distinguishable signals for the Si-C symmetrical vibration (see the Raman chapter for further clarification). Quantum chemical frequency calculations using the B3LYP/6-31G(d,p) method were performed for **1**, which gave the wavenumbers 590 cm^{-1} and 597 cm^{-1} for the SiC_2 symmetrical stretch of **1**, for the axial and equatorial conformers respectively. The wavenumber difference is therefore only 7 cm^{-1}, but a wavenumber difference of 10-20 cm^{-1} is usually desirable to achieve distinguishable signals for a system such as this. The non adequate wavenumber difference for **1** therefore resulted in an overlapped spectrum for both conformers **1a** and **1e**, instead of separated vibrational signals. The same frequency calculations of the wavenumbers for the symmetrical SiC_2-vibration ($\nu_s SiC_2$) for **15** on the other hand

predicted that the Raman vibrational signals for **15a** would appear at 594 cm^{-1}, but at 622 cm^{-1} for the **15e** conformer. This gives a wavenumber difference of 28 cm^{-1}, prompting the performance of the Raman analysis of **15**, in an attempt to gain information about **1**. There was not considered to be any need to study **15** any further than that, neither with respect to QC calculation nor experimentally, as **1** had already been studied extensively and repetition of these experiments was not expected to provide any additional information.

1-Fluoro-1-trifluorosilyl-1-silacyclohexane (**16**) was prepared with a combination of steps from the synthesis of **7** and **13** (see previous discussion). 1-Chloro-1-trichlorosilyl-1-silacyclohexane was first synthesized (again having ~ 25-30% impurities of brominated products) and used as the starting material for **16**. The third step involved the reaction of 1-chloro-1-trichlorosilyl-1-silacyclohexane and excess antomonytrifluoride at 0 °C. This process is demonstrates in scheme 3.4.1.6. The di-Grignard $BrMg(CH_2)_5MgBr$ was prepared in the traditional way described previously.

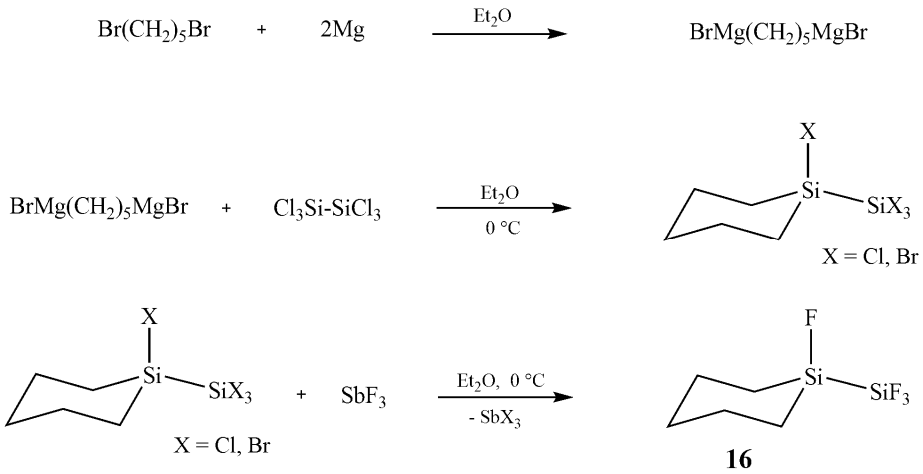

Scheme 3.4.1.6

Unfortunately at this time neither experimental nor theoretical results are available regarding the conformational behaviour of **16**, since it has only very recently been synthesized.

In the next subchapters the conformational analysis of **13** and **14** by various methods will be covered. To illustrate the experimental conformational analysis of the di-substituted silacyclohexane systems, **13** was chosen, as the most extensive data from each experimental method exists at this point in time for it. Data which will soon be published by our group. The Raman analysis of **15** will also be covered.

3.4.2 Low temperature ^{19}F- and ^{13}C-NMR spectroscopy

The ^{19}F NMR spectra for **13** were recorded at regular intervals from room temperature down to 126 K. At temperatures down to about 165 K the equilibrium between the two conformers (**13a** and **13e**) was still relatively fast compared to the NMR timescale giving only an averaged spectrum for the two conformers. At temperatures below 161 K the equilibrium is obviously slowing down and considerable broadening of the signal can clearly be seen as the temperature drops. At 137 K it becomes evident that two sets of peaks corresponding to the Si-F signal are forming, indicating the existence of a major and a minor conformer of **13**. According to a trend which appears to generally apply for cyclohexanes, the resonance signal appearing at lower frequency (lower ∂ value), can be assigned to the axial conformer [88-90]. Based on this trend the more intense signal was assigned to conformer **13a**, while the smaller signal was assigned to conformer **13e**. At 126 K the peaks have become well separated and an obvious intensity difference can be seen between the two signals. At this stage it can therefore be estimated that at 126 K more molecules of **13** possesses the conformer termed **13e** (having the methyl group in the equatorial position while having the fluorine group in the axial position) than the **13a** chair form.

Through DNMR-simulation of the spectra, the free energy of activation ($\Delta G^{\ddagger}$) and the total free energy change (ΔG) of the interconversion process of **13**, can be determined via calculations of the rate constant and the equilibrium constant respectively, as a function of temperature. Both the experimental and simulated spectra at various temperatures can be seen in figure 3.4.1. At 126 K it was found that $\Delta G^{\ddagger}_{\mathbf{13e} \rightarrow \mathbf{13a}}$ = 5.5 kcal/mol, with A = 0.26 kcal/mol, giving 75% abundance of the **13e** conformer (CH_3 equatorial, F axial).

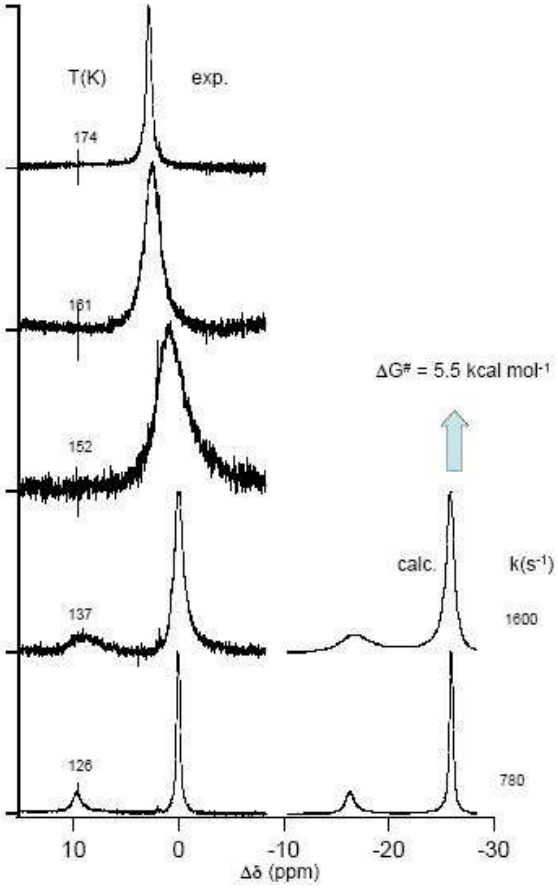

Figure 3.4.1: Experimental ^{19}F NMR spectra of **13** on the left and its simulated spectra on the right.

^{13}C-DNMR measurements of **14** were first performed, but unfortunately **14** crystallized out of the solvent mixture before reaching the coalescence temperature of any of the carbon signals of **14**, making the ^{13}C-DNMR analysis impossible. ^{19}F-DNMR measurements of **14** were then attempted and were found to be successful, but at this point $\Delta G^{\ddagger}_{e\rightarrow a}$ and k have not yet been evaluated. However, the preliminary evaluation of the data strongly indicates the preference of the conformer **14a**, having the CH_3 group in the axial position, while having the CF_3 group in the equatorial position.

3.4.3 GED analysis/measurements

Gas electron diffraction was performed for **13** by shooting beam of electrons at a molecular stream of **13**. After analysis of these measurements the "radial distribution function" (RDF) of **13** was obtained. This function describes the interaction between atoms within a molecule as a function of the distance between them (see figure 3.4.2). The measured function obtained shows a weighted average of **13e** and **13a**.

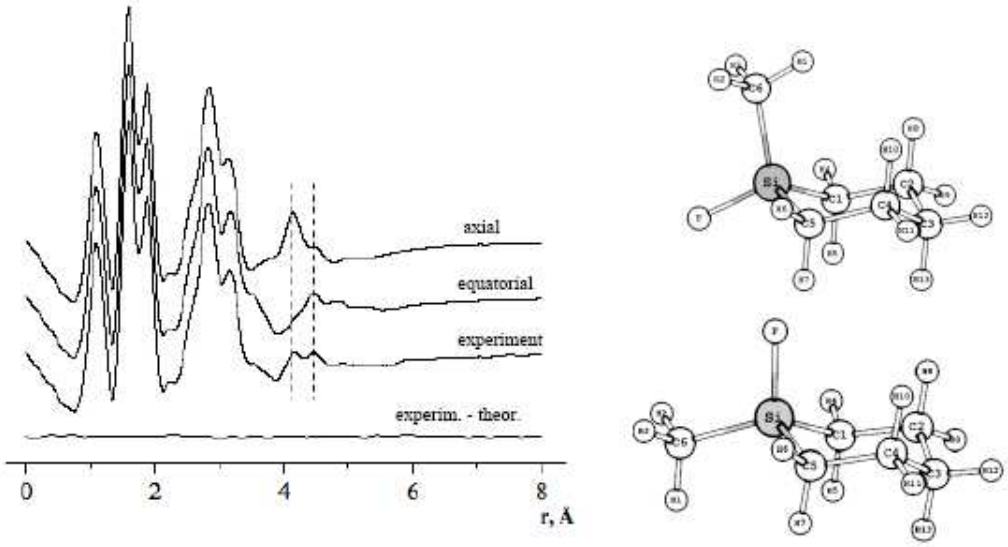

Figure 3.4.2: Experimental and theoretical radial distribution functions (RDF) of **13** (left) and molecular models of the axial and equatorial conformers (right).

Figure 3.4.2 also shows the calculated RDF curves for both the axial and the equatorial chair forms and it can be seen that the biggest difference between the curves is at r > 3 Å, due to the interaction between the methyl group and carbon atoms within the ring as well as for the nonbonded distance between the fluorine atom and ring atoms. By fitting these calculated functions in various ratios with the experimentally obtained function (until the least square method gave the lowest R value possible), the percentage of each chair form was obtained. These simulations predicted the conformer **13a (**having the CH_3 atom in the axial position) to be 45(6) % abundant, giving A = 0.11(13) at 282 K.

The GED measurements and analysis for **14** were performed in a similar way as described for **13**. According to the GED data the conformer **14e** (CH_3 equatorial, CF_3 axial), has 49(5) % abundance in the vapour of **14** at 262 K, while the conformer **14a** has 51(5) % abundance. This value corresponds to an *A* value of -0.02(11) kcal/mol.

3.4.4 Low temperature Raman measurements

Low temperature spectra were recorded for pure **13**, as well as for **13** in THF and in hexane solution at temperatures varying from 210 K to 300 K. The Raman spectrum of pure **13** at room temperature in the range 150-1450 cm^{-1} can be seen in figure 3.4.3.

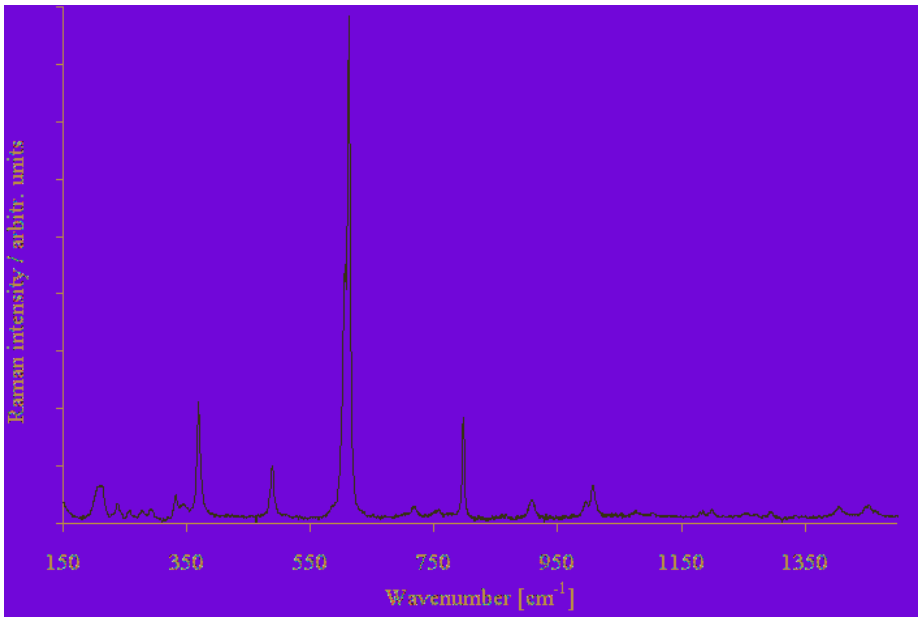

Figure 3.4.3: Raman spectrum of pure liquid **13** at room temperature.

The calculated wavenumbers (based on quantum chemical frequency calculations using the B3LYP/6-31G(d,p) method) for the symmetrical SiC_2-vibration ($\nu_s SiC_2$) for **13** are; 585 cm^{-1} for the conformer **13a** where the F-atom possesses the equatorial position and 597 cm^{-1} for the conformer **13e** in which the F-atom possesses the axial position.

Figure 3.4.4 shows the actual experimental values for the $\nu_s SiC_2$ vibrations of **13** appearing at 607 cm^{-1} and 614 cm^{-1}. The calculated values turned out to be a bit lower than the experimental values but nevertheless gave a correct overall picture of the vibrational Raman spectra and made the spectral interpretation easier. In contrast to what was seen for **1**, this small wavenumber difference was sufficient to give distinguished signals for both conformers of **13**. However, it can be seen in figure 3.4.4 that these signals are slightly overlapping.

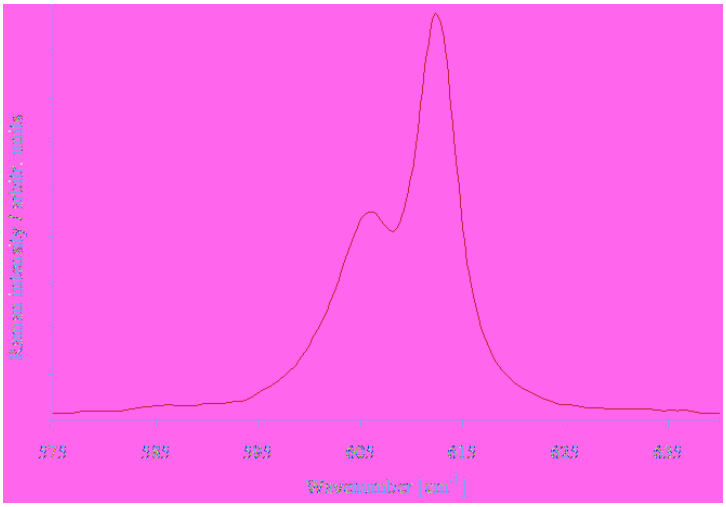

Figure 3.4.4: Magnified part of the Raman spectrum of pure **13** at room temperature, showing the Si-C stretching mode for the two chair conformers. According to the quantum chemical calculations the band at the left side (607 cm^{-1}) belongs to the **13a** conformer. The band at the right side (614 cm^{-1}) therefore belongs to the **13e** conformer.

Figure 3.4.5 shows the van't Hoff plots (by using equation 2.4.4.1) of pure liquid **13** using both deconvolutionised peak heights and peak areas. The calculated enthalpy differences from the van't Hoff analysis were found to be; $\Delta H_{e\rightarrow a,\ heights}$ = 0.50 kcal/mol using the deconvolutionised peak heights and $\Delta H_{e\rightarrow a,\ areas}$ = 0.61 kcal/mol using deconvolutionised peak areas. These values clearly predict the **13e** conformer to be energetically more stable then the **13a** conformer. It can also be predicted that **13e** (CH_3 equatorial, F axial) will be conformationally preferred, assuming that the entropy differences between the conformers are small.

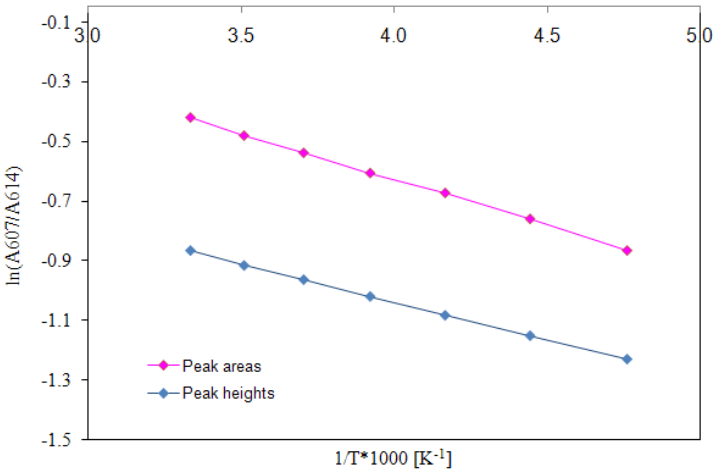

Figure 3.4.5: Van't Hoff plot of the band pair 607/614 cm^{-1} of pure **13** using peak heights $\Delta H_{e\rightarrow a,\ heights}$ = 0.50 kcal/mol and peak areas; $\Delta H_{e\rightarrow a,\ areas}$ = 0.61 kcal/mol.

It was interesting to see that at very low temperatures the substance **13** crystallized completely and a Raman spectrum was obtained showing only one stable conformer in the solid phase (see figure 3.4.6). The Raman spectra of pure **13** at 140 K and at 110 K were identical. At these temperatures the substance in the capillary was completely solid. X-ray diffraction measurements would be required to determine which conformer this is.

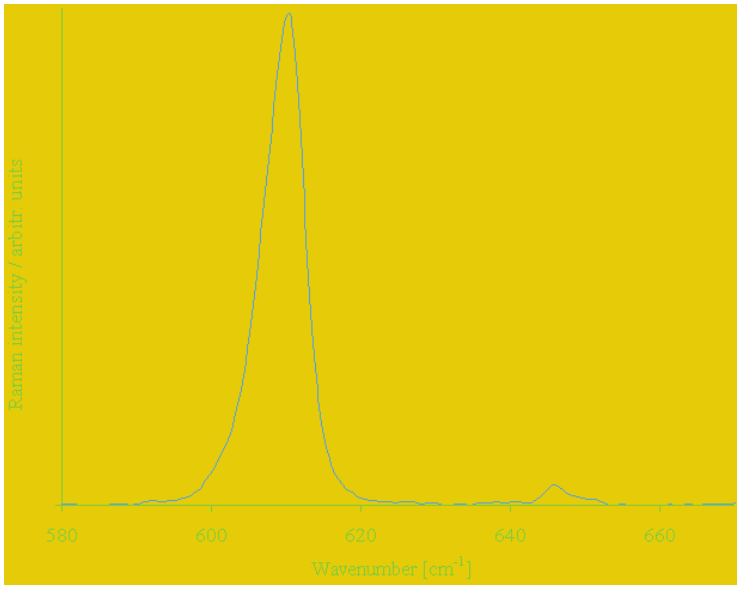

Figure 3.4.6: Magnified part of the Raman spectrum of pure **13** at 140 K, showing the Si-C stretching mode for only one conformer occurring at 610 cm^{-1}.

Compound **13** was also measured in THF and in hexane solution, where the **13e** conformer was also found to be the more stable conformer. The results are given in table 3.4.1.

Temperature dependent Raman measurements were performed for **14** in the temperature range of 300–210 K (neat liquid), 300–210 K (pentane solution) and 293–210 K (THF solution). This analysis predicted (similar to **13**) the **14e** conformer to be energetically more stable then the **14a** conformer. This leads to the prediction that **14e** (where the methyl group possesses the equatorial position) will be conformationally preferred, assuming that the entropy differences between the conformers are small. However, the DNMR analysis indicates that this is not the case as the **14a** conformer seems to be preferred in the liquid phase.

Temperature-dependent Raman measurements were performed for **15**, for neat liquid and for **15** in pentane, CH_2Cl_2 and THF solutions, in the temperature range of 300–210 K. The resulting enthalpies (see table 3.4.1) are in good agreement with the calculated ΔH values for **1** seen in table 3.3.3. Conformer populations cannot be calculated for **15** as Raman spectroscopy does not supply information about the entropies of this system. This is not of concern, as the conformer population of **15** should closely resemble that of **1**.

In table 3.4.1 the results from the analysis of low temperature Raman measurements of **13**, **14** and **15** are summarized. As was seen for the monosubstituted silacyclohexanes, the different polarities of the medium do not greatly affect the ΔH values.

Table 3.4.1: Summary of obtained enthalpy (ΔH) values from low temperature Raman analysis of the 1,1-disubstituted silacyclohexanes; **13**, **14** and **15**, using both peak heights and peak areas. All measurements are based on the analysis of the $\nu_s SiC_2$ vibrational mode. In all cases ΔH is the enthalpy difference between the axial and equatorial conformers i.e. $\Delta H_{e \rightarrow a}$.

	Method of deconvolution	**Vibrational mode**	**Neat liquid (ΔH) [kcal/mol]**	**Hexane solution (ΔH) [kcal/mol]**	**Pentane solution (ΔH) [kcal/mol]**	**CH_2Cl_2 solution (ΔH) [kcal/mol]**	**THF solution (ΔH) [kcal/mol]**
13 (Me_F)	Peak heights	$\nu_s SiC_2$	0.50	0.48	-	-	0.51
	Peak areas	$\nu_s SiC_2$	0.61	0.56	-	-	0.60
14 (Me_CF_3)	Peak heights	$\nu_s SiC_2$	0.73	0.67	-	-	0.78
	Peak areas	$\nu_s SiC_2$	0.60	0.58	-	-	0.61
15 (Me_D)	Peak heights	$\nu_s SiC_2$	0.16	-	0.16	0.16	0.17
	Peak areas	$\nu_s SiC_2$	0.14	-	0.13	0.15	0.15

3.4.5 Discussion

The 1,1-disubstitued silacyclohexanes **13**, **14** and **16** were prepared with the intention of being conformationally investigated by means of DNMR (either ^{19}F- or ^{13}C-DNMR), GED and variable Raman spectroscopy. Compound **15** was synthesized purely to be investigated by variable Raman spectroscopy to complete the investigation of **1**. As previously mentioned, no experimental data exists yet for the newly synthesized **16**. The available results to date will be outlined here below.

The results for **13** show that the simple additive model, presented in chapter 3.4.1. cannot be applied to the system as the **13e** conformer (CH_3 equatorial, F axial), did not have over 90% population. The GED results indicated that **13e** is only slightly preferred (55(5)% preference). QC calculations support this finding, although not quantitively, with MP2/6-31G** and B3LYP/6-31G** predicting 65% and 78% preference of the **13e** conformer, respectively [108]. However, ^{19}F-DNMR predicted over 75% of **13e**, but this has not yet been supported by theoretical methods for the liquid phase.

Experimental results also show that the simplistic additive model cannot be applied to **14**. If the model could be applied, **14e** should have over 90% population in the gas phase. GED, however, predicts that **14e** is 49(5)% preferred in the gas phase. QC calculations replicate this result to a certain degree, with MP2/6-31G** and B3LYP/6-31G** predicting 62% and 56% preference of **14e** [108]. If the additive model had been correct in the liquid phase, **14a** would have been slightly preferred. Incomplete DNMR analysis indicates preference of the conformer **14a** (CH_3 axial, CF_3 equatorial) which seems to match that prediction reasonably well. However, from the above results this seems more like a coincidence rather than verification of the credibility of the additive model.

The variable Raman spectroscopy results for **15** are found to be in good agreement with the QC results for **1**. It can therefore be concluded that the approach of performing variable Raman analysis on **15** in order to gain thermodynamic information about the liquid phase of **1**, was successful.

Examining the Raman results for **13**, **14** and **15**, a general trend is noticed that the enthalpy for the conformers possessing the methyl group in the equatorial position is lower, as was expected from the known behaviour of the relevant monosubstituted rings.

The results for **14** indicate a similar phenomenon that was also seen for compounds **2** and **7**. Comparing the Raman results with the DNMR results shows that entropic effects are vital in the conformational behaviour of this system, as Raman indicates that the **14e** conformation is energetically more stable, yet preliminary DNMR results indicate that **14a** is conformationally favoured. Compounds **2**, **7**, and **14** all have fairly large substituents and it appears that the less hindered rotation these groups experience in the equatorial position in solution leads to entropic gains that outweigh the energy gained in the energetically favourable, yet more hindered, axial position.

This new accumulation of experimental and theoretical data of the conformational behaviour and potential energy barriers of mono- and 1,1-disubstitued silacyclohexanes facilitates further predictions of the origin of these barriers and their nature i.e. with respect to hyperconjugation or steric repulsion. Lately there has been a great deal of discussion regarding hyperconjugation for both cyclohexanes and heterocyclohexanes (originally referred to as the gauche effect), making this data of considerable use [109-113].

4 Conformational investigation of disilanes

4.1 Conformational properties of CF_3Me_2Si-$SiMe_2CF_3$

4.1.1 Introduction

The rotational barrier of the E-E single bond between elements of group 14 (i.e. H_3E-EH_3, E = C, Si, Ge, Sn and Pb) has been extensively investigated over the last decades, with various experimental methods as well as theoretical calculations. As with ethane in organic structural chemistry, the bonding properties play an important role for the understanding of the structure mechanism and energetics of the homologous systems containing the heavier group 14 elements [41,114]. It has been established that the rotational barriers for internal rotation between the E-E bond for this series decreases downwards through the group [115]. Obviously the most information exists on ethane and its derivatives, however, a considerable amount of work has also been done on various disilanes.

When investigating Si-Si systems as opposed to C-C systems there are few things that must be considered including increased bond length, higher electron density, lower bond strength and lower torsional force constants accompanied by overall lower barriers for internal rotation. For example the central bond length in disilane is 0.84 Å longer than in ethane and the barrier for the hindered rotation of ethane was predicted to be 2.9 kcal/mol, for disilane this amounts to 1.2 kcal/mol [116,117].

The rotational barriers for H_3E-EH_3, E = C, Si, Ge, Sn and Pb can now be quite accurately calculated by theoretical methods. However, there has been much controversy regarding the origin of these barriers. In 2001 it seemed that a consensus had been reached, when Goodman et al. reported that the main source of the rotational barrier in ethane is hyperconjugation, not steric repulsive forces as previously thought [118]. The same authors (supported by Mo et al.) predicted, however, that the hyperconjugation effect favours the staggered configuration of disilane, although they claimed that it only plays a secondary role for disilane (and for digermane as well) [119,120]. They therefore predicted that the rotational barriers for disilane and digermane are in fact dominated by electrostatic repulsion. However,

more recently, Mo et al. reaffirmed that steric effects are the major factor that induces the rotational barrier of ethane, with only a slight impact from hyperconjugation stabilization [121].

A large number of publications exists to date concerning the conformational characteristics of various disilanes. It is not within the scope of this thesis to give a complete overview of all the work that has been done in this field, however, it is profitable to summarise some noteworthy results that are relevant to the work later presented in this thesis.

In 1972 Schleyer et al. confirmed a surprising prediction by both Mislow and Profeta and their co-workers, that the rotational barrier of hexamethyldisilane $Me_3Si\text{-}SiMe_3$ (1.06 kcal/mol) is almost the same as the one for the simplest disilane $H_3Si\text{-}SiH_3$ despite the presence of the six methyl groups [115,122,123]. Recent NMR investigation, however, predict the barrier to be about 1.65–1.70 kcal/mol [124].

Theoretical as well as experimental (Raman and GED) conformational studies have been performed over the years for more complicated disilane systems. These systems are among others; Me_3SiSiH_3, MeX_2SiSiX_2Me (with X = H, F, Cl, Br and I), $ClMe_2SiSiMe_2Cl$ and disilanes substituted with the bulky ^{t}Bu-group, e.g. $^t BuH_2SiSiH_2{}^t Bu$, $^t Bu_2HSiSiH{}^t Bu_2$ and $^t BuX_2SiSiX_2{}^t Bu$ [125-129].

The series $MeX_2Si\text{-}SiX_2Me$ (X = H, F, Cl, Br and I) was examined by Hassler et al. by means of Raman spectroscopy and ab initio calculations [130,131]. Both methods predicted a mixture of the two rotamers, anti and gauche in the liquid phase, where the anti rotamer was energetically preferred in all cases except for X= H where the gauche conformation was stabilized by 0.10 kcal/mol.

For $ClMe_2Si\text{-}SiMe_2Cl$, the global minimum was predicted to be the anti conformer by RHF/SBK calculations with E_{rel} of the gauche conformer being 1.3 kcal/mol [127]. These results for $ClMe_2Si\text{-}SiMe_2Cl$ were supported by Raman spectroscopy of both the solid (where only the anti conformer was found) and the liquid phase (where $E_{rel,\ gauche}$ was found to be 1.0 kcal/mol) of $ClMe_2Si\text{-}SiMe_2Cl$ [126]. GED

measurements, however, predicted the gauche conformer to be the most stable minimum in the gaseous phase [127].
Hassler et al. also studied very sterically hindered $^{t}BuX_2Si\text{-}SiX_2{}^{t}Bu$ (X = H, F, Cl, Br and I) [128,132,133]. Surprisingly, in contrast to all previous results for disilanes, $^{t}BuCl_2Si\text{-}SiCl_2{}^{t}Bu$ was calculated to have three conformational minima, however, only the staggered (anti) conformation could be seen by GED.

In order to further investigate heavily substituted disilanes, Hassler et al. were interested in $CF_3Me_2Si\text{-}SiMe_2CF_3$ as a model substance. A collaboration between our group, the Graz University of Technology and the School of Chemistry, University of Edinburgh was established for that purpose. This investigation will be presented in the next subchapters.

4.1.2 Synthesis of CF_3Me_2Si-$SiMe_2CF_3$

CF_3Me_2Si-$SiMe_2CF_3$ (1,2-bis(trifluoromethyl)-1,1,2,2-tetramethyl-disilane) (**17**) was, like **14**, prepared in slight variation to the standard preparation of F_3CSiCl_3 [107]. CF_3Br was first condensed in excess in vacuo into a reaction flask containing $ClMe_2Si$-$SiMe_2Cl$ (1,2-dichloro-1,1,2,2-tetramethyl-disilane) and CH_2Cl_2. The content of the flask was allowed to melt and its temperature was then maintained at –78 °C while it was reacted to equimolar $P(NEt_2)_3$ dissolved in CH_2Cl_2 (see scheme 4.1.2.1).

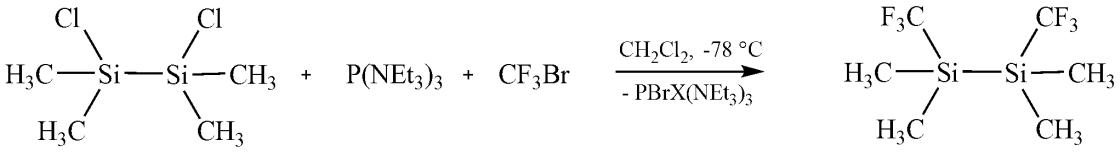

17

Scheme 4.1.2.1

Earlier results for **17** had predicted the existence of three local minima for internal rotation of the Si-Si bond, namely the anti, gauche and ortho rotamers (in figure 4.1.1 the Newman projections of these conformers can be seen) [134]. These result were interesting in light of the fact that they matched similar findings for *n*-Si_4Me_{10} and *n*-C_4F_{10}, however, no experimental reports exist yet, to the best of my knowledge, on this particular behaviour for unstrained disilanes and oligosilane chains [135-139]. The only exception is the preliminary result for $^tBuCl_2Si$-$SiCl_2{}^tBu$. Michl et al. reported that *n*-Si_4Me_{10} has three nonequivalent conformers with backbone dihedral angles ≈ ±165° (anti), ≈ ±55° (gauche) and ≈ ±90° (termed ortho by the authors) [135]. This is supported by GED [136]. The same authors also predicted the third ortho backbone rotamer in the n-C_4F_{10} system by ab initio calculations, for which Mid-IR matrix-isolation spectra directly predicted the existence of three nonequivalent rotamers [137,138]. Likewise the same three backbone conformers were computationally predicted for $SnMe_3SiMe_2SiMe_2SnMe_3$ and

$SiMe_3SiX_2SiX_2SiMe_3$ chains with X = H, F, Cl, Br, I and experimentally by Raman matrix-isolation study for $SiCl_3SiCl_2SiCl_2SiCl_3$ [140-142].

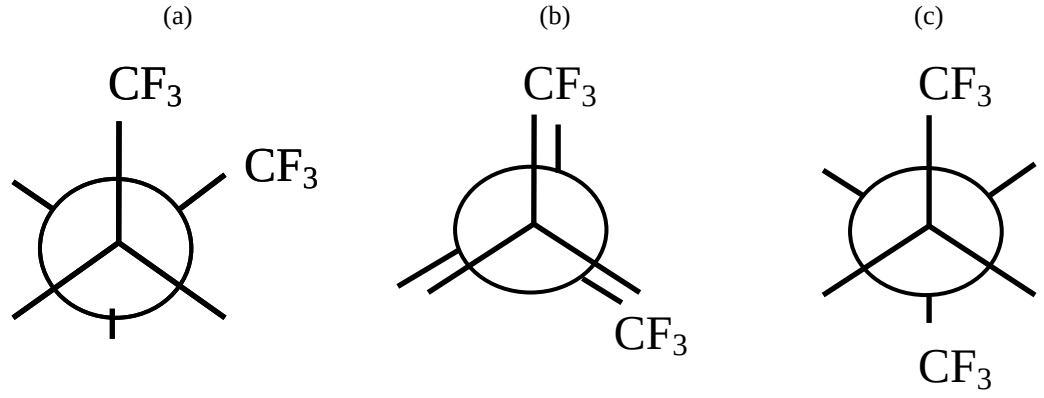

Figure 4.1.1: Newman projections of the three enantiomeric pairs of nonequivalent conformers of **17**: (a) gauche (b) ortho and (c) anti.

In the following subchapters the results of the currently available conformational investigation of **17** will be covered. These data include results from newly repeated variable Raman spectroscopy, GED measurements and high level quantum chemical calculation [143]. If the early predictions of the possible presence of three pairs of enantiomeric conformers, in the liquid state and/or the gaseous state, are correct, then **17** could be a useful system that could facilitate further elucidation of this interesting backbone behaviour. It could also help to clarify whether the size and type of the substituents are affecting the numbers of stable conformations of individual bonding systems, as for example *n*-Si_4H_{10} (as opposed to the previously discussed *n*-Si_4Me_{10}) only showed two stable rotamers [144].

4.1.3 Temperature dependent Raman measurements

Both high and low temperature-dependent Raman measurements were performed for **17** in the temperature range of 297-373 K (neat liquid), 300-225 K (cyclopentane solution) and 297-373 K (cyclopentane solution). The room temperature spectrum of **17** in the range of 200-1600 cm^{-1} can be seen in figure 4.1.2.

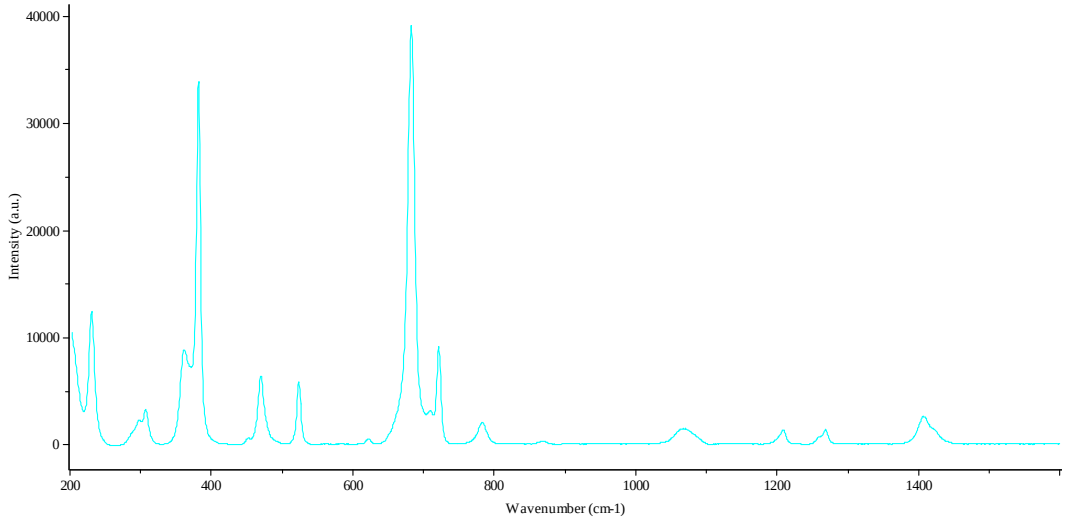

Figure 4.1.2: Raman spectrum of pure liquid **17** at room temperature (24 °C) in the range: 200 - 1600 cm^{-1}.

Quantum chemical calculations (6-31G*/SCF) were used to assign the active Raman vibrational modes. The νSiC^F mode of **17** was found to be extremely sensitive to the backbone configuration. Three peaks were predicted to correspond to the νSiC^F vibrational mode in the Raman spectrum of **17**, calculated to appear at 354 cm^{-1}, 364 cm^{-1} and 377 cm^{-1} each corresponding to a different enantiomeric conformer, namely the gauche, ortho and the anti conformer, respectively. The three bands in the experimental Raman spectra of pure liquid **17** at room temperature (see figure 4.1.2), appearing at 360 cm^{-1}, 369 cm^{-1} and 380 cm^{-1} were assigned to the gauche, ortho and the anti rotamer, respectively. This was in agreement with the theoretical values.

The ρCF_3 vibrational mode was also calculated to show intensive signals in the Raman spectrum of **17**. Unfortunately even though it was predicted to show appreciable wavenumber difference between the anti and gauche conformers, the

wavenumber difference between the gauche and ortho conformers was predicted to be negligible. These signals were therefore very likely to appear as one signal in the Raman spectrum, making the van't Hoff analysis for that band triplet unreliable.

The experimental temperature variable Raman spectra of **17**, show that the bands for the νSiC^F modes for the three rotamers change with temperature. This is shown in figure 4.1.3 for **17** in cyclopentane solution which also demonstrates that one rotamer could be crystallized out of the cyclopentane solution at 225K where the band pair corresponding to the gauche and ortho rotamers disappears completely. This reveals that the anti conformer is clearly preferred in the solid state. These crystals are currently being studied by means of X-ray crystal diffraction. The results will soon be available.

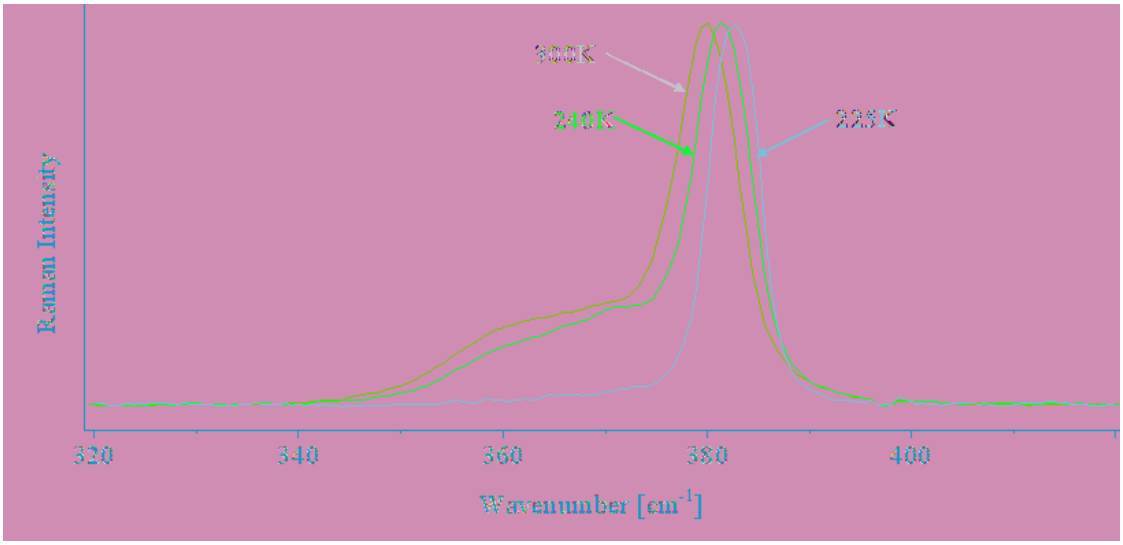

Figure 4.1.3: Magnified part of the Raman spectra of the spectral bands 360/369/380 cm^{-1} (belonging to the gauche, ortho and anti conformers respectively) for the νSiC^F mode of **17** in cyclopentane solution at 300, 240 and 225K in the range: 320 - 420 cm^{-1}.

From figure 4.1.3 it can also be seen that the bands for the ortho and gauche conformers of **17** overlap enormously (hardly surprising, considering that the wavenumber difference between these two conformers is only 9 cm^{-1}). Due to distinguishable features of the curves in figure 4.1.3 deconvolution of the band pair

(ortho and gauche) made their Raman analysis possible. After deconvolution of the spectral bands, the relative enthalpies were calculated using the van't Hoff equation 2.4.4.1.

Various properties currently available for the three conformers deducted from the newly performed analysis of **17** are shown in table 4.1.1. The relative enthalpies of the three conformers are shown with anti being the lowest in energy.

Table 4.1.1: Properties of the three conformers of **17** using the $vSiC^F$ mode: Wavenumber [cm^{-1}], torsion angle [°] and experimental average ΔH [kcal/mol][143].

Conformer	**Anti**	**Ortho**	**Gauche**
SiC^F stretching band [cm^{-1}][a]	380	369	360
Torsion angle [°][b]	170.8	101.1	55.7
Experimental average ΔH_{rel} [kcal/mol][c]	0.0	0.13	1.12

[a] Raman experimental values
[b] MP2/6-31G*
[c] Experimental average of ΔH [kcal/mol] values obtained from Van't Hoff plots of **17** after band fitting. The ΔH values for low-temperature (300-240K) and high-temperature Raman measurements (297-373 K) in cyclopentane solution were taken into consideration; the ΔH values for heights and areas of the fitted bands were also taken into consideration (in total four ΔH values were used to get the average ΔH values shown in above table).

4.1.4 Ab initio calculations

All ab initio calculations for **17** were performed by our collaborators at the School of Chemistry, University of Edinburgh [143]. An extensive scan of the torsional potential energy surface of **17** was performed at various levels of theory in order to locate all potential energy minima, i.e. all stable rotamers for **17**.

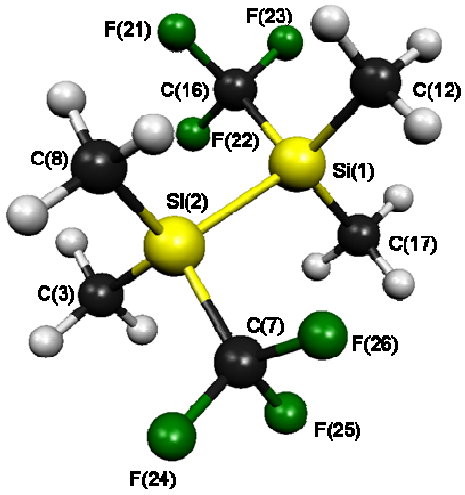

Figure 4.1.4: Atom labelling system of **17**.

By examining figure 4.1.5 which shows a compilation of the potential energy scans for different methods, it can be found that at the lowest level of theory used (HF/6-31G*) gives one energy minimum [C(16)-Si(1)-Si(2)-C(7) = 180°, corresponding to the anti position] with a further two possible minima being the gauche (τC(16)-Si(1)-Si(2)-C(7) = 55.7°) and *ortho* (τC(16)-Si(1)-Si(2)-C(7) = 101.1°) positions (see figure 4.1.4 for atomic labelling). The MP2 level of theory (6-31G*) gave three definite conformers at similar positions to the Hartree Fock level of theory, namely the gauche [τC(16)-Si(1)-Si(2)-C(7) = 55.7°], *ortho* [τC(16)-Si(1)-Si(2)-C(7) = 101.1°] and *anti* [τC(16)-Si(1)-Si(2)-C(7) = 170.9°]. This is in agreement with earlier documented results using similar levels of theory [134]. These three conformers, however, did not persist at higher levels of theory. MP2 (6-311G*) calculations predicted the near disappearance of the gauche minimum while at the MP2 (6-311+G*) level, both the gauche and ortho rotamers had vanished, leaving only the

anti [τC(16)-Si(1)-Si(2)-C(7) = 171.6°] minimum. To confirm these results MP2 calculations were performed using a double-ζ augmented basis set (aug-cc-pVDZ). These calculations also yielded only the anti conformer [τC(16)-Si(1)-Si(2)-C(7) = 170.0°]. Minor features were observed were the other two conformational minima used to be.

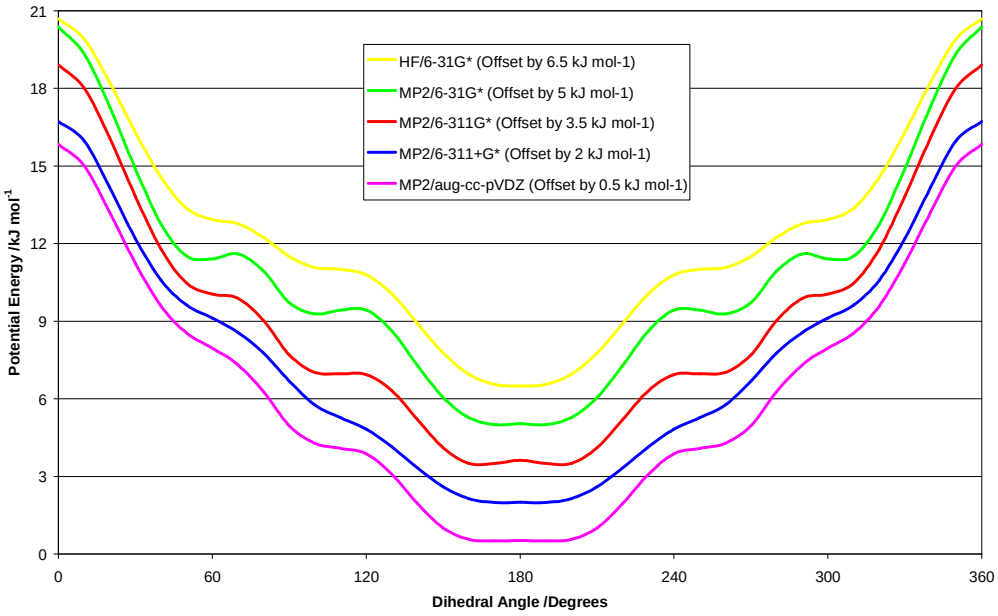

Figure 4.1.5: Compilation of the potential-energy scans of the C(16)-Si(1)-Si(2)-C(7) torsion angle of **17** using various levels of theory.

4.1.5 Gas electron diffraction (GED) analysis

Based on the results from the ab initio calculations, the assumption was made that only one real rotamer of **17** exits in the gaseous phase, that being the anti rotamer (calculated as having C_2-symmetry). Optimisation parameters obtained from the MP2 calculations were used to model the structure of the system, which was then used to perform the GED measurements of **17**. The experimental radial distribution curve and theoretical radial distribution function calculations for **17** can be seen in figure 4.1.6.

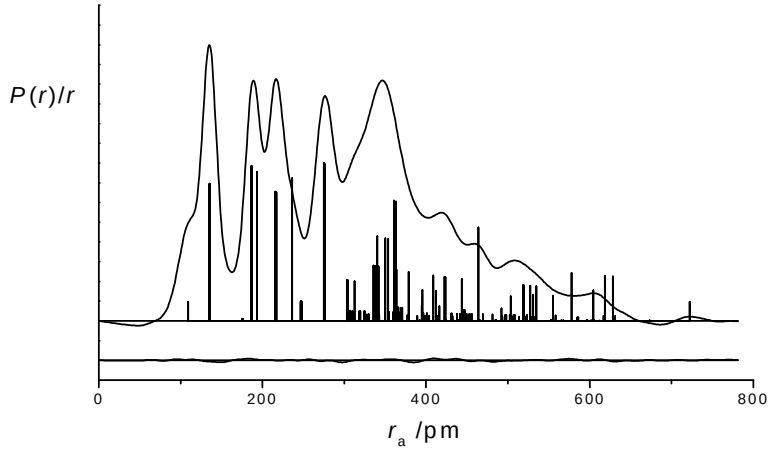

Figure 4.1.6: Experimental radial distribution curve functions and theoretical radial distribution function calculations for **17**, along with the difference between the experimental and theoretical data [143].

The results from the GED measurements supported the results obtained from the high level ab initio calculations of **17**, indicating that only the anti rotamer is present in the gaseous vapour of **17**. This is, however, in disagreement with the results from the temperature dependent Raman measurements of **17.**

4.1.6 Discussion

In the introduction to this chapter the known conformational properties of $ClMe_2Si\text{-}SiMe_2Cl$, the starting material for **17**, were presented. Its investigations indicate a mixture of two stable conformers gauche and anti, with the anti being favoured. It seems, however, that **17** behaves differently.

Earlier results for **17** predicted three non-equivalent enantiomeric rotamers of **17** (gauche, ortho and anti), by performing MP2/6-31G* potential-energy scans and variable-temperature Raman measurements [134]. Very recent high level calculations and experimental GED results, however, indicate the existence of only the anti rotamer [143]. New Raman measurements were therefore repeated for **17**, attaining both low and high temperature Raman spectra for neat liquid of **17** and for **17** in cyclopentane solution, again indicating a mixture of three rotamers of **17** in the liquid phase. Upon solidification the spectral band corresponding to the gauche and ortho rotamers disappeared completely (see figure 4.1.3), clearly demonstrating the preference for the anti conformer in the solid state of **17** [143]. This behaviour is similar to the surprising results for $^tBuCl_2Si\text{-}SiCl_2{}^tBu$ mentioned previously, as GED indicated only one conformer for the gaseous phase, despite calculations predicting three conformational minima [128,132,133]. Both $^tBuCl_2Si\text{-}SiCl_2{}^tBu$ and **17** are fairly heavily substituted and sterically hindered and this may explain the why only one conformer is conformationally viable in the gaseous phase.

Another possible explanation for this unfamiliar behaviour of **17** could be that in the liquid phase three rotamers do exist for **17**, with solvent effects stabilizing the three conformers. When going to the gaseous phase these rotamers may then collapse into the potential energy minima corresponding to the anti conformation. Presently both Onsager solvent shell calculations and X-ray crystal diffraction are being performed and those results will soon be available. The solvents calculation of **17** will hopefully elucidate whether these three rotamers are found at higher levels of theory (with sufficiently large basis sets) in solvent solution, along with providing further information about the backbone behaviour of this disilane.

DNMR analysis of **17** would be very interesting, as it would provide further information about what conformers of **17** exist in the liquid phase along with predicting the conformational population distributions of the observed conformers. The DNMR results would also allow a comparison with the results for **2** and **7**. Both of those systems exhibited a conformational change when going from the liquid phase to the gas phase, as seems to be the case for **17**. These three compounds all contain fairly bulky substitutents (CF_3 in both **2** and **17**, and SiH_3 in **7**). Results for **17** may allow us to understand whether this liquid/gas conformational change is due to size of the substituent or whether something else is at work. Unfortunately it is very likely that the rotational barrier of **17** is too low for DNMR to be viable (as discussed in the DNMR chapter).

5 Nitrogen and phosphorous containing silacyclohexane systems

5.1 Introduction

When attempting to synthesize the monosubstituted silacyclohexane 1-methylamine-1-silacyclohexane (**18**), there was also the possibility that bis(silacyclohexane)-methyl-amine (**19**) could be the product (see scheme 5.1.1). This ignited curiosity as to which product would be preferred, or whether a mixture would be observed.

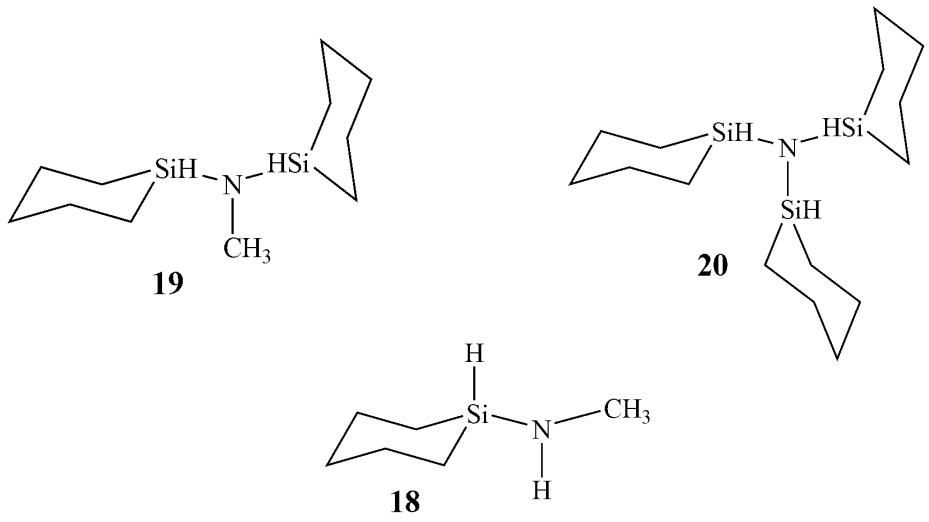

Scheme 5.1.1

It turned out, confirmed by ^{1}H, $^{13}C\{H\}$, and $^{29}Si\{H\}$ NMR spectroscopy, that only product **19** was formed. These results prompted our group to embark upon a different path of investigation, attempting to connect three silacyclohexanes rings to a nitrogen atom and synthesize tri(silacyclohexane)amine (**20**) as well (see scheme 5.1.2), by use of similar reaction conditions.

As mentioned earlier in chapter 3.3.2, compound **9** was successfully synthesized (see scheme 5.1.2) and an investigation of its conformational behaviour was a fruitful one.

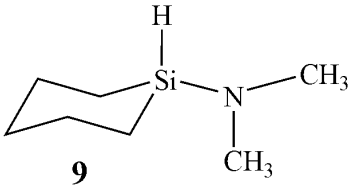

9

Scheme 5.1.2

This along with the potential method of synthesis shown above for the nitrogen containing silacyclohexane series, fuelled interest as to whether any member of the following analogous phosphorus series (**21**-**23**) could also be synthesized (see scheme 5.1.3).

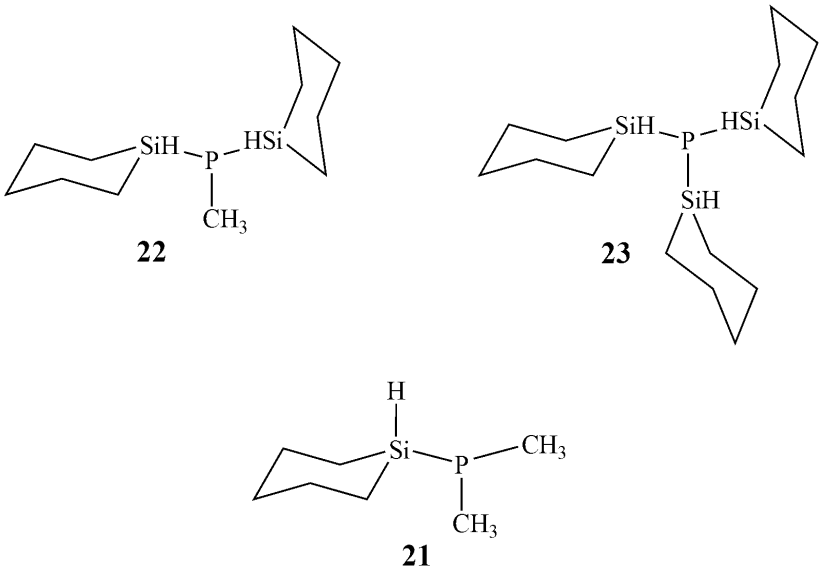

22 **23** **21**

Scheme 5.1.3

5.2 Synthesis of nitrogen containing silacyclohexane systems

Compound **19** was prepared under same reaction condition as **9** in slight variation to a standard preparation of $Et_2SiN(Me)_2$ and similar silanes [61]. Gaseous methylamine was condensed under vacuum into a reaction flask containing cyclohexane which was used as a solvent during the reaction. Chlorosilacyclohexane was then reacted with 2 equivalents of methylamine using a cooler maintained at –78 °C for 12 hours. This reaction is demonstrated in scheme 5.2.1 below.

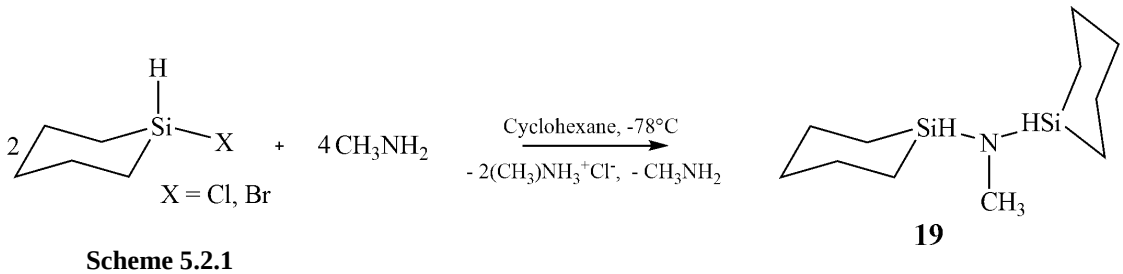

Scheme 5.2.1

In an attempt to synthesize **20**, the same reaction conditions as for the synthesis of **9** and **19** were used, where anhydrous gaseous ammonia was condensed under vacuum into a reaction flask containing cyclohexane. Chlorosilacyclohexane was then reacted with 3 equivalents of the ammonia using a cooler maintained at –78 °C for 12 hours. In scheme 5.2.2 the desired reaction can be seen:

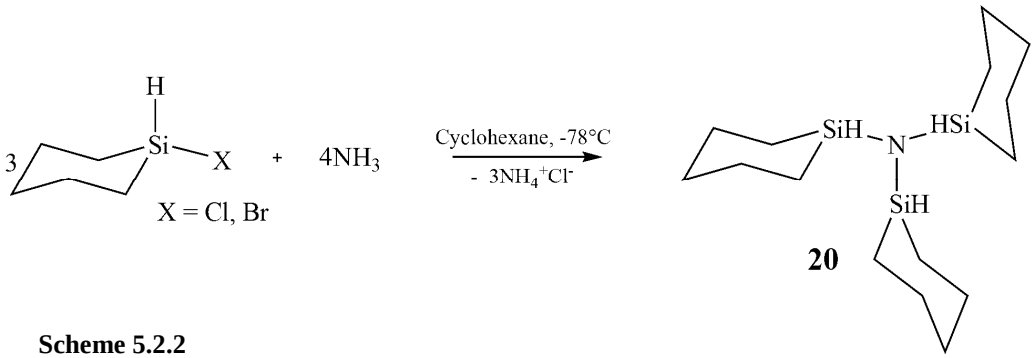

Scheme 5.2.2

It turned out that the ammonium nitrogen only formed two N-Si bonds, connecting two silacyclohexane groups instead of the desired three during the reaction, leading

to the formation of Bis(silacyclohexane)amine (**24**). The actual reaction that took place is demonstrated in scheme 5.2.3.

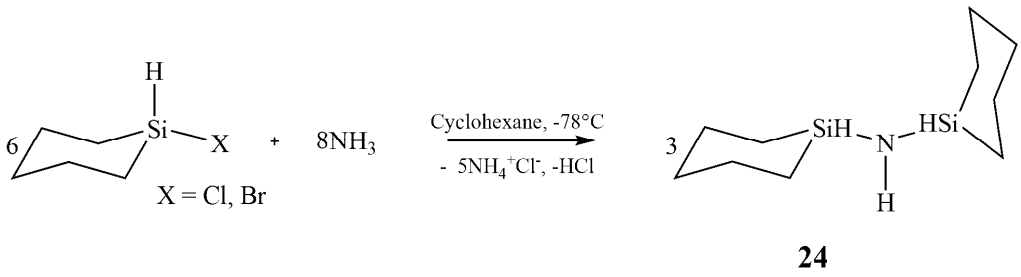

24

Scheme 5.2.3

A variation of the methods was then attempted in order to force the third silacyclohexane group upon the ammonia. That method involved anhydrous NH_3 gas being condensed into a ampule containing chlorosilacyclohexane. The ampule was at that point sealed off in vacuum and placed in a -84 °C cooling bath were it was allowed to stand for 24 hours and slowly warm up to room temperature. The ampule was then left untouched for two weeks before it was opened, to make sure that the reactants would have enough time to fully react. Even this didn't do the trick and analysis by means of ^{1}H, $^{13}C\{H\}$, and Si{H} NMR spectroscopy as well as MS measurements, again confirmed the formation of **24**.

5.3 An attempt to synthesize phosphorous containing silacyclohexane systems

An attempt was made to synthesize the monosubstituted silacyclohexane having dimethylphosphine as the substituent, namely compound **21**, to further add to our database of conformational behaviour of such systems. Compound **21** was the first attempt for the synthesis of any member of the phosphorous linking silacyclohexane series. Similar reaction conditions as for **9**, **19** and the former method used for **24** were applied, now having the reaction taking place under reduced pressure in order to avoid all unnecessary loss of the gaseous dimethylphosphine. In scheme 5.3.1 the desired reaction is shown.

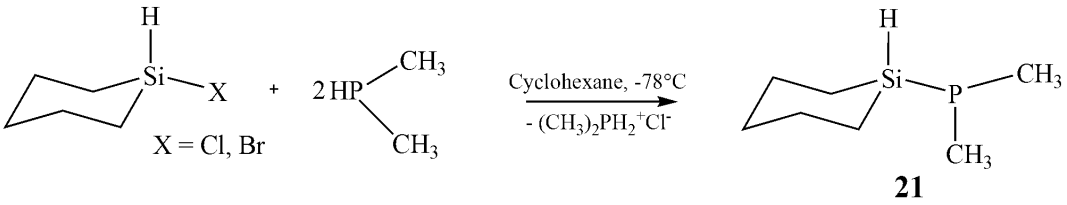

Scheme 5.3.1

Unfortunately it turned out that the silacyclohexane didn't react with the gaseous dimethylphosphine at all, giving no reaction product. No further attempts have been made so far in order to synthesize **21**, **22** and **23**, since no suitable method for these syntheses has yet been found.

5.4 Preliminary conformational investigations of 19

Preliminary QC calculations have been done on the three conformers that are predicted to be lowest in energy for **19**, namely the conformer with both the rings having the nitrogen in the axial position (ax-ax), the conformer with both the rings having the nitrogen in the equatorial position (eq-eq) and the conformer where the nitrogen atom is in the equatorial position for one ring but the axial position for the other ring [145]. These conformers can be seen in figure 5.4.1. The calculations were performed at the B3LYP/(6-31+G*) level of theory and the relative energies can be seen in table 5.4.1. According to these preliminary calculations the eq-eq conformer appears to be the most energetically stable. Obviously more extensive conformational analysis is needed.

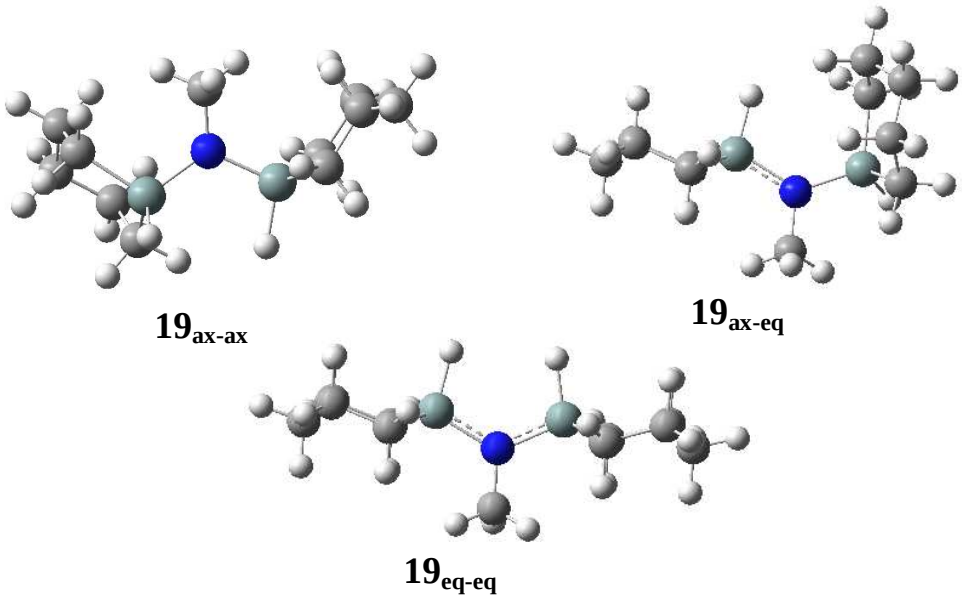

Figure 5.4.1: The calculated structures of the three conformers of **19** that are predicted to be lowest in energy.

Conformer	E_{rel} [kcal/mol]
eq-eq	0
ax-eq	1.4
ax-ax	2.6

Table 5.4.1: The relative energies of the predicted three main conformers of **19**, calculated using B3LYP (6-31+G*).

5.5 Discussion

Efforts were made to synthesize series of novel monosubstituted silacyclohexanes linked together by nitrogen and phosphorus.

The impetus for that work, ignited when compound **19** was formed when attempting the synthesis of **18**, using the same reaction condition as for previously described **9**. Attempts where then made to attach three silacyclohexane rings to a nitrogen atom to form **20**, but to little avail. However, the unexpected compound **24** was formed instead in all these attempts.

Conformational studies of **19** and **24** are a noteworthy challenge. It will be interesting to find out how many conformational states these systems possesses and to see how many of them will be populated under ambient condition. Samples of **19** and **24** intended for DNMR measurements, have been prepared for that purpose and will be measured in the near future. Furthermore, preliminary QC calculations for three potentially stable conformers of **19**, have been performed. More extensive theoretical investigations of **19** and **24** are needed, which will hopefully, along with the possible results from the prospective DNMR analysis, elucidate conformational properties of these novel systems.

Applying the same synthetic route as for **9**, **19** and **24**, in an attempt to form analogous phosphorus series, unfortunately gave no results.

6 Summary

6.1 Project overview

The main target of the present work was to synthesize a number of monosubstituted silacyclohexanes as well as a few 1,1-disubstituted silacyclohexanes, in order to further improve the understanding of the conformational behaviour of silicon containing ring systems. In this thesis the synthesis and the conformational analysis of four kinds of silicon containing systems have been addressed. This is outlined here below.

1. Monosubstituted silacyclohexanes; $C_5H_{10}SiHX$ with X = F, Cl, Br, I, SiH_3, OMe, $N(Me)_2$, ^tBu, CN and N_3 (**3-12**), were synthesized with the purpose of investigating their conformational properties by means of GED, DNMR and temperature dependent Raman spectroscopy.

2. The following 1,1-disubstituted silacyclohexane rings, $C_5H_{10}SiXY$ with X = Me and Y = F, X = Me and Y = CF_3 as well as X = SiF_3 and Y = F (**13**, **14** and **16**) were synthesized, so as to be investigated with respect to their conformational properties, using the same methods as described above. $C_5H_{10}SiXY$ with X = Me and Y = D (**15**) was synthesized in order to be investigated by Raman spectroscopy and to complete the investigation of $C_5H_{10}SiHMe$.

3. $CF_3Me_2Si\text{-}SiMe_2CF_3$ (**17**) was synthesized and its seemingly unusual conformational properties were investigated by GED, temperature dependent Raman spectroscopy and QC calculations.

4. The novel compounds $(C_5H_{10}SiH)_2NMe$ (**19**) and $(C_5H_{10}SiH)_2NH$ (**24**) were synthesized and the process of conformational analysis was initiated by performing preliminary QC calculations for **19**.

Not all the experimental measurements have been completed, nevertheless it is an ongoing project that will be finished in the not too distant future.

6.2 Results summary and discussion

6.2.1 Monosubstituted silacyclohexane systems

In this thesis it has been shown that monosubstituted silacyclohexanes do not follow the trends set by the corresponding cyclohexane derivatives. The *A* values for the monosubstituted silacyclohexanes were found to be substantially lower than for the corresponding cyclohexane analogues and in all cases except for one, they show a preference of the axial conformation. Interesting results are encountered for **7** in the liquid phase. DNMR and Raman seem to give conflicting results, as DNMR predicts a preference of the equatorial conformer while Raman ΔH values indicate that the axial conformer is energetically more stable. The same behaviour was also previously seen for **2** in the liquid phase. This indicates that entropic effects are playing a large part for both systems, but as of yet this has not been verified.

6.2.2 1,1-disubstituted silacyclohexane systems

A general trend was noticed that the methyl group preferred the equatorial position in all three of the methyl containing 1,1-disubstituted silacyclohexane systems as was expected from the previous findings of the behaviour of the methyl group in monosubstituted silacyclohexanes. The results for **13** and **14** indicate that the additive model described previously cannot be applied and more sophisticated model is required to predict the conformational behaviour of 1,1-disubstituted silacyclohexanes. The results for **14** indicate behaviour similar to what was previously seen for both **2** and **7**. DNMR predicts that the CF_3 substituent favours the equatorial position in the liquid phase, yet Raman shows that conformation to be energetically less favourable. As mentioned before, this points to the key role that entropic effects play in these systems but that has not yet been verified. CF_3 and SiH_3 are both comparatively large substituents and are likely to be able to rotate more freely in the equatorial position. This increased entropy may outweigh the energetic gain obtained in the more hindered axial position. Theoretical solvent calculations are required to study this further.

6.2.3 $CF_3Me_2SiSiMe_2CF_3$

The interesting backbone behaviour of the sterically strained disilane **17** was investigated. The results indicated that there is only one conformer in the gaseous phase, while three rotamers were observed in the liquid phase. These contrasting results for the liquid and gaseous phase were also observed for **2** and **7**. It remains to be seen whether this is due to the size of the substituent or whether this is purely down to solvent effects. Theoretical solvent calculations are being performed to help elucidate what is going on in the liquid phase of this system.

6.2.4 Nitrogen and phosphorous containing silacyclohexane systems

In this part of the present work, novel compounds **19** and **24** were made, where two silacyclohexane rings were linked together by a nitrogen atom. To date only preliminary CQ calculations have been performed for these compounds. However, more extensive conformational investigations by ^{13}C-DNMR and QC calculations will be performed in the near future. Further attempts were made to both force the third silacyclohexane ring upon the nitrogen and to form analogous a phosphorus series, without success.

7 Experimental procedures

7.1 General information

All syntheses were carried out in absence of oxygen and moisture under an inert atmosphere of nitrogen or argon, employing standard Schlenk techniques for all manipulations. All solvents were dried using appropriate drying agents and were continuously distilled prior to use. Et_2O, pentane and cyclohexane were dried by continuous distillation over sodium wire. Benzophenone was used to indicate the dryness of these solvents, as the product of these chemicals in the absence of air and water is a dark blue ketyl. For pentane, triglyme or diglyme was additionally added to increase the solubility of the benzophenone. CH_2Cl_2 was dried over CaH_2.

Na, $MeSiCl_3$, $HSiCl_3$, $Cl_3Si\text{-}SiCl_3$, $MgSO_4$, $LiAlD_4$, ZnI_2, Me_3SiI, PEG400, $NH_2(Me)$ and $NH(Me)_2$ were purchased from Aldrich, while $MeSiCl_3$, $Br(CH_2)_5Br$, $P(NEt_2)_3$, MeOH, $CDCl_3$, H_2SO_4, ^tBuLi and CD_2Cl_2 were obtained from Acros. Mg (shavings), $LiAlH_4$, $Cl(CH_2)_5Cl$, Et_3N, HF, SbF_3, PhBr, NaCN and NaN_3 were purchased from Merck. CF_3Br was purchased from Pfaltz & Bauer and $Cl(Me)_2Si\text{-}Si(Me)_2Cl$ was purchased from ABCR GmbH & Co. GK. HCl and HBr were purchased from Fluka and I_2 was purchased from BDH chemicals Ltd. The gaseous solvents $CHFCl_2$ and CHF_2Cl were purchased from Sigma-Aldrich. Other solvents were purchased either from Sigma-Aldrich (pentane and ethylacetate), Acros (diglyme and triglyme), Merck (CH_2Cl_2) or Fluka (Et_2O). If not otherwise stated, chemical substances were used as purchased from the commercial sources. Chemical substances used as starting materials were prepared following procedures found in literature (see the respective chapters).

Whenever chlorosilacyclohexane and chloromethylsilacyclohexane were used as the starting materials, they typically contained up to 30% of the respective bromo derivatives as reported in their synthesis chapters. In the following experimental descriptions these substance mixtures will, however, be referred to as chlorosilacyclohexane and chloromethylsilacyclohexane.

7.2 Experimental

Chlorosilacyclohexane: $Br(CH_2)_5Br$ (126.5 g, 550.1 mmol) disolved in Et_2O (300-400 mL) was added in a dropwise manner to a solution of Mg (29.4 g, 1210.3 mmol) and Et_2O (80-100 mL). After the complete addition, the reaction mixture was boiled for two hours and then stirred overnight. The di-Grignard $BrMg(CH_2)_5MgBr$ was filtered with glass wool into a dropping funnel and then slowly added to a solution of Cl_3SiH (72.7 g, 536.4 mmol) and Et_2O (300-400 mL), while stirring at 0 C°. A lot of white reaction salt was formed during the reaction. After stirring overnight, the Et_2O was distilled off the reaction mixture and replaced by pentane. The reaction mixture was then filtered under nitrogen and the salt was discarded. Distillation of the reaction mixture at 123-136 °C and 1 atm, yielded 48.2 g of chlorosilacyclohexane with ~ 10-30% impurities of partly brominated products.

Chloromethylsilacyclohexane: $Br(CH_2)_5Br$ (126.5 g, 550.1 mmol) disolved in Et_2O (300-400 mL) was added in a dropwise manner to a solution of Mg (29.4 g, 1210.3 mmol) and Et_2O (80-100 mL). After the complete addition, the reaction mixture was boiled for two hours and then stirred overnight. The di-Grignard $BrMg(CH_2)_5MgBr$ was filtered with glass wool into a dropping funnel and then slowly added to a solution of Cl_3SiMe (80.2 g, 536.4 mmol) and Et_2O (300-400 mL), while stirring at 0 C°. A lot of white reaction salt was formed during the reaction. After stirring overnight, the Et_2O was distilled off the reaction mixture and replaced by pentane. The reaction mixture was then filtered under nitrogen and the salt was discarded. Distillation of the reaction mixture at 137-157 °C and 1 atm yielded, 55.6 g of chloromethylsilacyclohexane with ~ 10-30% impurities of partly brominated products.

1-Fluoro-1-silacyclohexane (3). 40% HF (8 g, 160 mmol) was slowly added to chlorosilacyclohexane (21.5 g, 160 mmol) at –30 °C. The reaction mixture was allowed to stand in the cooling bath and warm up slowly to room temperature. Afterwards it was transferred to a separation funnel, the aqueous phase was discarded and the organic layer was dried over $MgSO_4$. The desired product was collected by distillation under reduced pressure (54 °C, 180 Torr) as a colourless liquid, found to

be analytically pure by NMR spectroscopy. Yield: 5.56 g (47.0 mmol, 29%). ^{1}H NMR (400 MHz, $CDCl_3$): δ= 0.77–0.83 (m, 2H, $CH_{2(ax/eq)}$), 0.87–0.97 (m, 2H, $CH_{2(ax/eq)}$), 1.37–1.54 (m, 2H, CH_2), 1.67–1.84 (m, 4H, CH_2), 4.81 (d, $^{2}J_{H–F}$ = 54 Hz, 1H, SiH). ^{13}C{^{1}H} NMR (101 MHz, $CDCl_3$): δ= 13.2 (d, $^{2}J_{F–C}$ = 11.1 Hz), 23.2 (d, $^{3}J_{F–C}$ = 1.0 Hz), 29.2. ^{19}F NMR (376 MHz, $CDCl_3$): δ= –180.8 (dtm, $^{2}J_{H-F}$ = 54 Hz, $^{3}J_{H–F}$ = 11.1 Hz, $^{1}J_{Si–F}$ = 290 Hz). ^{29}Si NMR (79 MHz, $CDCl_3$): δ= 13.9 (d, $^{1}J_{Si–F}$ = 290 Hz). MS (EI, 70 eV): *m/z* (%) 118 (20) [M^+], 99 (100) [M^+ –F].

1-Phenyl-1-silacyclohexane: PhMgBr (14.9 g, 82.0 mmol) was slowly added to chlorosilacyclohexane (10.0 g, 74.0 mmol) dissolved in Et_2O (90 mL), while stirring at 0 °C. The diethylether was distilled off the reaction mixture and replaced by pentane. The reaction mixture was then filtered under nitrogen and reduced pressure and the salt was discarded. Distillation of the reaction mixture under reduced pressure (112-115 °C, 25 Torr) yielded 12.42 g (70.0 mmol, 95%) of pure 1-phenyl-1-silacyclohexane.

1-Chloro-1-silacyclohexane (4) method 1: Anhydrous HCl (2.4 g, 66.0 mmol) was condensed into a 100 mL ampule containing 1-phenyl-1-silacyclohexane (10.5 g, 60.0 mmol) and the ampule was then sealed off in vacuum. The ampule was inserted in a –78 °C cooling bath (methanol/dry ice bath). Dry Ice was added to the cooling bath on a regular basis for the next two days. The content of the ampule was then allowed to stand in the cooling bath and slowly warm up to room temperature. After opening the ampule, all volatile components were condensed on a N_2(l) cooled finger. The desired product was collected (after the benzene by-product had been removed) by distillation under nitrogen at 120-122 °C (4.68 g, 58%) as a colourless liquid. The product was purified further using preparative GC. Analytically pure colourless liquid was attained, confirmed by NMR spectroscopy. ^{1}H NMR (400 MHz, $CDCl_3$): δ= 0.94–1.06 (m, 2H, CH_2), 1.32–1.42 (m, 1H, $CH_{2(ax/eq)}$), 1.52–1.60 (m, 1H, $CH_{2(ax/eq)}$), 1.72–1.85 (m, 4H, CH_2), 4.85-4.87 (m, 1H, SiH). ^{13}C{^{1}H} NMR (101 MHz, $CDCl_3$): δ= 14.8, 23.1, 29.0. ^{29}Si NMR (79 MHz, $CDCl_3$): δ= 7.9. MS (EI, 70 eV): *m/z* (%) 134 (90), 106 (100), 63 (76); HRMS: *m/z* calcd for $C_5H_{11}SiCl$(35) 134.0319, found 134.0312.

1-Chloro-1-silacyclohexane (4) method 2: $ClMg(CH_2)_5MgCl$ (15.6 g, 82.0 mmol) was slowly added to trichlorosilane (10.0 g, 74.3 mmol) dissolved in Et_2O (90 mL), while stirring at 0 °C. A lot of white reaction salt was formed during the reaction. The dietylether was distilled off the reaction mixture and replaced by pentane. The reaction mixture was then filtered under nitrogen and reduced pressure and the salt was discarded. Distillation of the reaction mixture under nitrogen (120-122 °C), yielded 1.60 g (11.9 mmol, 16%) of 1-chloro-1-silacyclohexane.^{1}H NMR (400 MHz, $CDCl_3$): δ = 0.94–1.06 (m, 2H, CH_2), 1.32–1.42 (m, 1H, $CH_{2(ax/eq)}$), 1.52–1.60 (m, 1H, $CH_{2(ax/eq)}$), 1.72–1.85 (m, 4H, CH_2), 4.85-4.87 (m, 1H, SiH). $^{13}C\{^1H\}$ NMR (101 MHz, $CDCl_3$): δ = 14.8, 23.1, 29.0. ^{29}Si NMR (79 MHz, $CDCl_3$): δ = 7.9.

1-Bromo-1-silacyclohexane (5): Anhydrous HBr (5.3 g, 66.0 mmol) was condensed into a 100 mL ampule containing 1-phenyl-1-silacyclohexane (10.5 g, 60.0 mmol) and the ampule was then sealed off in vacuum. The ampule was inserted in a –78 °C cooling bath (methanol/dry ice bath). Dry Ice was added to the cooling bath on a regular basis for the next two days. The content of the ampule was then allowed to stand in the cooling bath and slowly warm up to room temperature. After opening the ampule, all volatile components were condensed on a N_2(l) cooled finger. The desired product was collected (after the benzene by-product had been removed) by distillation under nitrogen at 138-140 °C (7.78 g, 72%) as a colourless liquid. The product was purified further using preparative GC. Analytically pure colourless liquid was attained, confirmed by NMR spectroscopy. ^{1}H NMR (400 MHz, $CDCl_3$): δ = 1.06–1.18 (m, 4H, CH_2), 1.33–1.43 (m, 1H, $CH_{2(ax/eq)}$), 1.54–1.62 (m, 1H, $CH_{2(ax/eq)}$), 1.72–1.87 (m, 4H, CH_2), 4.84-4.86 (m, 1H, SiH). $^{13}C\{^1H\}$ NMR (101 MHz, $CDCl_3$): δ: = 14.7, 23.3, 29.0. ^{29}Si NMR (79 MHz, $CDCl_3$): δ = -21.9. MS (EI, 70 eV): *m*/*z* (%) 178 (79), 150 (100), 109 (54); HRMS: *m/z* calcd for $C_5H_{11}SiBr(79)$ 177.9813, found 177.9845.

1-Iodo-1-silacyclohexane (6). Iodotrimethylsilane (13.9 g, 69.4 mmol) was slowly added to a solution of chlorosilacyclohexane (8.5 g, 63.1 mol) in CH_2Cl_2 (220 mL) under vigorous stirring. After complete addition, the reaction mixture was stirred for three days, following a filtration of the reaction salt under nitrogen and reduced pressure. The salt was then discarded and the desired product was collected (after

CH_2Cl_2 had been removed) by distillation under nitrogen at 108-110 °C and 50 Torr (8.10 g, 35.8 mmol, 57%) as a colourless liquid, found to be analytically pure by NMR spectroscopy. ^{1}H NMR (400 MHz, $CDCl_3$): δ = 1.16–1.24 (m, 2H, $CH_{2(ax/eq)}$), 1.26–1.36 (m, 2H, $CH_{2(ax/eq)}$), 1.37–1.45 (m, 1H, $CH_{2(ax/eq)}$), 1.54–1.64 (m, 1H, $CH_{2(ax/eq)}$), 1.68–1.78 (m, 2H, CH_2), 1.79–1.88 (m, 2H, CH_2), 4.80 (s, $^1J_{H–Si}$ = 224.3 Hz, 1H, SiH). ^{13}C{^{1}H} NMR (101 MHz, $CDCl_3$): δ = 14.2, 23.7, 28.9. ^{29}Si{^{1}H} NMR (79 MHz, $CDCl_3$): δ = -16.0.

1-Chloro-1-trichlorosilyl-1-silacyclohexane: $Br(CH_2)_5Br$ (23.5 g, 102.3 mmol) disolved in Et_2O (180 mL) was added in a dropwise manner to a solution of Mg (5.7 g, 235.2 mmol) and Et_2O (50 mL). After the complete addition, the reaction mixture was boiled for two hours and then stirred overnight. The di-Grignard $BrMg(CH_2)_5MgBr$ was filtered with glass wool into a dropping funnel and then slowly added to a solution of Cl_3Si-$SiCl_3$ (25.0 g, 93.0 mmol) and Et_2O (100 mL), while stirring at 0 C°. A lot of grey reaction salt was formed during the reaction. After stirring overnight, the Et_2O was distilled off the reaction mixture and replaced by pentane. The reaction mixture was then filtered under nitrogen and the salt was discarded. Distillation of the reaction mixture under reduced pressure (110-111 °C, 5 Torr) yielded 17.60 g (65.6 mmol, 71%) of 1-chloro-1-trichlorosilyl-1-silacyclohexane with ~ 25-30% impurities of partly brominated products.

1-Silyl-1-silacyclohexane (7): 1-Chloro-1-trichlorosilyl-1-silacyclohexane (12.8 g, 47.7 mmol) dissolved in Et_2O (60 mL) was slowly added to a solution of $LiAlH_4$ (2.1 g, 54.9 mmol) and Et_2O (80 mL) while stirring at 0 °C. After boiling for 12 hours most of the Et_2O was removed from the solution and replaced by pentane. The reaction mixture was filtered under nitrogen and reduced pressure and the salt was discarded. All volatile components were then condensed on a N_2(l) cooled finger. The desired product was collected by distillation at 131-132° C and 500 Torr. Further purification was achieved by preparative GC, attaining an analytically pure colourless liquid confirmed by NMR spectroscopy. Yield: 3.84 g (29.5 mmol, 60%). ^{1}H NMR (400 MHz, $CDCl_3$): δ = 0.76–0.84 (m, 2H, $CH_{2(ax/eq)}$), 0.93–1.00 (m, 2H, $CH_{2(ax/eq)}$), 1.39–1.52 (m, 2H, CH_2), 1.68–1.82 (m, 4H, CH_2), 3.09 (d, 3H, $^3J_{H–H}$ = 3.0 Hz, $^1J_{Si–H}$ = 187 Hz, SiH_3), 3.91-3,95 (m, 1H, SiH). ^{13}C{^{1}H} NMR (101 MHz,

$CDCl_3$): δ = 9.6, 25.6, 29.6 (CH_2). $^{29}Si\{^1H\}$ NMR (79 MHz, $CDCl_3$): δ = -19.9 (s, SiH), -102.0 (s, $^1J_{Si–Si}$ = 77 Hz, SiH_3). MS (EI, 70 eV): *m/z* (%) 130 (22), 116 (35), 72 (100); HRMS: *m/z* calcd for $C_5H_{14}Si_2$ 130.0634, found 130.0627.

1-Metoxy-1-silacyclohexane (8): Solution of triethylamine (30.0 g, 297.1 mmol), methanol (9.5 g, 297.1 mmol) and Et_2O (120 mL) was slowly added to chlorosilacyclohexane (20.0 g, 148.5 mmol) dissolved in Et_2O (400 mL) while stirring. After continued stirring overnight, the reaction mixture was filtered under nitrogen and reduced pressure and the salt was discarded. The solvents were then distilled off and the product was collected at 115 –117 °C and 1 atm. Yield: 15.37 g (118 mmol, 79%). ^1H NMR (400 MHz, $CDCl_3$): δ = 0.77–0.81 (m, 4H, CH_2), 1.32–1.49 (m, 2H, $CH_{2(ax/eq)}$), 1.56–1.65 (m, 2H, $CH_{2(ax/eq)}$), 1.73–1.83 (m, 4H, CH_2), 3.49 (s, 3H OMe), 4.50–4.51 (m, 1H, $^1J_{Si–H}$ = 197 Hz, SiH). $^{13}C\{^1H\}$ NMR (101 MHz, $CDCl_3$): δ = 12.4, 23.7, 29.5 (CH_2), 51.8 (OMe). ^{29}Si NMR (79 MHz, $CDCl_3$): δ = 4.3 (dq, $^1J_{Si–H}$ = 197 Hz). MS (EI, 70 eV): *m/z* (%) 129 (100), 102.1 (64); HRMS: *m/z* calcd for $C_6H_{14}OSi$ 130.0814, found 130.0799.

1-Dimethylamine-1-silacyclohexane (9): $(Me)_2NH$ (19.1 g, 423.7 mmol) was condensed into a reaction flask containing cyclohexane (140 mL). The reaction flask was equipped with dry ice/ethylacetate cooler and a dropping funnel containing chlorosilacyclohexane (15.0 g, 111.4 mmol) which was slowly added to the solution under stirring. The dry ice/ethylacetate cooler was maintained at –78 °C for 12 hours. After the complete addition the reaction mixture was boiled for about 5 hours, still having the dry ice/ethylacetate cooler to minimize the loss of dimethylamine. The solution was stirred further overnight, while the dry ice/ethylacetate cooling bath slowly warmed up to room temperature. The reaction mixture was then filtered under nitrogen and reduced pressure and the salt was discarded. The desired product was collected (after the cyclohexane had been removed) by distillation under nitrogen at 144-146 °C (10.97g, 76.6 mmol, 69%) as a colourless liquid. Analytically pure liquid was attained, confirmed by NMR spectroscopy. ^1H NMR (400 MHz, $CDCl_3$): δ = 0.62–0.71 (m, 2H, $CH_{2(ax/eq)}$), 0.79–0.85 (m, 2H, $CH_{2(ax/eq)}$), 1.18–1.31 (m, 1H, $CH_{2(ax/eq)}$), 1.45–1.50 (m, 1H, $CH_{2(ax/eq)}$), 1.51–1.57 (m, 2H, $CH_{2(ax/eq)}$), 2.48 (s, 6H, $N(CH_3)_2$), 4,22 (t, 1H, $^3J_{H-H}$ = 4.7 Hz, $^1J_{Si-H}$ = 191 Hz, SiH). $^{13}C\{^1H\}$ NMR (101

MHz, $CDCl_3$): δ = 11.9, 24.4, 29.8 (CH_2), 38,6 ($N(CH_3)_2$). ^{29}Si NMR (79 MHz, $CDCl_3$): δ = -5.2 (dm, $^1J_{Si\text{-}H}$ = 191 Hz). MS (EI, 70 eV): *m/z* (%) 143 (100), 72 (71); HRMS: *m/z* calcd for $C_7H_{17}NSi$ 143.1130, found 143.1148.

1-Tertbuthyl-1-silacyclohexane (10). Solution of ^{t}BuLi in pentane (60 mL, 90.0 mmol) was slowly added to chlorosilacyclohexane (11.5 g, 85.4 mmol) dissolved in Et_2O (130 mL) at –78 °C (dry ice cooling bath) under stirring. The reaction mixture was allowed to stand in the cooling bath and slowly warm up to room temperature and was then additionally stirred for 12 hours. The ether was distilled off the reaction mixture and replaced by pentane (150-200 mL). The solution was filtered under nitrogen and the reaction salt (after being washed with pentane) was discarded. The desired product was collected by distillation at 125-126 °C and 1 atm, as a colourless liquid, found to be analytically pure by NMR spectroscopy. Yield: 10.33 g (66.1 mmol, 77%). ^1H NMR (400 MHz, $CDCl_3$): δ = 0.51–0.61 (m, 2H, $CH_{2(ax/eq)}$), 0.85–0.88 (m, 1H, $CH_{2(ax/eq)}$), 0.89–0.92 (m, 1H, $CH_{2(ax/eq)}$), 0.97 (s, 9H, $C(CH_3)_3$), 1.12–1.24 (m, 1H, $CH_{2(ax/eq)}$), 1.44–1.55 (m, 2H, CH_2), 1.65–1.73 m, 1H, $CH_{2(ax/eq)}$), 1.97–2.05 (m, 2H, CH_2), 3.59 (tt, $^3J_{H–H}$ = 6.6 Hz, $^3J_{H–H}$ = 1.5 Hz, $^1J_{Si–H}$ = 177 Hz, 1H, SiH). $^{13}C\{^1H\}$ NMR (101 MHz, $CDCl_3$): δ = 8.0, 15.9 ($C(CH_3)_3$), 25.1, 27.1 ($C(CH_3)_3$), 29.9. $^{29}Si\{^1H\}$ NMR (79 MHz, $CDCl_3$): δ = -0.6.

1-Cyano-1-silacyclohexane (11). Sodium cyanide (6.1 g, 123.9 mmol) was dried by continuous heating under vacuum for 24 hours and was then added to a stirred mixture of zinc iodide (0.17 g, 0.5 mmol), polyethylene glycol (1.4 g) and chlorosilacyclohexane (13.9 g, 103.2 mmol) dissolved in CH_2Cl_2 (35 mL). After vigorous stirring for 24 hours, the reaction mixture was filtered under nitrogen and reduced pressure and the salt was discarded. The solvent was then removed from the reaction mixture and the desired product was collected by distillation under nitrogen at 152-153 °C and 1 atm (9.06 g, 72.3 mmol, 70%). Analytically pure liquid was attained, confirmed by NMR spectroscopy. ^1H NMR (400 MHz, $CDCl_3$): δ = 0.82–0.90 (m, 2H, $CH_{2(ax/eq)}$), 1.01–1.09 (m, 2H, $CH_{2(ax/eq)}$), 1.24–1.34 (m, 1H, $CH_{2(ax/eq)}$), 1.59–1.67 (m, 1H, $CH_{2(ax/eq)}$), 1.68–1.79 (m, 2H, CH_2), 1.85–1.95 (m, 2H, CH_2), 4.20-4.22 (m, $^1J_{H–Si}$ = 222 Hz, 1H, SiH). $^{13}C\{^1H\}$ NMR (101 MHz, $CDCl_3$): δ = 8.5, 23.6, 28.6, 124.1 (CN). $^{29}Si\{^1H\}$ NMR (79 MHz, $CDCl_3$): δ = -36.1.

1-Azide-1-silacyclohexane (12). Sodium azide (3.5 g, 53.5 mmol) was dried by continuous heating under vacuum for 24 hours and was then added to a stirred mixture of zinc iodide (0.07 g, 0.2 mmol), polyethylene glycol (0.6 g) and chlorosilacyclohexane (6.0 g, 44.6 mmol) dissolved in CH_2Cl_2 (25 mL). After stirring of the reaction mixture for one week, the reaction mixture was filtered under nitrogen and reduced pressure and the salt was discarded. The solvent was then removed from the reaction mixture and the desired product was collected by distillation under nitrogen at 79-80 °C and 23 Torr (4.01 g, 28.4 mmol, 64%) as a colourless liquid. ^{1}H NMR (400 MHz, $CDCl_3$): δ = 0.81–0.89 (m, 2H, $CH_{2(ax/eq)}$), 0.92–0.99 (m, 2H, $CH_{2(ax/eq)}$), 1.33–1.43 (m, 1H, $CH_{2(ax/eq)}$), 1.45–1.58 (m, 1H, $CH_{2(ax/eq)}$), 1.68–1.83 (m, 4H, CH_2), 4.61 (m, $^1J_{H–Si}$ = 216 Hz, 1H, SiH). ^{13}C{^{1}H} NMR (101 MHz, $CDCl_3$): δ= 11.7, 23.4, 29.0. ^{29}Si{^{1}H} NMR (79 MHz, $CDCl_3$): δ= -4.0.

1-Fluoro-1-methyl-1-silacyclohexane (13): Antimony trifluoride (2.2 g, 12.2 mmol) was dried by continuous heating under vacuum for three days prior to use and was then transferred into a 70 mL Schlenk tube containing chloromethylsilacyclohexane (3.7 g, 25.2 mmol). The reaction mixture was stirred at 0 °C for a couple of hours, with the solution soon turning red and then dark brown. The ice bath was allowed to melt and warm up to room temperature and the solution was stirred overnight. The product was then condensed into a trap held at –196 K, as a colourless liquid. Further purification was achieved by the use of preparative GC, attaining an analytically pure substance. Yield: 2.99 g (22.6 mmol, 90%). ^{1}H NMR (400 MHz, $CDCl_3$). δ = 0.22 (d, $^3J_{H–F}$ = 7.4 Hz, 3H, CH_3), 0.58–0.68 (m, 2H, $CH_{2(ax/eq)}$), 0.83–0.90 (m, 2H, $CH_{2(ax/eq)}$), 1.30–1.39 (m, 1H, $CH_{2(ax/eq)}$, 1.47–1.56 (m, 1H, $CH_{2(ax/eq)}$, 1.68–1.76 (m, 4H, CH_2). ^{13}C{^{1}H} NMR (101 MHz, $CDCl_3$): δ = -2.6 (d, CH_3, $^2J_{F–C}$ = 14.8 Hz), 14.6 (d, CH_2, $^2J_{F–C}$ = 12.7 Hz), 24.0, 29.5 (CH_2); ^{19}F NMR (376 MHz, $CDCl_3$): δ = –168.4 - (-168.5) (m, $^3J_{H–F}$ = 7.4 Hz, $^1J_{Si–F}$ = 286 Hz). ^{29}Si{^{1}H} NMR (79 MHz, $CDCl_3$): δ= 27.5 (d, $^1J_{Si–F}$ = 286 Hz). MS (EI, 70 eV): *m*/*z* (%) 132 (100), 89 (98).

1-Trifluoromethyl-1-methyl-1-silacyclohexane (14): CF_3Br (13.2 g, 88.9 mmol) was condensed into a reaction flask containing chloromethylsilacyclohexane (10.0 g, 67.3 mmol) and CH_2Cl_2 (30 mL). A –78 °C cooling bath (acetone/dry ice bath) was placed under the reaction system and when the content of the flask had reached the

temperature of the bath, a solution of $P(NEt_2)_3$ (16.6 g, 67.3 mmol) in CH_2Cl_2 (20 mL) was slowly added while stirring. The cooling bath was removed and after continued stirring at room temperature overnight, the colourless solution had turned orange. All volatile components were then condensed on a N_2(l) cooled finger. The solvent was distilled off and the product was collected by distillation under nitrogen at 129.5-130.0 °C. Yield: 8.92 g, 73 %. ^{1}H NMR (400 MHz, $CDCl_3$): δ = 0.25 (s, 3H, CH_3), 0.66–0.73 (m, 2H, $CH_{2(ax/eq)}$), 0.97–1.03 (m, 2H, $CH_{2(ax/eq)}$), 1.28–1.38 (m, 1H, $CH_{2(ax/eq)}$), 1.51–1.60 (m, 1H, $CH_{2(ax/eq)}$), 1.67–1.83 (m, 4H, CH_2). ^{13}C{^{1}H} NMR (101 MHz, $CDCl_3$): δ = -7.1 (d, CH_3, $^3J_{F–C}$ = 1.3 Hz), 9.3 (d, CH_2, $^3J_{F–C}$ = 1.3 Hz), 23.5, 29.1 (CH_2), 131.9 (q, CF_3, $^1J_{C-F}$ = 323 Hz). ^{19}F NMR (376 MHz, $CDCl_3$): δ = –65.4 (s, $^2J_{Si–F}$ = 36 Hz). ^{29}Si{^{1}H} NMR (79 MHz, $CDCl_3$): δ = -1.5 (d, $^2J_{Si–F}$ = 36 Hz). MS (EI, 70 eV): *m/z* (%) 182 (3), 113 (100), 85 (100). HRMS: *m/z* calcd for $C_6H_{13}Si$ (M – CF_3) 113.0787, found 113.0769.

1-Deuterium-1-methyl-silacyclohexane (15): Solution of chloromethylsilacyclohexane (11.9 g, 80.3 mmol) and diethylether (180 mL) was slowly added to a solution of $LiAlD_4$ (1.0 g, 23.9 mmol) and diethylether (250 mL) while stirring at 0 °C. After boiling for 12 hours most of the diethylether was removed from the solution and replaced by pentane. The reaction mixture was then filtered under nitrogen and reduced pressure and the salt was discarded. The solvents were then distilled off and the product was collected at 105.6 –106.0 °C and 1 atm. Yield: 4.7 g (31.4 mmol, 40%).

^{1}H NMR (400 MHz, $CDCl_3$): δ = 0.09 (s, 3H, CH_3), 0.51–0.58 (m, 2H, $CH_{2(ax/eq)}$), 0.78–0.85 (m, 2H, $CH_{2(ax/eq)}$), 1.27–1.38 (m, 1H, $CH_{2(ax/eq)}$), 1.44–1.53 (m, 1H, $CH_{2(ax/eq)}$), 1.56–1.66 (m, 2H, CH_2), 1.71–1.81 (m, 2H, CH_2). ^{13}C{^{1}H} NMR (101 MHz, $CDCl_3$): δ = -5.7, 11.6, 24.8, 29.9. ^{29}Si{^{1}H} NMR (79 MHz, $CDCl_3$): δ = -17.2 (t, $^1J_{Si-D}$ = 28 Hz)

1-Fluoro-1-trifluorosilyl-1-silacyclohexane (16): Antimony trifluoride SbF_3 (9.2 g, 51.5 mmol) was dried by continuous heating under vacuum for three days prior to use in an 100 mL ampule. 1-Chloro-1-trichlorosilyl-1-silacyclohexane (9.5 g, 35.5 mmol) was then transferred into the SbF_3 containing ampule and the reaction mixture was stirred at 0 °C for couple of hours. Soon after the mixing of the reactants, the

solution turned dark grey (almost black). The ice bath was allowed to melt and warm up to a room temperature and the solution was stirred overnight. The product was then condensed on a N_2(l) cooled finger, leaving the $SbCl_3$ reaction salt and the unreacted SbF_3 behind in the reaction ampule. The condensation of the reaction mixture was repeated a couple of times. However, at present the product still needs to be purified further. ^{1}H NMR (400 MHz, $CDCl_3$): δ = 1.10–1.15 (m, 4H, CH_2), 1.39–1.49 (m, 1H, $CH_{2(ax/eq)}$), 1.51–1.60 ((m, 1H, $CH_{2(ax/eq)}$), 1.64–1.81 (m, 2H, CH_2), 1.87–1.97 (m, 2H, CH_2). ^{13}C{^{1}H} NMR (101 MHz, $CDCl_3$): δ = 14.1 (dq, $^2J_{F–C}$ = 8.7 Hz, $^3J_{F–C}$ = 2.8 Hz), 22.8 (d, $^3J_{F–C}$ = 1.5 Hz), 28.5. ^{19}F NMR (376 MHz, $CDCl_3$): δ = –121.6 (d, $^3J_{F–F}$ = 9.7 Hz, $^1J_{Si–F}$ = 372 Hz, SiF_3), the other signal still hasn't been found. ^{29}Si{^{1}H} NMR (79 MHz, $CDCl_3$): δ = -62.7 (qd, $^1J_{Si–F}$ = 372 Hz, $^2J_{Si–F}$ = 56 Hz), the other signal still hasn't been found.

1,2-Bis(trifluoromethyl)-1,1,2,2-tetramethyl-disilane (17): CF_3Br (25.1 g, 168.3 mmol) was condensed into a reaction flask containing $ClMe_2Si$-$SiMe_2Cl$ (15.0 g, 80.1 mmol) and CH_2Cl_2 (40 mL). A –78 °C cooling bath (acetone/dry ice bath) was placed under the reaction system and when the content of the flask had reached the bath temperature, a solution of $P(NEt_2)_3$ (39.6 g, 160.3 mmol) in CH_2Cl_2 (30 mL) was added slowly under stirring. The cooling bath was removed and after continued stirring at room temperature overnight, the colourless solution had turned orange. All volatile components were then condensed into a trap held at –196 °C. The solvent was then distilled off and the product was collected by distillation under nitrogen at 129-130 °C. Yield: 8.83 g, 44 % (colourless semi solid at room temperature); ^{1}H NMR (400 MHz, $CDCl_3$, 25 °C, TMS): δ = 0.43 (s, 12 H, CH_3). ^{13}C{^{1}H} NMR (101 MHz, $CDCl_3$, 25 °C, TMS): δ = -7.4 (s, CH_3), 132.1 (q, CF_3, $^1J_{C-F}$ = 322 Hz). ^{19}F NMR (376 MHz, $CDCl_3$, 25°C, $CFCl_3$): δ = -61.6 (s, $^2J_{Si-F}$ = 38 Hz). ^{29}Si{^{1}H} NMR (79 MHz, $CDCl_3$, 25 °C, TMS): δ = -13.0 (qq, $^2J_{Si-F}$ = 38 Hz, $^3J_{Si-F}$ = 3.0 Hz).

Bis(1-silacyclohexane)-methyl-amine (19): $(CH_3)NH_2$ (6.9 g, 222.8 mmol) was condensed into a reaction flask containing cyclohexane (130 mL), equipped with a cooler system. A Dry ice/ethylacetate mixture was then added into the cooler system and the content of the flask was allowed to melt and adjust to the new temperature of the system. A solution of chlorosilacyclohexane (10.0 g, 74.3 mmol) was then slowly

added to the reaction mixture under vigorous stirring. After the complete addition, the reaction mixture was boiled for 5 hours still having the dry ice/ethylacetate cooler to minimize the loss of $(CH_3)NH_2$. The dry ice/ethylacetate cooler was maintained at –78 °C for additional 12 hours and then the cooling mixture slowly warmed up to room temperature. The reaction mixture was filtered under nitrogen and reduced pressure and the salt was discarded. The solvent was then distilled off the solution and the product was collected at 135.9-137.0 °C and 15 Torr. Yield: 6.77 g (29.8 mmol, 40%). ^{1}H NMR (400 MHz, $CDCl_3$): δ = 0.66–0.76 (m, 4H, $CH_{2(ax/eq)}$), 0.80–0.87 (m, 4H, $CH_{2(ax/eq)}$), 1.13–1.23 (m, 2H, $CH_{2(ax/eq)}$), 1.41–1.61 (m, 6H, $CH_{2(ax/eq)}$), 1.86–1.95 (m, 4H, $CH_{2(ax/eq)}$), 2.53 (s, 3H, NCH_3), 4.30 (tt, 2H, $^3J_{H\text{-}H}$ = 5.5 Hz, $^3J_{H\text{-}H}$ = 1.2 Hz, $^1J_{Si–H}$ = 192 Hz, SiH). $^{13}C\{^1H\}$ NMR (101 MHz, $CDCl_3$): δ = 12.9, 24.8, 29.8 (CH_2), 31.3 (NCH_3). $^{29}Si\{^1H\}$ NMR (79 MHz, $CDCl_3$): δ = -7.7. MS (EI, 70 eV): *m/z* (%) 227 (19), 213 (100), 143 (42); HRMS: *m/z* calcd for $C_{11}H_{25}Si_2N$ 227.1526, found 227.1521.

Bis(1-silacyclohexane)amine (24) method 1: NH_3 was condensed into an ampule and dried over sodium alloy for 24 hours. The anhydrous NH_3 (2.96 g, 173.80 mmol) was then condensed into a reaction flask containing cyclohexane (130 mL). The reaction flask was equipped with dry ice/ethylacetate cooler and a dropping funnel containing chlorosilacyclohexane (15.0 g, 111.4 mmol) which was slowly added to the solution under stirring. The dry ice/ethylacetate cooler was maintained at –78 °C for 12 hours. After the complete addition, the reaction mixture was boiled for about 5 hours, still having the dry ice/ethylacetate cooler to minimize the loss of ammonia. The solution was stirred further overnight, while the dry ice/ethylacetate cooling bath slowly warmed up to room temperature. The reaction mixture was then filtered under nitrogen and reduced pressure and the salt was discarded. The solvent was then distilled off the solution and the product was collected at 100.0-100.1 °C and 8 Torr. ^{1}H NMR (400 MHz, $CDCl_3$): δ = 0.30–0.48 (bs, 1H, NH), 0.56–0.65 (m, 4H, $CH_{2(ax/eq)}$), 0.80–0.89 (m, 4H, $CH_{2(ax/eq)}$), 1.22–1.32 (m, 2H, $CH_{2(ax/eq)}$), 1.45–1.59 (m, 6H, $CH_{2(ax/eq)}$), 1.75–1.85 (m, 4H, $CH_{2(ax/eq)}$), 3.35 (q, 2H, $^1J_{Si–H}$ = 193 Hz, SiH). $^{13}C\{^1H\}$ NMR (101 MHz, $CDCl_3$): δ = 14.9, 24.4, 29.7 (CH_2). $^{29}Si\{^1H\}$ NMR (79 MHz, $CDCl_3$): δ = -12.3. MS (EI, 70 eV): *m/z* (%) 214 (100) [M^+], 177 (43).

Bis(1-silacyclohexane)amine (24) method 2: NH_3 was condensed into an ampule and dried over sodium alloy for 24 hours. The anhydrous NH_3 (0.61 g, 35.82 mmol) was then condensed into a 100 mL ampule containing chlorosilacyclohexane (5,12 g, 38.02 mol) and the ampule was sealed off in vacuum. The ampule was then inserted in a -84 °C cooling bath (ethyl acetate slush) were it was allowed to stand the next 24 hours and slowly warm up to room temperature. After opening the ampule and removing the white reaction salt, the product was condensed on a N_2(l) cooled finger as a colourless liquid. ^{1}H NMR (400 MHz, $CDCl_3$): δ = 0.30–0.48 (bs, 1H, NH), 0.56–0.65 (m, 4H, $CH_{2(ax/eq)}$), 0.80–0.89 (m, 4H, $CH_{2(ax/eq)}$), 1.22–1.32 (m, 2H, $CH_{2(ax/eq)}$), 1.45–1.59 (m, 6H, $CH_{2(ax/eq)}$), 1.75–1.85 (m, 4H, $CH_{2(ax/eq)}$), 3.35 (q, 2H, $^1J_{Si–H}$ = 193 Hz, SiH). ^{13}C{^{1}H} NMR (101 MHz, $CDCl_3$): δ= 14.9, 24.4, 29.7 (CH_2). ^{29}Si{^{1}H} NMR (79 MHz, $CDCl_3$): δ= -12.3.

7.3 Measurements and experimental apparatuses

General NMR measurements: ^{1}H, $^{13}C\{H\}$,^{19}F, ^{29}Si and $^{29}Si\{H\}$ NMR spectra were recorded on Brucker AVANCE 400 MHz spectrometer. Chemical shifts are reported in δ (ppm) downfield from TMS and are referenced to solvent residual signals. NMR spectra for all the compounds synthesized in this work are available as electronic supplementary material on an attached CD. In the appendix ^{1}H, $^{13}C\{H\}$, ^{19}F and $^{29}Si\{H\}$ NMR spectra for **3**, **13** and **17** are given, and for compounds **19** and **24** ^{1}H, $^{13}C\{H\}$ and $^{29}Si\{H\}$ NMR spectra are given.

Low-temperature NMR measurements: ^{13}C-DNMR and ^{19}F-DNMR spectra were recorded on Brucker AC 250 PFT-NMR spectrometer. The Freon solvent mixture was prepared in 1:1:3 ratio of CD_2Cl_2, $CHFCl_2$ and CHF_2Cl for the low-temperature ^{13}C- and ^{19}F NMR measurements of **3**, **7**, **8**, **9**, **13** and **14**. Sufficient amount of CD_2Cl_2 (~0,2 mL) was placed in NMR tubes (connected to a vacuum line), containing the sample under investigation. The mixtures in the NMR tubes were degassed before proceeding further by repeatedly freezing and thawing them. The Freon substances used; $CHFCl_2$ (bp: 8.9 °C) and CHF_2Cl (bp: -40.7 °C) were then condensed under vacuum into the NMR tubes and then sealed off. The pyrophoric SiD_4 solvent was prepared prior to use and was condensed into a NMR tube (connected to the vacuum line) containing the sample of **7** and the tube was then sealed off under vacuum.

A type K (Chromel/Alumel) thermocouple was used to calibrate the temperature of the probe. The thermocouple was placed in a dummy tube both the day before and the day after the actual NMR readings were taken. It is estimated that the temperature is accurate within 2 K. The numerical data analysis program IGOR (WaveMetrics) was used for manipulation of the NMR spectra. Simulations of the line shapes of the NMR spectra were performed using PC version of the DNMR program (QCPE program no. 633; Indiana University, Bloomington, IN, USA).

GED measurements: The Electron diffraction intensities of **3**, **7**, **13** and **14** were measured with a Gasdiffraktograph KD-G2, both at 25 and 50 cm nozzle-to-plate

distances, with an accelerating voltage of about 60 kV [146]. ZnO powder diffraction patterns allowed the determination of the electron wavelength. While the experiment was in progress, the sample was kept at -10 °C and the nozzle and inlet system were at room temperature. An Agfa Duoscan HiD scanner was used to analyse the photographic plates (Kodak Electron Image Plates, 18x13 cm). The program SCAN3 was used to obtain the total scattering intensity curves [147].

Compound **17** was recorded using the Edinburgh gas diffraction apparatus, with an accelerating voltage of around 40 kV (corresponding to a electronic wavelength of *ca*. 6.0 pm) [148]. Both the sample and the nozzle were maintained at 293K and nozzle-to-plate distances of 127.45 and 285.32 mm were used. The scattering intensities were recorded on Kodak Electron Image films. The electron wavelengths were determined from the scattering patterns of benzene vapour. These patterns were recorded immediately after the compound patterns and analysed in the same way in an attempt to eliminate systematic errors in wavelengths and camera distances. An Epson Expression 1680 Pro flatbed scanner was used to measure the scattering intensities, which were then converted to optical densities as a function of the scattering variable *s*, using an established program [149]. Data reduction and least-squares refinements were carried out using the ed@ed v2.4 program, employing the scattering factors of Ross et al. [150,151].

Low-temperature Raman measurements: Raman spectra for samples of **3-5**, **7-9**, **13-15** and **17** were recorded with a Jobin Yvon T64000 spectrometer equipped with a triple monochromator and a CCD camera. For recording spectra at high and low temperatures, liquid samples were placed into 1 mm capillary glass tubes and then sealed off under nitrogen flow. The capillaries were stood on a copper block, cooled with liquid nitrogen and the temperature was monitored with a thermocouple. The samples were irradiated by the green 532 nm line of a frequency doubled Nd-YAG Laser (Coherent, DPSS model 532-20, 20 mW). To prevent any deposition of ice at low temperatures the copper block was put in a continuous flow cryostat, Oxford instruments OptistatCF^{TM}, using liquid nitrogen for cooling.

Mass spectroscopy: Compound **3** was recorded using MA Varian, Saturn 2000 spectrometer. Mass spectra for **24** were obtained with a Microtof Brucker

spectrometer from Brucker Daltonios. Interpretation of the mass spectra was performed by standard techniques [119]. Mass spectra for **4**, **5**, **7**, **8**, **9**, **13**, **14** and **19** were obtained with MASPEC II system (II32/1235) spectrometer. All available MS spectra to date are available as electronic supplementary material on an attached CD. In the appendix MS spectra for **3**, **13**, **19** and **24** are given.

8 References

1. Greenwood, N. N.; Earnshaw, A. *Chemistry of the Elements*, Second ed.; Butterworth-Heinemann: Oxford, 1997.
2. Elschenbroich, C. *Organometallics*; WILEY-VCH Verlag GmbH & Co: Weinheim, Germany, 2006.
3. Haaland, A.; Rypdal, K.; Stuger, H.; Volden, H. V. *Acta Chem. Scand* **1994,** *48*, 46.
4. Carrell, H. L.; Donohue, J. *Acta Crystallogr.* **1972,** *28B*, 1566.
5. Wehle, D.; Scheuermann, H.-J.; Fitjer, L. *Chem. Ber.* **1986,** *119*, 3127.
6. Smith, Z.; Almenningen, A.; Hengge, E.; Kovar, D. *J. Am. Chem. Soc.* **1982,** *104*, 4362.
7. Hassel, O. *Tidsskr. Kjemi Bergvesen Met.* **1943** *3*, 32.
8. Arnason, I.; Thorarinsson, G. K.; Matern, E. Z. *Anorg. Allg. Chem.* **2000,** *626*, 853.
9. Favero, L. B.; Caminati, W.; Arnason, I.; Kvaran, A. *J. Mol. Spectrosc.* **2005,** *229*, 188.
10. Arnason, I.; Kvaran, Á.; Bodi, A. *Int. J. Quantum Chem.* **2006,** *106*, 1975.
11. Dixon, D. A.; Komornicki, A. *J. Phys. Chem.* **1990,** *94*, 5630.
12. Leventis, N.; Hanna, S. B.; Sotiriou-Leventis, C. *J. Chem. Educ.* **1997,** *74*, 813.
13. Lambert, J. B.; Keske, R. G. *J. Org. Chem.* **1966,** *31*, 3429.
14. Lehn, J. M.; Riddell, F. G.; Price, B. J.; Sutherland, I. O. *J. Chem Soc. (B)* **1967**, 387.
15. Anet, F. A. L.; Yavari, I. *J. Am. Chem. Soc.* **1977,** *99*, 2794.
16. Lambert, J. B.; Keske, R. G.; Weary, D. K. *J. Am. Chem. Soc.* **1967,** *89*, 5921.
17. Claeson, G.; Androes, G.; Calvin, M. *Ibid.* **1961,** *83*, 4357.
18. Ionescu, A. R.; Bérces, A.; Zgierski, M. Z.; Whitfield, D. M.; Nukada, T. *J. Phys. Chem. A* **2005,** *109*, 8096.
19. Weldon, A. J.; Vickrey, T. L.; Tschumper, G. S. *J. Phys. Chem. A* **2005,** *109*, 11073.
20. Friebolin, H.; Kabuss, S.; Maier, W.; Lüttringhaus, A. *Tetrahedron Letters* **1962**, 683.
21. Freeman, F.; Cha, C. *J. Phys. Org. Chem.* **2004,** *17* 32.

22. Köpf, H.; Block, B.; Schmidt, M. *Chem. Ber.* **1968,** *101*, 272.
23. Lambert, J. B.; Mixan, C. E.; Johnson, D. H. *J. Am. Chem. Soc.* **1973,** *95*, 4634.
24. Jensen, F. R.; Bushweller, C. H. *Tetrahedron Letters* **1968**, 2825.
25. Murray, R. W.; Kaplan, M. L. *Tetrahedron* **1969,** *25*, 1651.
26. Bushweller, C. H.; O'Neil, J. W.; Vilkofsky, H. S. *Tetrahedron* **1971,** *27*, 3065.
27. Casarini, D.; Lunazzi, L.; Mazzanti, A. *J. Org. Chem.* **1998,** *63*, 9125.
28. Casarini, D.; Lunazzi, L.; Mazzanti, A. *Tetrahedron* **1998,** *54*, 13181.
29. Arnason, I.; Thorarinsson, G. K.; Matern, E. *J. Mol. Struct. (Theochem)* **1998,** *454*, 91.
30. Arnason, I.; Matern, E. J. *Mol. Struct. (THEOCHEM)* **2001,** *544*, 61.
31. Arnason, I.; Oberhammer, H. *J. Mol. Struct.* **2001,** *598*, 245.
32. Arnason, I.; Kvaran, A.; Jonsdottir, S.; Gudnason, P. I.; Oberhammer, H. *J. Org. Chem.* **2002,** *67*, 3827.
33. Favero, L. B.; Velino, B.; Caminati, W.; Arnason, I.; Kvaran, A. *J. Phys. Chem. A* **2006,** *110*, 9995.
34. Favero, L. B.; Velino, B.; Caminati, W.; Arnason, I.; Kvaran, A. *Organometallics* **2006,** *25*, 3813.
35. Girichev, G. V.; Giricheva, N. I.; Bodi, A.; Gudnason, P. I.; Jonsdottir, S.; Kvaran, A.; Arnason, I.; Oberhammer, H. *Chem. Eur. J.* **2007,** *13*, 1776.
36. Bodi, A.; Kvaran, Á.; Jonsdottir, S.; Antonsson, E.; Wallevik, S. Ó.; Arnason, I.; Belyakov, A. V.; Baskakov, A. A.; Hölbling, M.; Oberhammer, H. *Organometallics* **2007,** *26*, 6544.
37. Hölbling, M.; Flock, M.; Hassler, K. *ChemPhysChem* **2007,** *8*, 735.
38. Tekautz, G.; Binter, A.; Hassler, K.; Flock, M. *ChemPhysChem* **2006,** *7*, 421.
39. Pitzer, K. S. *Disc. Faraday Soc.* **1951,** *10*, 66.
40. Kivelson., D. *J. Chem. Phys* **1954,** *22*, 1733.
41. Eliel, E. L.; Wilen, S. H.; Mander, L. N. *Stereochemistry of Organic Compounds*; Wiley-Interscience Publication, John Wiley & Sons: New York, 1994.
42. Eliel, E. L. *Conformational analysis*; Wiley: Chichester, 1998; Vol. 1.
43. Bischoff, C. A. *Ber. Dtsch. Chem. Ges.* **1890,** *23*, 623.
44. Sachse, H. *Ber. Dtsch. Chem. Ges.* **1890,** *23*, 1363.
45. Sachse, H. *Z. Phys. Chem.* **1892,** *10*, 203.
46. Mohr, E. R. *J. Prakt. Chem.* **1918,** *98*, 315.

47. Bushweller, C. H. In *Conformational Behavior of Six-Membered Rings*; Juaristi, E. Ed.; VCH Publishers, Inc.: New York, 1995.
48. Barton, D. H. R. *Experientia* **1950,** *6*, 316.
49. Barton, D. H. R. *Top. Stereochem.* **1971,** *6*, 1.
50. Bott, G.; Field, L. D.; Sternhell, S. *J. Am. Chem. Soc.* **1980,** *102*, 5618.
51. Hesek, D.; Hembury, G. A.; Drew, M. G. B.; Borovkov, V. V.; Inoue, Y. *J. Am. Chem. Soc.* **2001,** *123* 12232.
52. Clayden, J.; Vallverdú, L.; Clayton, J.; Helliwell, M. *Chem. Commun.* , 561
53. Binsch, G. *Top. Stereochem.* **1968,** *3*, 97.
54. Sandstrom, J. *Dynamic NMR spectroscopy*; Academic Press: New York, 1982.
55. Oki, M. *Application of Dynamic NMR to Organic Chemistry*; VCH puplisher: Deerfield Beach, Florida, 1985.
56. Shanan-Atidi, H.; Bar-Eli, K. H. *J. Phys. Chem.* **1970,** *74*, 961.
57. Hinchley, S. L.; Wann, D. A.; Rankin, D. W. H. *Int. J. Quantum Chem.* **2005,** *101*, 878.
58. Sipachev, V. A. *J Mol Struct (Theochem)* **1985,** *121*, 143.
59. Sipachev, V. A. *in: Advances in Molecular Structure Research*; JAI Press: New York, 1999 Vol. 5.
60. Brain, T.; Morrison, C. A.; Parsons, S.; Rankin, D. W. H. *J. Chem. Soc. Dalton Trans* **1996**, 4589.
61. Blake, A. J.; Brain, P. T.; McNab, H.; Miller, J.; Morrison, C. A.; Parsons, S.; Rankin, D. W. H.; Robertson, H. E.; Smart, B. A. *J Phys Chem* **1996,** *100*, 12280.
62. Mizel, N. W.; Rankin, D. W. H. *J. Chem. Soc. Dalton Trans* **2003**, 3650.
63. Andersen, B.; Seip, H. M.; Strand, T. G.; Stolevik, R. *Acta Chem. Scand.* **1969,** *23*, 3224.
64. Wilson, E. B.; Decius, J. C.; Cross, P. C. *Molecular Vibrations, The Theory of Infrared and Raman Vibrational Spectra*; McGraw-Hill Book Company, 1955.
65. Chalmers, J. M.; Griffiths, P. R., Eds. *Handbook of Vibrational Spectroscopy*; Wiley & Sons Ltd: Chichester, 2002; Vol. 1
66. Klaboe, P. *Vib. Spectrosc.* **1995,** *9*, 3.
67. LabSpec software version 3.03t, HORIBA Jobin Yvon, http://www.jobinyvon.com

68. Gudnason, P. I. *Kísilinnihaldandi sexhringir*, M.Sc thesis, Univeristy of Iceland, 2003.
69. Leong, M. K.; Mastryukov, V. S.; Boggs, J. E. *J. Phys. Chem.* **1994,** *98*, 6961.
70. Carleer, R.; Anteunis, M. J. O. *Org. Magn. Reson.* **1979,** *12*, 673.
71. Quellette, R. J. *J. Am. Chem. Soc.* **1974,** *96*.
72. Frierson, M. R.; Iman, M. R.; Zalkow, V. B.; Allinger, N. L. *J. Org. Chem.* **1988,** *53*, 5248.
73. Wiberg, K. B.; Hammer, J. D.; Castejon, H.; Bailey, W. F.; DeLeon, E. L.; Jarret, R. M. *J. Org. Chem.* **1999,** *64*, 2085.
74. Della, E. W. *J. Am. Chem. Soc.* **1967,** *89*, 5221.
75. Schneider, H.-J.; Hoppen, V. *J. Org. Chem.* **1978,** *43*, 3866.
76. Weigert, F. J. *J. Org. Chem.* **1980** *45*, 3476.
77. Wolniewicz, A.; Dmowski, W. *Journal of Fluorine Chemistry* **2001,** *109*, 95.
78. Taskinen, E. *Struct. Chem.* **1998,** *9*, 411.
79. West, R. *J. Am. Chem. Soc.* **1954,** *76*, 6012.
80. Schott, V. G.; Schneider, P.; Kelling, H. Z. *Anorg. Allg. Chem.* **1973,** *398*, 293.
81. Fritz, G.; Kummer, D. *Chem. Ber.* **1961,** *94*, 1143.
82. Metz, S.; Burschka, C.; Platte, D.; Tacke, R. *Angew. Chem. Int. Ed.* **2007,** *46*, 7006.
83. Negrebetsky, V. V.; Taylor, P. G.; Kramarova, E. P.; Bylikin, S. Y.; Belavin, I. Y.; Shipov, A. G.; Bassindale, A. R.; Baukov, Y. I. *J. Organomet. Chem.* **2006,** *691*, 3976.
84. Welsh, K. M.; Michl, J.; West, R. *J. Am. Chem. Soc.* **1988,** *110*, 6689.
85. Pacl, Z.; Sakoubková, M.; Papoušková, Z.; Chvalovský, V. *Coll. Czech. Chem. Commun.* **1971,** *36*, 1588.
86. Gompper, K. *Untersuchungen zur Metallorganischen Synthese von 1,3,5,7-Tetrasilaadamantanen*, Dissertation, Universität Karlsruhe, 1979.
87. Du, Y. F.; Cao, Y. Q.; Dai, Z.; Chen, B. H. *J. Chem. Res.* **2004**, 223.
88. Aliev, A. E.; Harris, K. D. M. *J. Am. Chem. Soc.* **1993,** *115*, 6369.
89. Booth, H. *Progress in NMR Spectroscopy*; Pergamon Press: Oxford, UK, 1969; Vol. 5.
90. Kalinowski, H.-O.; Berger, S.; Braun, S. *13C-NMR-Spektroskopie*; Georg Thieme Verlag: Stuttgart, Germany, 1984.

91. Frisch, M. J.; Trucks, G. W.; Schlegel, H. B. *Gaussian 03*; revision C.02, Gaussian, Inc: Wallingford. CT, 2004.
92. Jensen, F. R.; Bushweller, C. H.; Beck, B. H. *J. Am. Chem. Soc.* **1969,** *91*, 344.
93. Bugay, D. E.; Bushweller, C. H.; Danehey, C. T.; Hoogasian, S.; Blersch, J. A.; Leenstra, W. R. *J. Phys. Chem.* **1989,** *93*, 3908.
94. Subbotin, O. A.; Sergeyev, N. M. *J. Am. Chem. Soc.* **1975,** *97*, 1080.
95. Schneider, H.-J.; Hoppen, V. J. *J. Org. Chem.* **1978,** *43*, 3866.
96. Chu, P.-S.; True, N. S. *J. Phys. Chem.* **1985,** *89*, 5613.
97. Scharpen, L. H. *J. Am. Chem. Soc.* **1972,** *94*, 3737.
98. Shen, Q.; Peloquin, J. M. *Acta Chem. Scand. A* **1988,** *42*, 367.
99. Hoefner, D.; Lesko, S. A.; Binsch, G. *Org. Magn. Reson.* **1978,** *11*, 179.
100. Penman, K. G.; Kitching, W.; Adcock, W. *J. Org. Chem.* **1989,** *54*, 5390.
101. Cho, S. G.; Rim, O. K.; Kim, Y.-S. *J. Mol. Struct. (THEOCHEM)* **1996,** *364*, 59.
102. Shen, Q.; Rhodes, S.; Cochran, J. C. *Organometallics* **1992,** *11*, 485.
103. Weldon, A. J.; Tschumper, G. S. *Int. J. Quant. Chem.* **2007,** *107*, 2261.
104. Booth, H. *J. Chem. Soc. Chem. Commun.* **1973**, 945.
105. Björnsson, R. *Theoretical studies of silicon containing six-membered rings*, M.Sc thesis, Univeristy of Iceland, 2008.
106. Hagen, A. P.; McAmis, L. L. In *Inorganic synthesis*; Basolo, F. Ed.; McGraw-Hill bookcompany, 1976; p. 139.
107. Beckers, H.; Bürger, H.; Bursch, P.; Ruppert, I. *J. Organomet. Chem.* **1986,** *316*, 41.
108. Girichev, G. V.; Giricheva, N. I. Personal communication, Ivanovo State University, 2008.
109. Alabugin, I. V.; Zeidan, T. A. *J. Am. Chem. Soc.* **2002,** *124*, 3175
110. Ribeiro, D. S.; Rittner, R. *J. Org. Chem.* **2003,** *68*, 6780.
111. Taddei, F.; Kleinpeter, E. *J. Mol. Struct. (Theochem)* **2004,** *683*, 29.
112. Taddei, F.; Kleinpeter, E. *J. Mol. Struct. (Theochem)* **2005,** *718*, 141.
113. Kleinpeter, E.; Rolla, N.; Koch, A.; Taddei, P. *J. Org. Chem.* **2006,** *71*, 4393.
114. Urban, J.; Schreiner, P. R.; Vacek, G.; Schleyer, P. v. R.; Huang, J. Q.; Leszczynski, J. *Chem. Phys. Letters* **1997,** *264*, 441.
115. Schleyer, P. v. R.; Kaupp, M.; Hampel, F.; Bremer, M.; Mislow, K. *J. Am. Chem. Soc.* **1992** *114*, 6791.

116. Herzberg, G. *Molecular Spectra and Molecular Structure*; Van Nostrand: New York, 1997; Vol. III.
117. Beagley, B.; Conrad, A. R.; Freeman, J. M.; Monaghan, J. J.; Norton, B. G.; Halywell, G. C. *J. Mol. Struct.* **1972,** *11*, 371.
118. Pophristic, V.; Goodman, L. *Nature* **2001,** *411*, 565.
119. Goodman, L.; Pophristic, V.; Wang, W. *J. Phys. Chem. A* **2001,** *105*, 7454.
120. Song, L.; Lin, Y.; Wu, W.; Zhang, Q.; Mo, Y. *J. Phys. Chem. A* **2005,** *109*, 2310.
121. Mo, Y.; Gao, J. *Acc. Chem. Res.* **2007,** *40*, 113.
122. Mislow, K.; Stackhouse, J.; Hummel, J. P. *Tetrahedron* **1977,** *33*, 1925.
123. Profeta, S. J.; Unwalla, R. J.; Cartledge, F. K. *J. Comp. Chem.* **1989,** *I0*, 99.
124. Aksnes, D. W.; Kimtys, L. *Acta Chem. Scand.* **1995,** *49*, 722.
125. Mohamed, T. A. *J. Mol. Struct. (Theochem)* **2003,** *635*, 161.
126. Jähn, A.; Schenzel, K.; Zink, R.; Hassler, K. *Spectroschim. Acta Part A* **1999,** *55*, 2677.
127. Kveseth, K. *Acta Chem. Scand.* **1979,** *A33*, 453.
128. Hnyk, D.; Fender, R. S.; Robertsson, H. E.; Rankin, D. W. H.; Brühl, M.; Hassler, K.; Schenzel, K. *J. Mol. Struct.* **1995,** *346*, 215.
129. Hinchley, S. L.; Robertson, H.; Parkin, A.; Rankin, D. W. H.; Tekautz, G.; Hassler, K. *Dalton Transactions* **2004,** *5*, 759.
130. Zink, R.; Hassler, K.; Ramek, M. *Vib. Spectrosc.* **1998,** *18*, 123.
131. Ernst, M.; Schenzel, K.; Jähn, A.; Hassler, K. *J. Mol. Struct.* **1997,** *412*, 83.
132. Smart, B. A.; Robertson, H. E.; Mitzel, N. W.; Rankin, D. W. H.; Zink, R.; Hassler, K. *J. Chem. Soc., Dalton Trans.* **1997**, 2475.
133. Hinchley, S. L.; Smart, B. A.; Morrison, C.; Robertson, H. E.; Rankin, D. W. H.; Coxall, R. A.; Parsons, S.; Zink, R.; Siegl, H.; Hassler, K.; Mawhorter, R. *J. Chem. Soc., Dalton Trans.* **2001**, 2916.
134. Zink, R.; Hassler, K.; Roth, A.; Eujen, R. In *Organosilicon Chemistry IV*; Auner, N.; Weis, J. Eds.; Wiley-VCH: Weinheim, 2000.
135. Michl, J.; West, R. *Acc. Chem. Res.* **2000,** *33*, 821.
136. Belyakov, A. V.; Haaland, A.; Shorokhov, D. J.; West, R. *J. Organomet. Chem.* **2000,** *597*, 87.
137. Albinsson, B.; Michl, J. *J. Am. Chem. Soc.* **1995,** *117*, 6378.
138. Albinsson, B.; Michl, J. *J. Phys. Chem.* **1996,** *100*, 3418.

139. Albinson, B.; Teramae, H.; Downing, J. W.; Michl, J. *Chem. Eur. J.* **1996,** *2*, 529.
140. Hummeltenberg, R.; Hassler, K.; Uhlig, F. *J. Organomet. Chem.* **1999,** *592*, 198.
141. Zink, R.; Tekautz, G.; Kleewein, A.; Hassler, K. *ChemPhysChem* **2001,** *6*, 377.
142. Zink, R.; Magnera, T. F.; Michl, J. *J. Phys. Chem.* **2000,** *104*, 3829.
143. Lennox, F.; Masters, S. L.; Hassler, K. Personal communication, University of Edinburgh and Graz University of Technology, 2008.
144. Teramae, H.; Michl, J. *Mol. Cryst. Liq. Cryst.* **1994,** *256*, 149.
145. Björnsson, R. Personal communication, Reykjavík, 2008.
146. Oberhammer, H. *Molecular Structure by Diffraction Methods*; The Chemical Society: London, 1976; Vol. 4
147. Atavin, E. G.; Vilkov, L. V. *Instrum. Exp. Tech.* **2002,** *45*, 745.
148. Huntley, C. M.; Laurenson, G. S.; Rankin, D. W. H. *J. Chem. Soc., Dalton Trans.* **1980**, 954.
149. Fleischer, H.; Wann, D. A.; Hinchley, S. L.; Borisenko, K. B.; Lewis, J. R.; Mawhorter, R. J.; Robertson, H. E.; Rankin, D. W. H. *Dalton Trans.,* **2005**, 3221.
150. Hinchley, S. L.; Robertson, H. E.; Borisenko, K. B.; Turner, A. R.; Johnston, B. F.; Rankin, D. W. H.; Ahmadian, M.; Jones, J. N.; Cowley, A. H. *Dalton Trans.*, **2004**, 2469.
151. Ross, A. W.; Fink, M.; Hilderbrandt, R. In *International Tables for Crystallography*; Wilson, A. J. C. Ed.; Kluwer Academic Publishers: Dordrecht, Netherlands, 1992; p. 245.

9 Curriculum vitae

Name: Sunna Ólafsdóttir Wallevik
Date of birth: 7th September, 1982
Place of birth: Reykjavík, Iceland
Citizenship: Icelandic
E-mail address: sow@hi.is

Education:

Four year High school degree from Menntaskólinn á Egilsstöðum, May 2002.

- One semester spent in the High school of Geometry, Latina, Italy, winter 2000.

B.Sc. degree in chemistry from the University of Iceland, February 2006.

M.Sc. degree in inorganic chemistry from the University of Iceland. Expected graduation in October 2008.

- One semester spent in the University of Ottawa, Ottawa, Cananda, autumn 2006.
- Approximately one month spent in the Graz University of Technology, Graz, Austria, autumn 2007.

Committees:

Editor of the school paper of the primary school of Egilsstaðir.
(Period 1999)

Advisor for chemistry students - University of Iceland.
(Period 2004-2005)

On the editorial board of the chemistry paper Snefill – The paper of chemistry-, biochemistry- and chemical engineering students of Iceland.
(Period 2005)

On the preparation committee for the Icelandic national team for the International Olympiad in Chemistry – On the committee for the experimental part of the qualification competition. (Period 2006 and 2007)

Working experience:

Vallanes: Icelandic farm. (Period 1997-2000)

Home for disabled people, Egilsstaðir – Taking care of disabled people.
(Period 2000-2002)

Camping Marina di Venezia, Italy – Reception work.
(Period: summer 2001)

The Icelandic Building Research Institute - Research work in cement based materials. (Period: 2002-2004)

Science Institute, University of Iceland – Research work in inorganic chemistry.
(Period: summer 2004 and 2005)

University of Iceland - Part time laboratory teaching in analytical chemistry.
(Period: Winter 2006 and 2007)

University of Iceland - Part time laboratory teaching in general chemistry N.
(Period: autumn 2007)

University of Iceland - Part time laboratory teaching in inorganic chemistry IV.
(Period: Winter 2007 and 2008)

Science Institute, University of Iceland – M.Sc. research work in inorganic chemistry. (Period: January 2006 – July 2008)

Innovation Center Iceland – research work in the thermal and rheological properties of well cement. (Period: July 2008 – present day)

10 Publications and presentations regarding this thesis:

1. Wallevik, S. Ó.; Björnsson, R.; Arnason, I., **Conformational behavior of monosubstituted silacyclohexanes**; The 15th International Symposium on Organosilicon Chemistry, June 1.-6th 2008, Jeju, Korea.

2. Wallevik, S. Ó.; Arnason, I., **Conformational behavior investigated by Raman spectroscopy**; Natural Science Symposium 2008, March 14th-15th 2008, Reykjavík, Iceland.

3. Bodi, A.; Kvaran, Á.; Jónsdóttir, S.; Antonsson, E.; Wallevik, S. Ó.; Arnason, I.; Belyakov, A. V.; Baskakov, A. A.; Hölbling, M.; Oberhammer, H., **Conformational Properties of 1-Fluoro-1-silacyclohexane, $C_5H_{10}SiHF$: Gas Electron Diffraction, Low-Temperature NMR, Temperature-Dependent Raman Spectroscopy, and Quantum Chemical Calculations**; *Organometallics* 2007, *26*, 6544.

4. Wallevik, S. Ó.; Arnason, I., **Stellingajafnvægi rannsakað með Raman greiningu**; The Icelandic Chemical Society Symposium, November 17th 2007, Reykjavík, Iceland.

5. Wallevik, S. Ó.; Björnsson, R.; Kvaran, Á.; Jónsdóttir, S; Arnason, I.; Bodi, A.; Girichev, G. V.; Giricheva, N. I, **Conformational properties of 1-fluoro-1-methyl-1-silacyclohexane. Are *A* values additive?**; 12th European Symposium on Gas Electron Diffraction, June 24th – 28th 2007, Blaubeuren, Germany.

6. Björnsson, R.; Wallevik, S. Ó.; Arnason, I.; Bodi, A.; Hölbling, M., **Substituent effects in silacyclohexanes: Theory vs. experiment**; 12th European Symposium on Gas Electron Diffraction, June 24th – 28th 2007, Blaubeuren, Germany.

The following papers are in preparation:

1. Arnason, I.; Kvaran, Á.; Jonsdottir, S.; Wallevik, S. Ó.; Björnsson, R.; Bodi, A.; Belyakov, A. V.; Basakov, A. A.; Hassler, K.; Oberhammer, H., **Conformational Properties of 1-Silyl-1-silacyclohexane, $C_5H_{10}SiHSiH_3$: Gas Electron Diffraction, Low-Temperature NMR, Temperature-Dependent Raman Spectroscopy, and Quantum Chemical Calculations.** To be submitted.

2. Arnason, I.; Kvaran, Á.; Jonsdottir, S.; Wallevik, S. Ó.; Arnason, Bodi, A.; G. V. Girichev N. I.; Giricheva; Hassler, K., et al., **Conformational Properties of 1-Fluoro-1-methyl-silacyclohexane and 1-Trifluoromethyl-1-methyl-silacyclohexane, $C_5H_{10}SiCH_3F$ and $C_5H_{10}SiCH_3CF_3$: Gas Electron Diffraction, Low-Temperature NMR, Temperature-Dependent Raman Spectroscopy, and Quantum Chemical Calculations.** In preparation.

3. Arnason, I.; Kvaran, Á.; Jonsdottir, S.; Wallevik, S. Ó.; Belyakov, A. V.; Basakov, A. A.; Hassler, K.; et al., **Conformational Properties of 1-Chloro-1-silacyclohexane and 1-Bromo-1-silacyclohexane, $C_5H_{10}SiHCl$ and $C_5H_{10}SiHBr$: Gas Electron Diffraction, Low-Temperature NMR, Temperature-Dependent Raman Spectroscopy, and Quantum Chemical Calculations.** In preparation.

4. Bodi, A.; Kvaran, Á.; Jonsdottir, S.; Wallevik, S. Ó.; Arnason, I.; Belyakov, A. V.; Basakov, A. A.; Hassler, K.; Oberhammer, H., **Conformational Properties of 1-Methoxy-1-silacyclohexane and 1-Dimethylamine-1-silacyclohexane, $C_5H_{10}SiHOCH_3$ and $C_5H_{10}SiHN(CH_3)_2$: Gas Electron Diffraction, Low-Temperature NMR, Temperature-Dependent Raman Spectroscopy, and Quantum Chemical Calculations.** In preparation.

5. Bodi, A.; Kvaran, Á.; Jonsdottir, S.; Wallevik, S. Ó.; Arnason, I.; G. V. Girichev N. I.; Giricheva; Hassler, K.; et al., **Conformational Properties of 1-Cyano-1-silacyclohexane and 1-Azide-1-silacyclohexane; $C_5H_{10}SiHCN$ and $C_5H_{10}SiHN_3$: Gas Electron Diffraction, Low-Temperature NMR,**

Temperature-Dependent Raman Spectroscopy, and Quantum Chemical Calculations. In preparation.

6. Bodi, A.; Kvaran, Á.; Jonsdottir, S.; Wallevik, S. Ó.; Arnason, I.; Oberhammer, H., **Conformational Investigation of the novel Compounds; Bis(1-silacyclohexane)-methyl-amine and Bis(1-silacyclohexane)amine, $(C_5H_{10}SiH)_2NMe$** and **$(C_5H_{10}SiH)_2NH$.** In preparation.

7. Arnason, I.; Kvaran, Á.; Jonsdottir, S.; Wallevik, S. Ó.; et al., **Conformational Properties of 1-Tertbuthyl-1- silacyclohexane, $C_5H_{10}SiH^tBu$: Gas Electron Diffraction, Low-Temperature NMR, Temperature-Dependent Raman Spectroscopy, and Quantum Chemical Calculations.** In preparation.

8. Bodi, A.; Kvaran, Á.; Jonsdottir, S.; Wallevik, S. Ó.; Arnason, I.; Belyakov, A. V.; Basakov, A. A.; Hassler, K.; Oberhammer, H., **Conformational Properties of 1-Iodo-1-silacyclohexane, $C_5H_{10}SiHI$: Gas Electron Diffraction, Low-Temperature NMR, Temperature-Dependent Raman Spectroscopy, and Quantum Chemical Calculations.** In preparation.

9. Papers regarding $C_5H_{10}SFSiF_3$, $CF_3Me_2Si\text{-}SiMe_2CF_3$ and $C_5H_{10}SiMeD$ may soon be prepared.

11 Appendix

Appendix A: ^{1}H NMR spectrum of 3

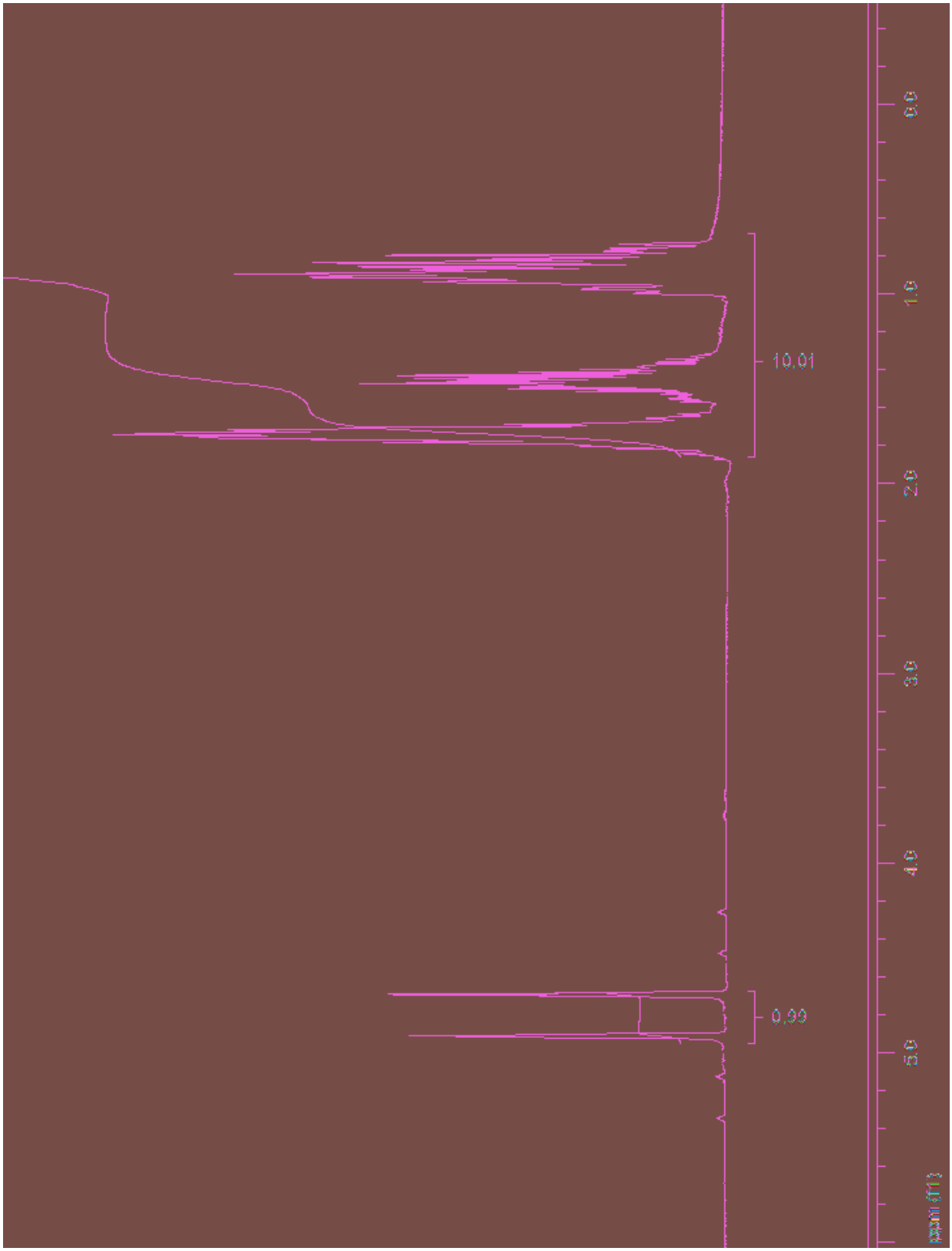

Appendix B: ^{13}C NMR spectrum of 3

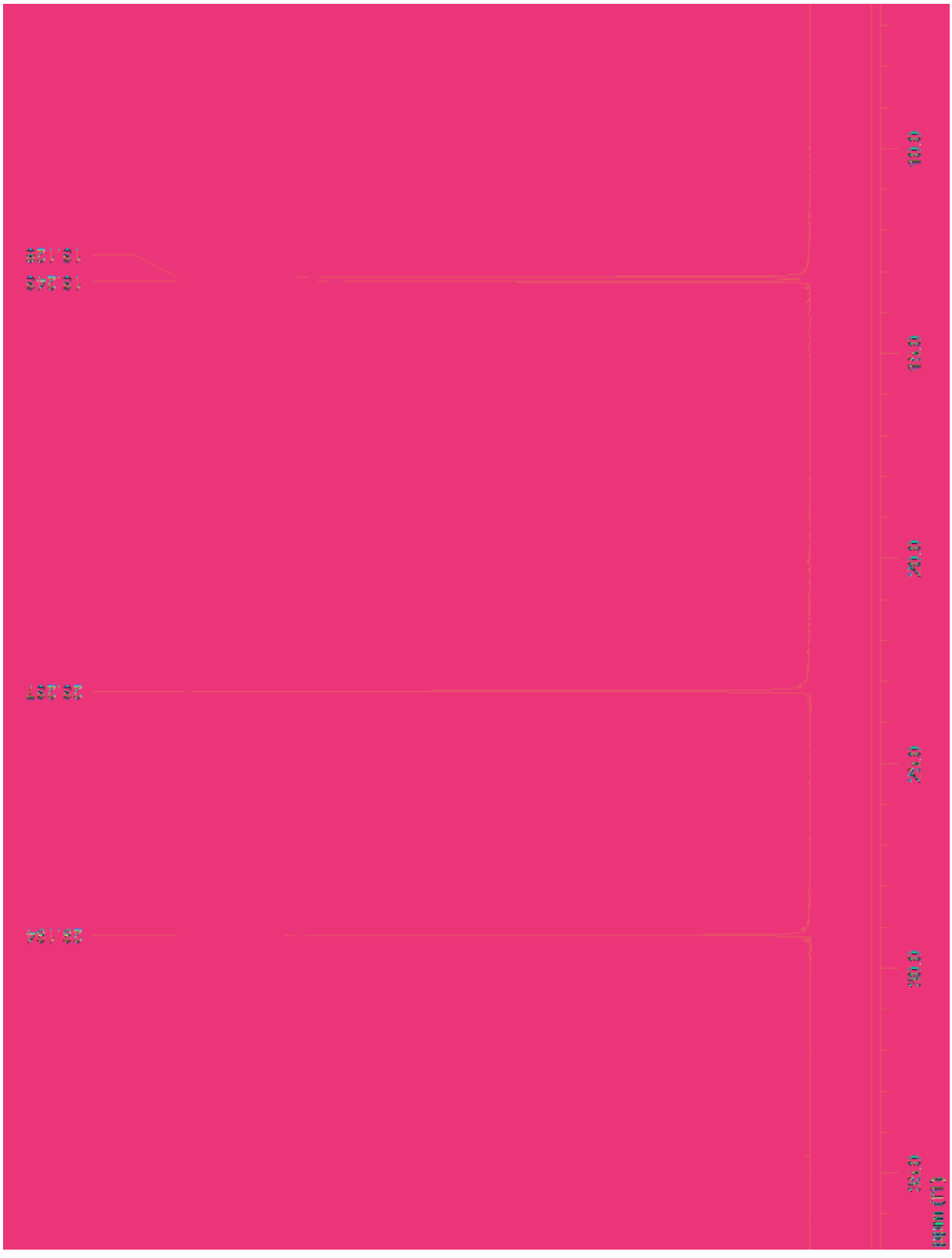

Appendix C: ^{29}Si NMR spectrum of 3

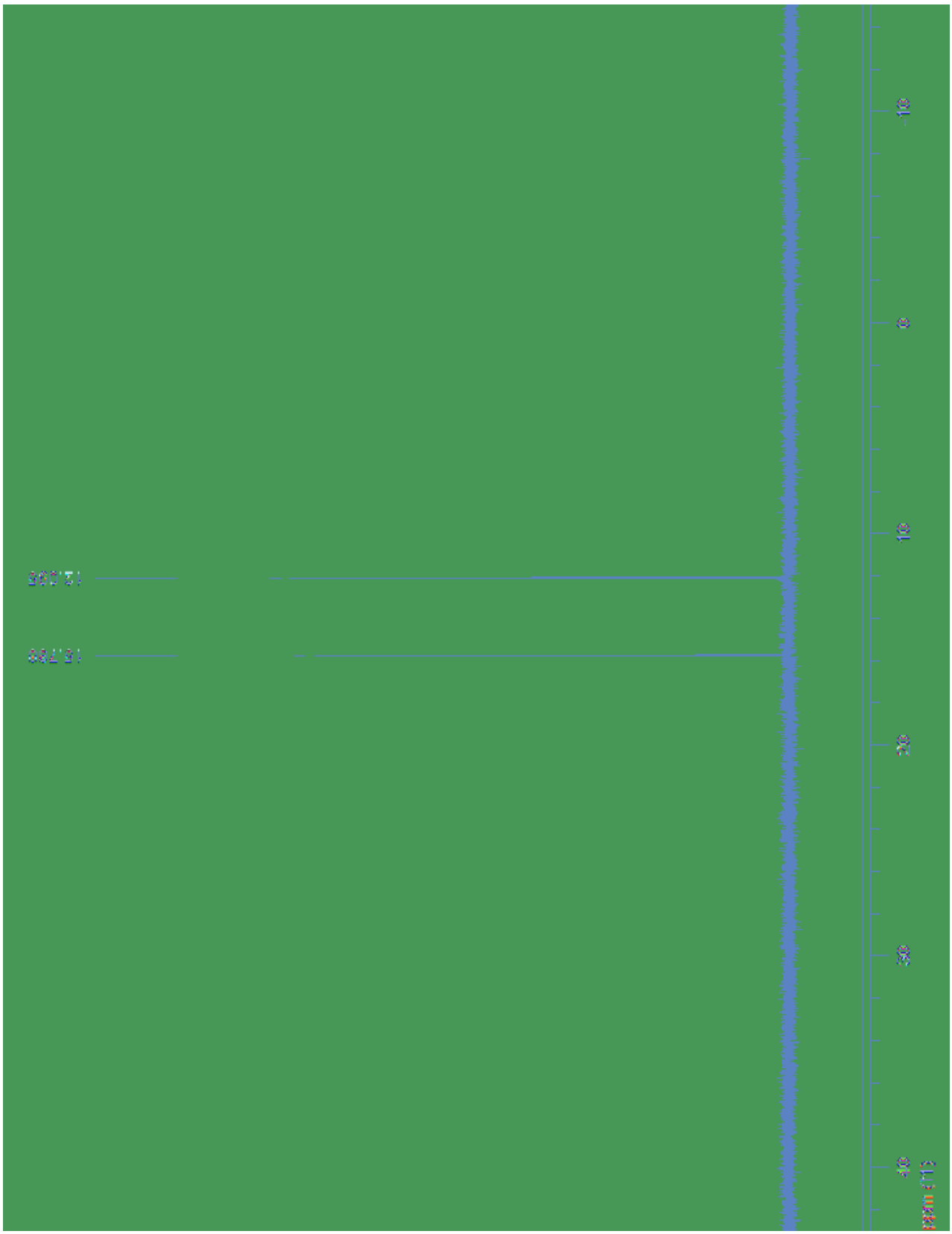

Appendix D: ^{19}F NMR spectrum of 3

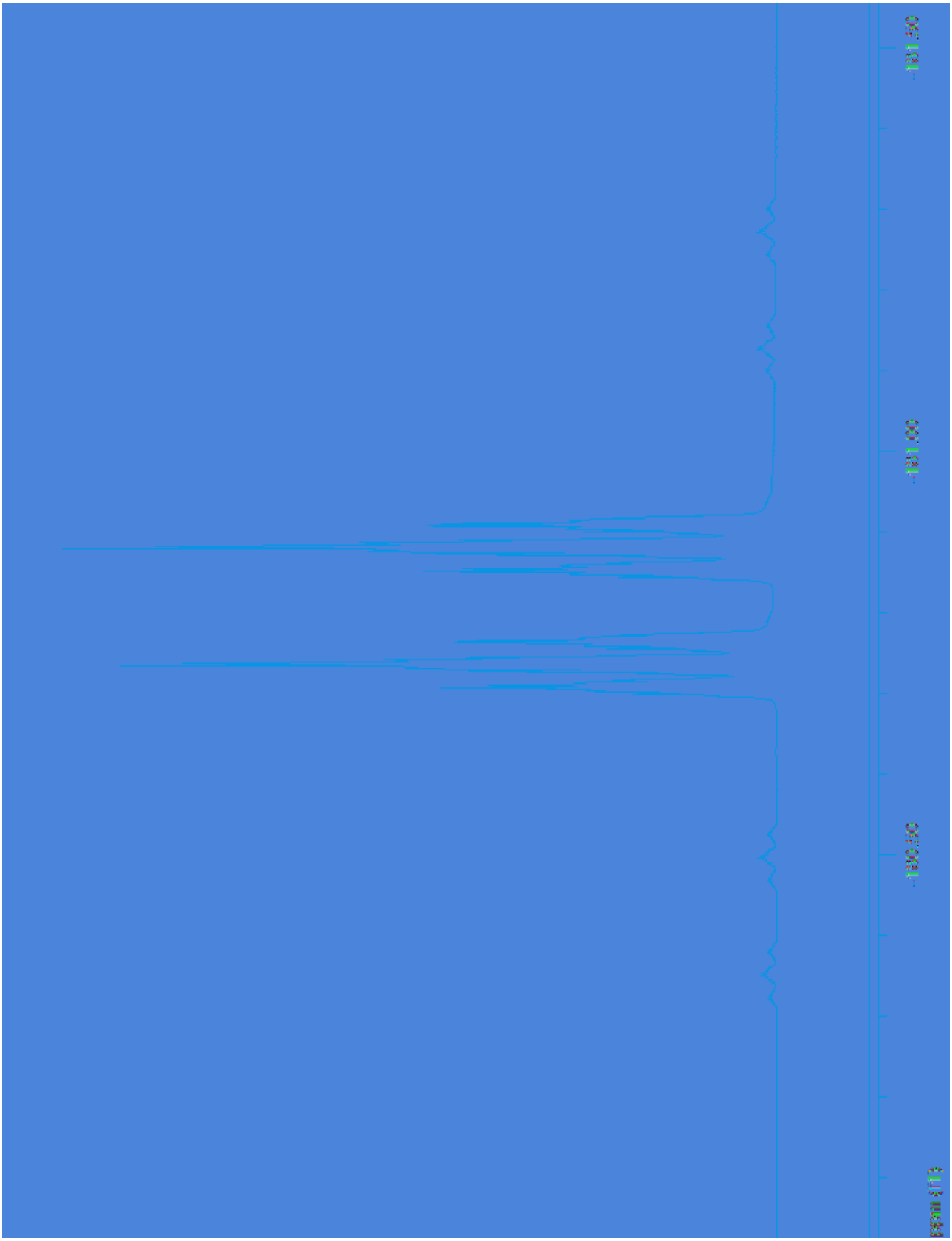

Appendix E: MS spectrum of 3

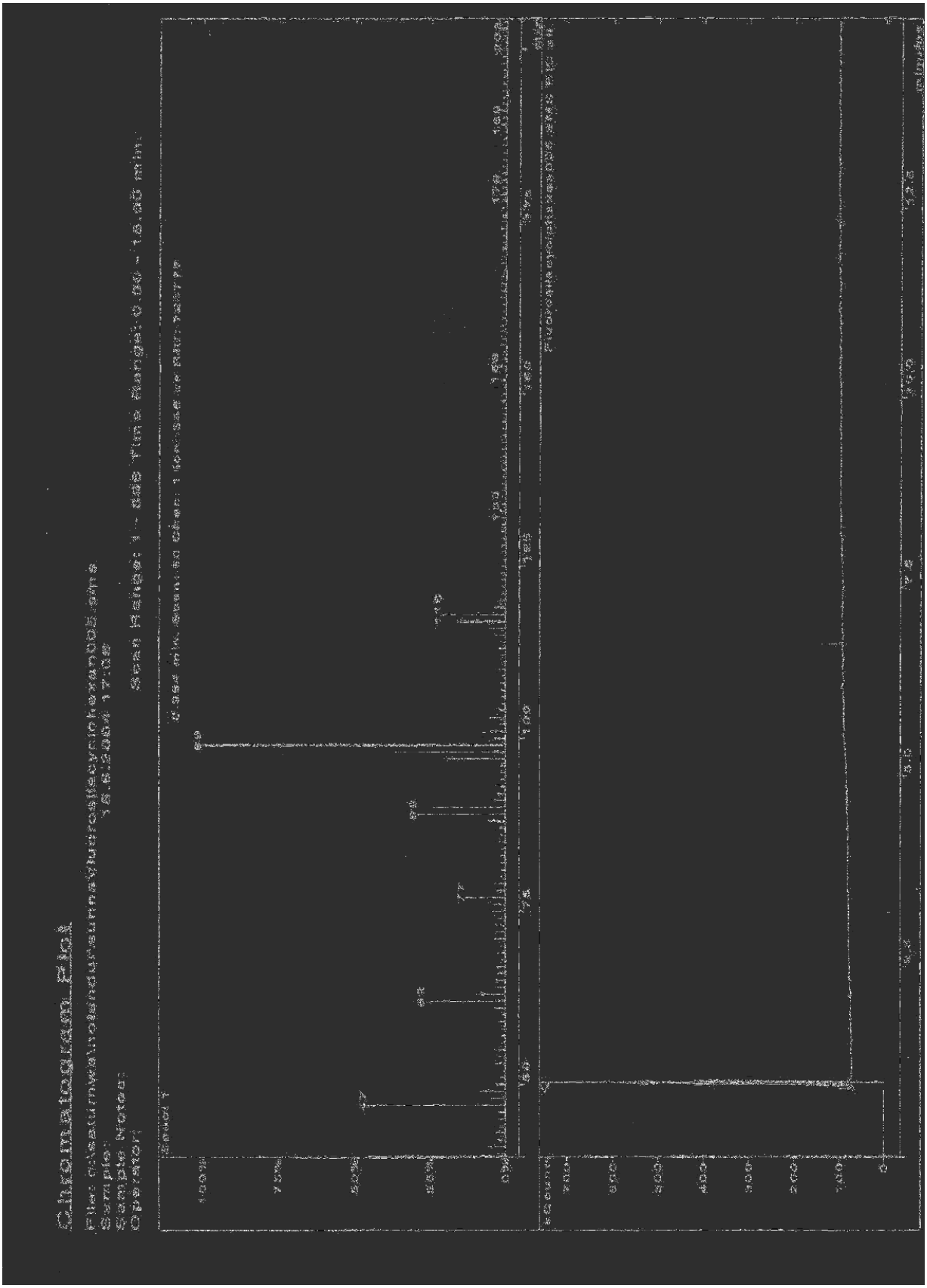

Appendix F: ^{1}H NMR spectrum of 13

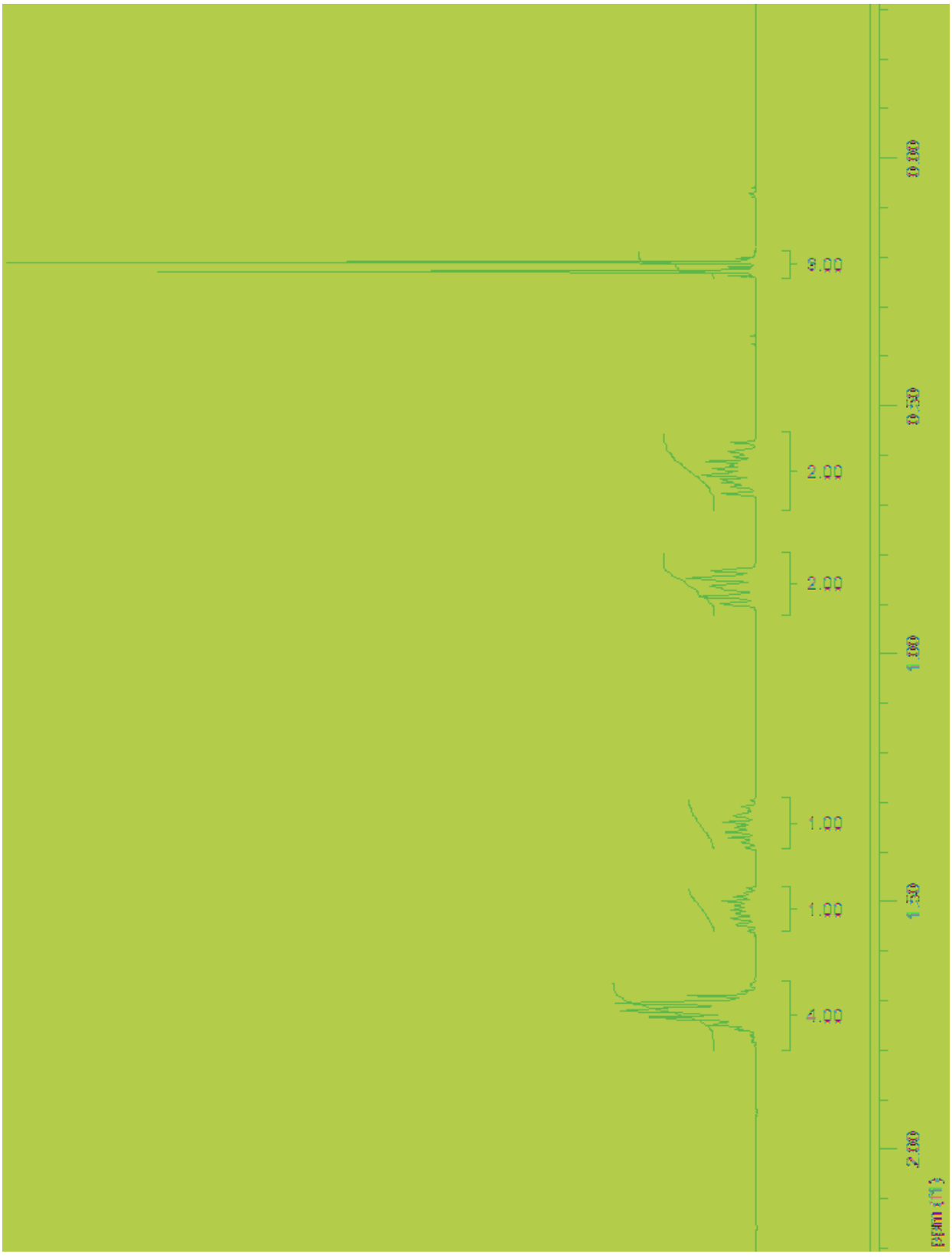

Appendix G: ^{13}C NMR spectrum of 13

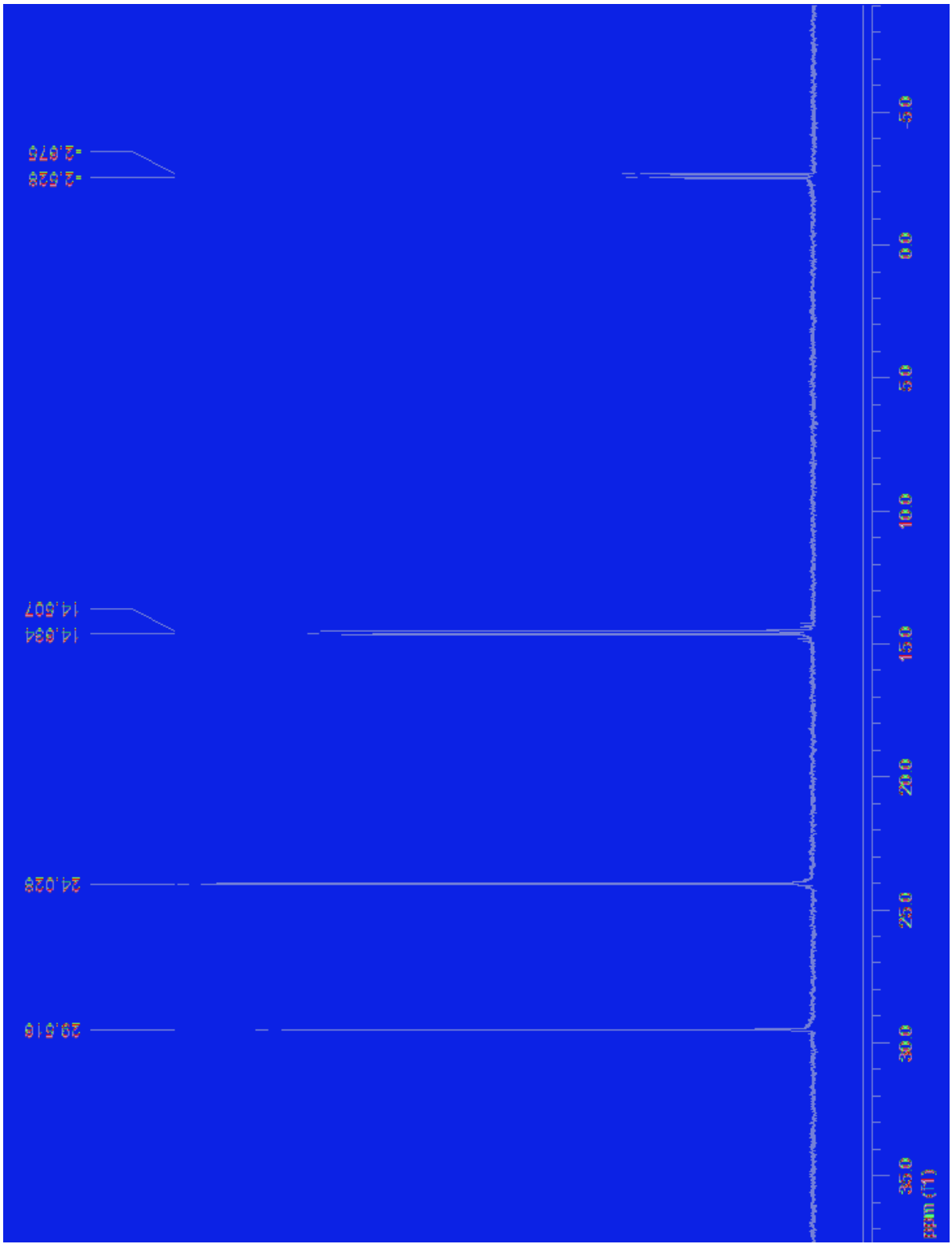

Appendix H: ^{29}Si NMR spectrum of 13

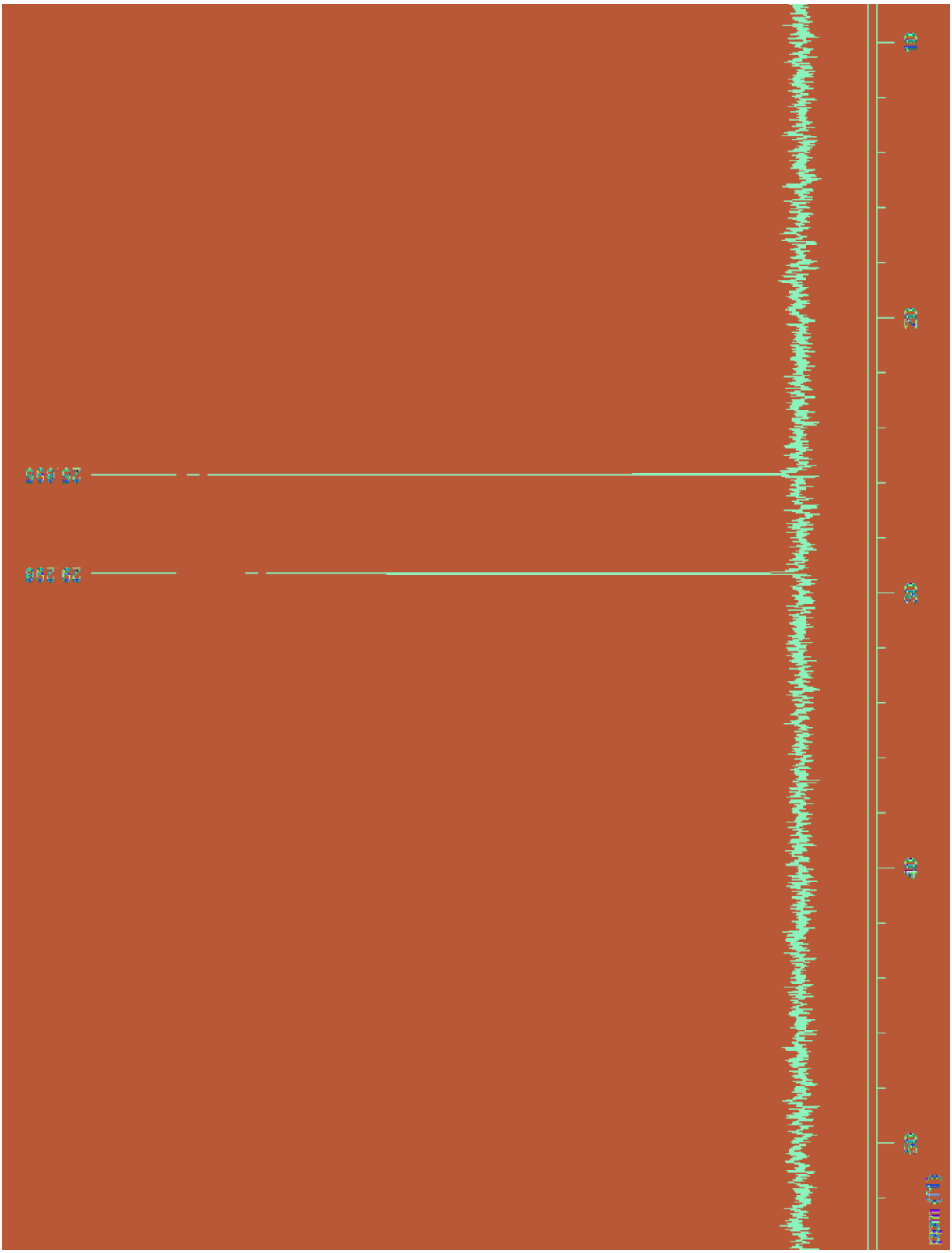

Appendix I: ^{19}F NMR spectrum of 13

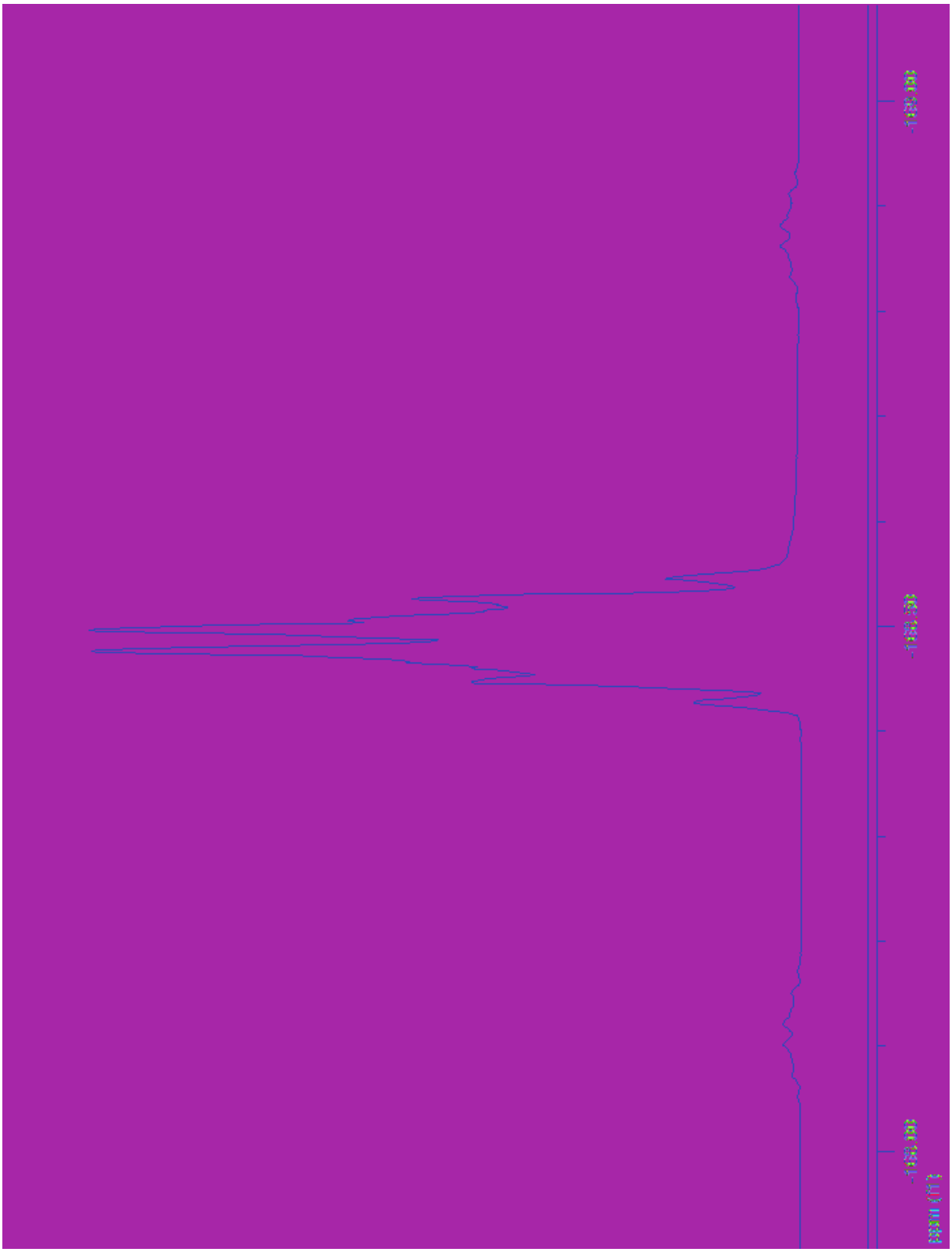

Appendix J: MS spectrum of 13

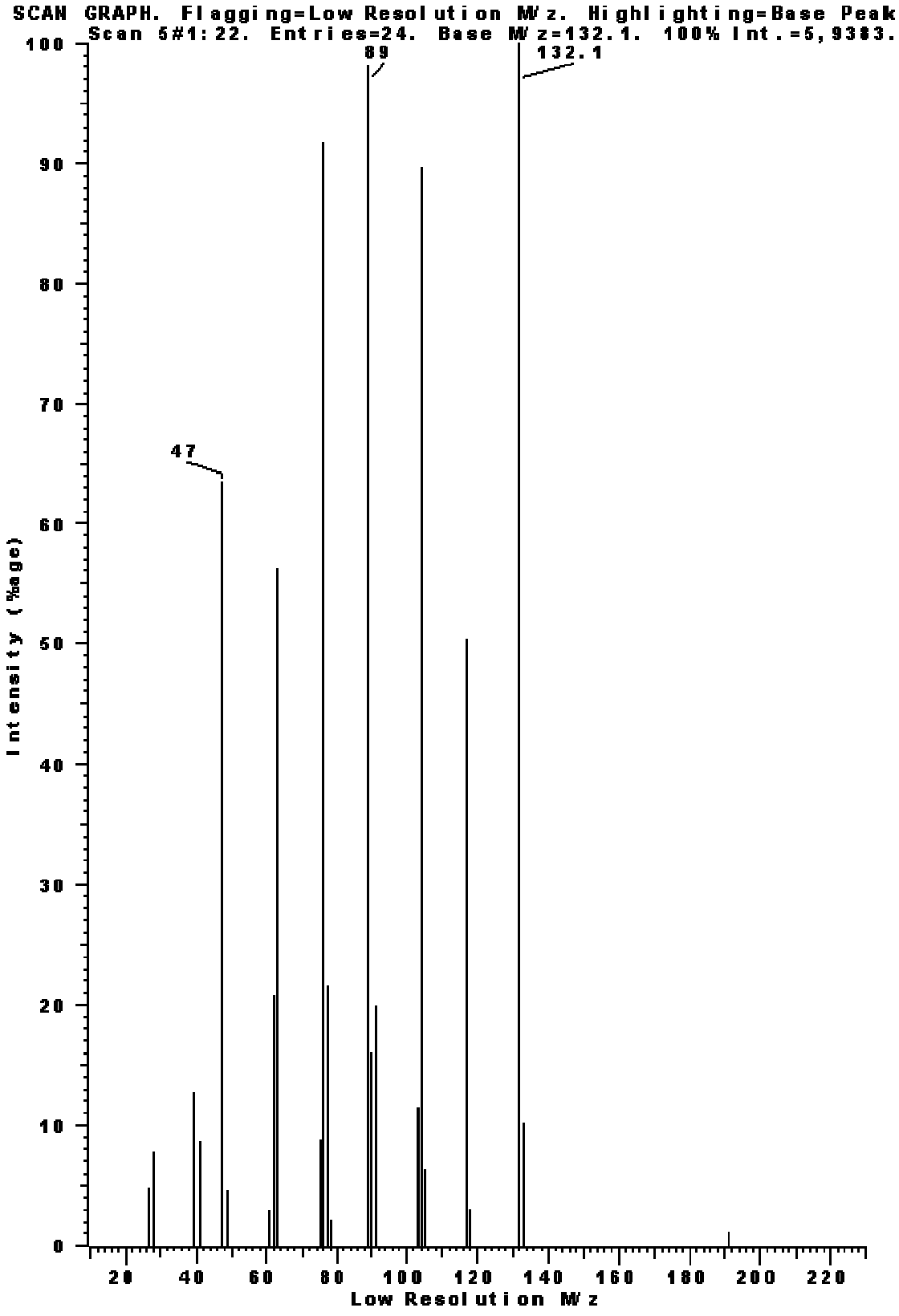

Appendix K: ^{1}H NMR spectrum of 17

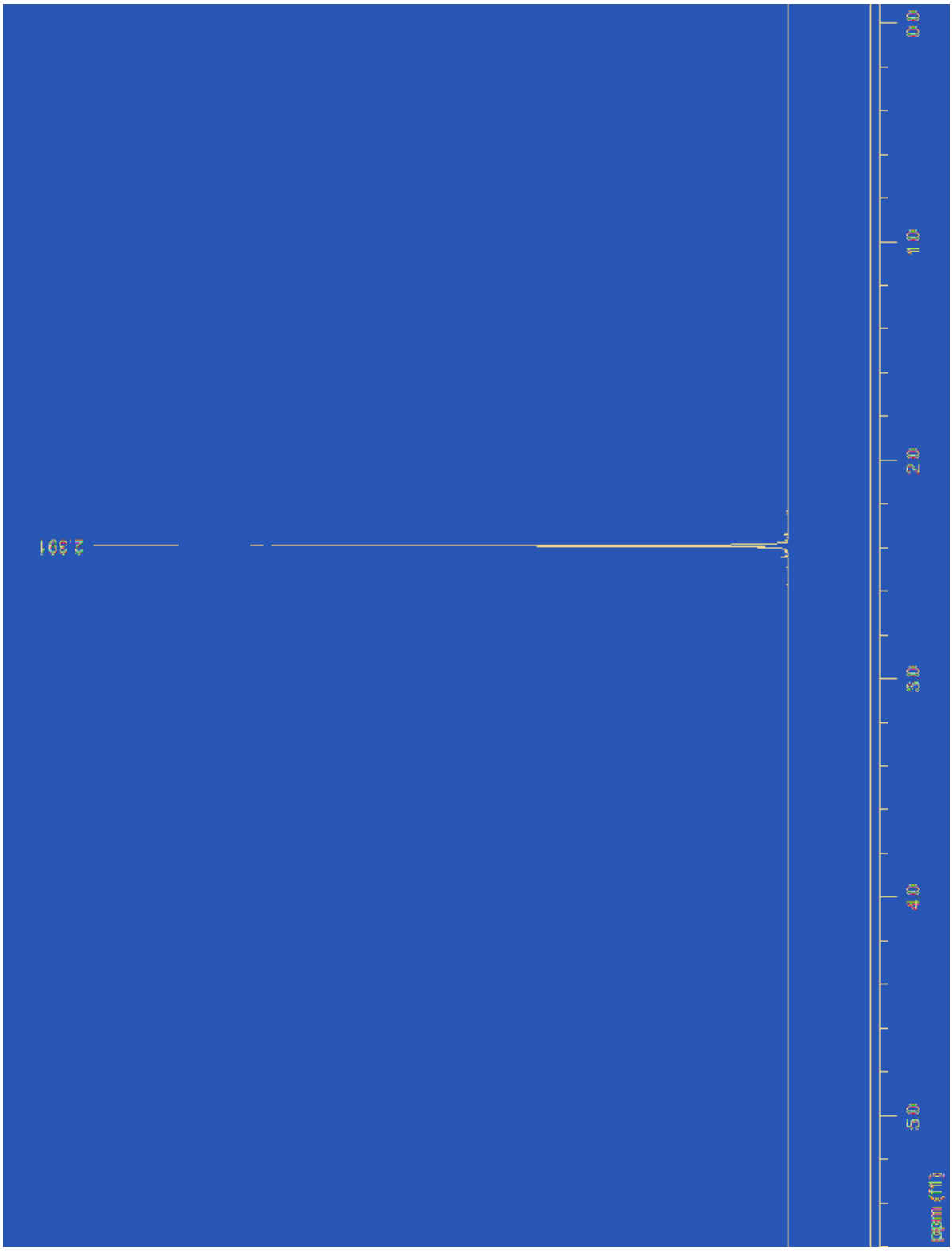

Appendix L: ^{13}C NMR spectrum of 17

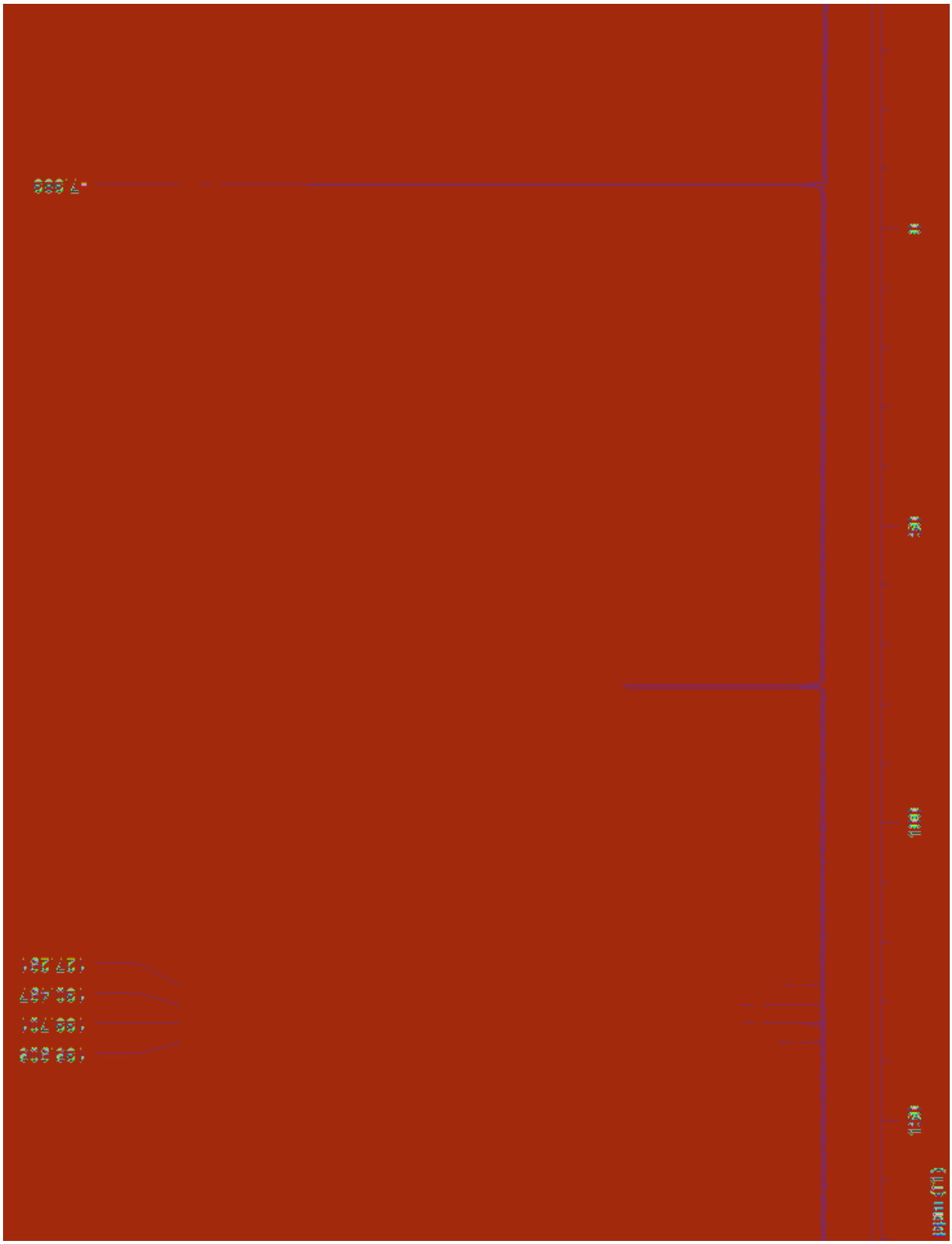

Appendix M: ^{29}Si NMR spectrum of 17

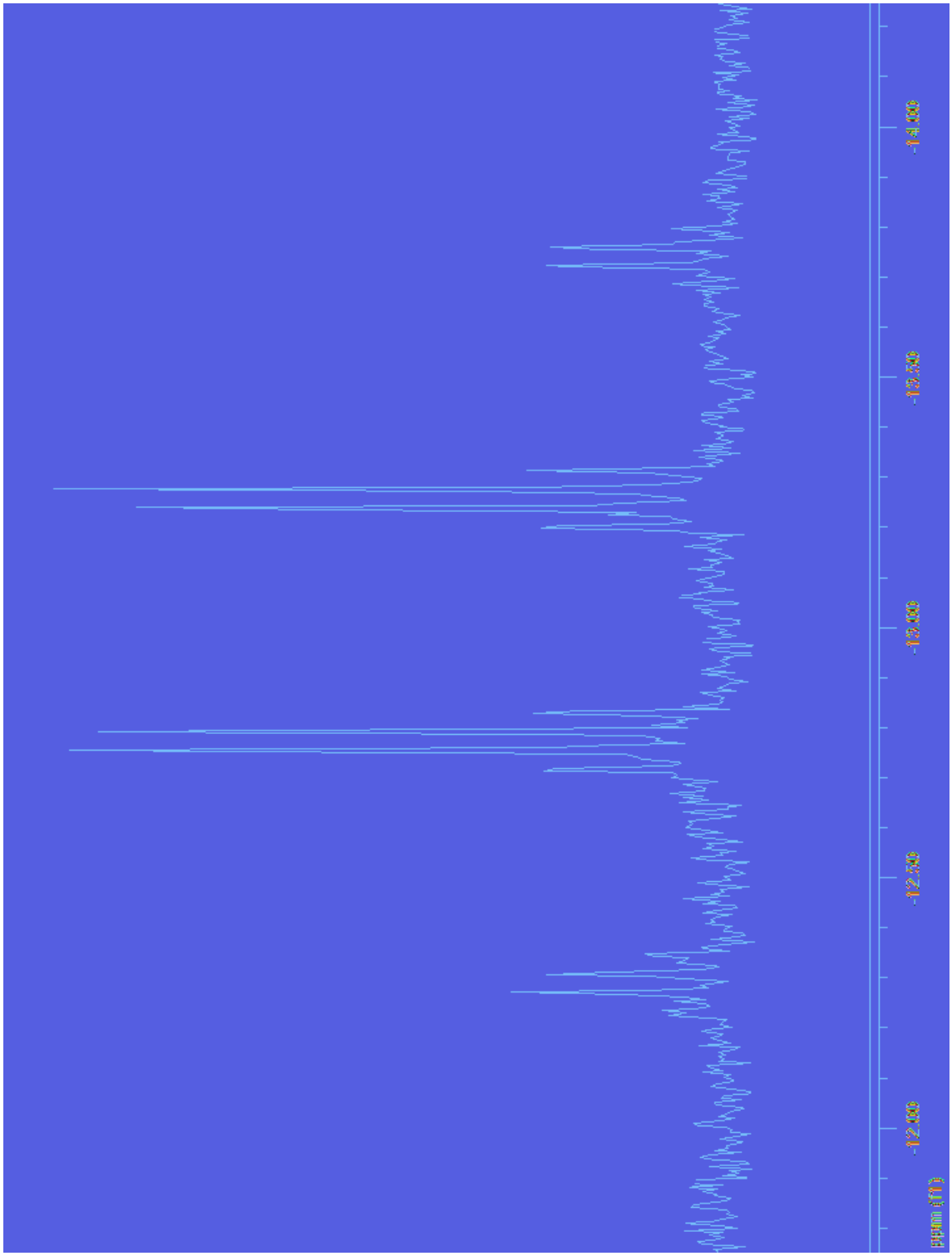

Appendix N: ^{19}F NMR spectrum of 17

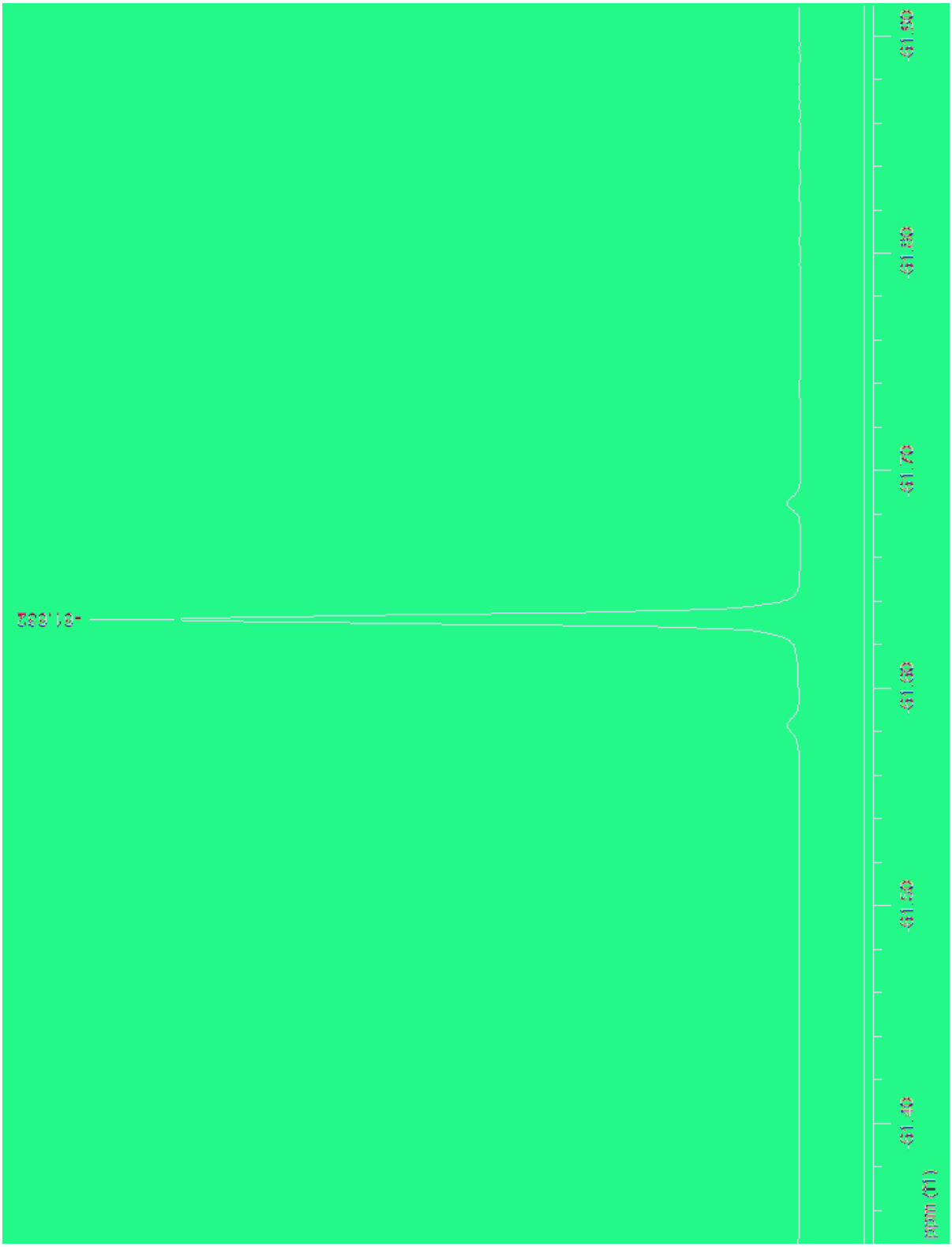

Appendix O: ^{1}H NMR spectrum of 19

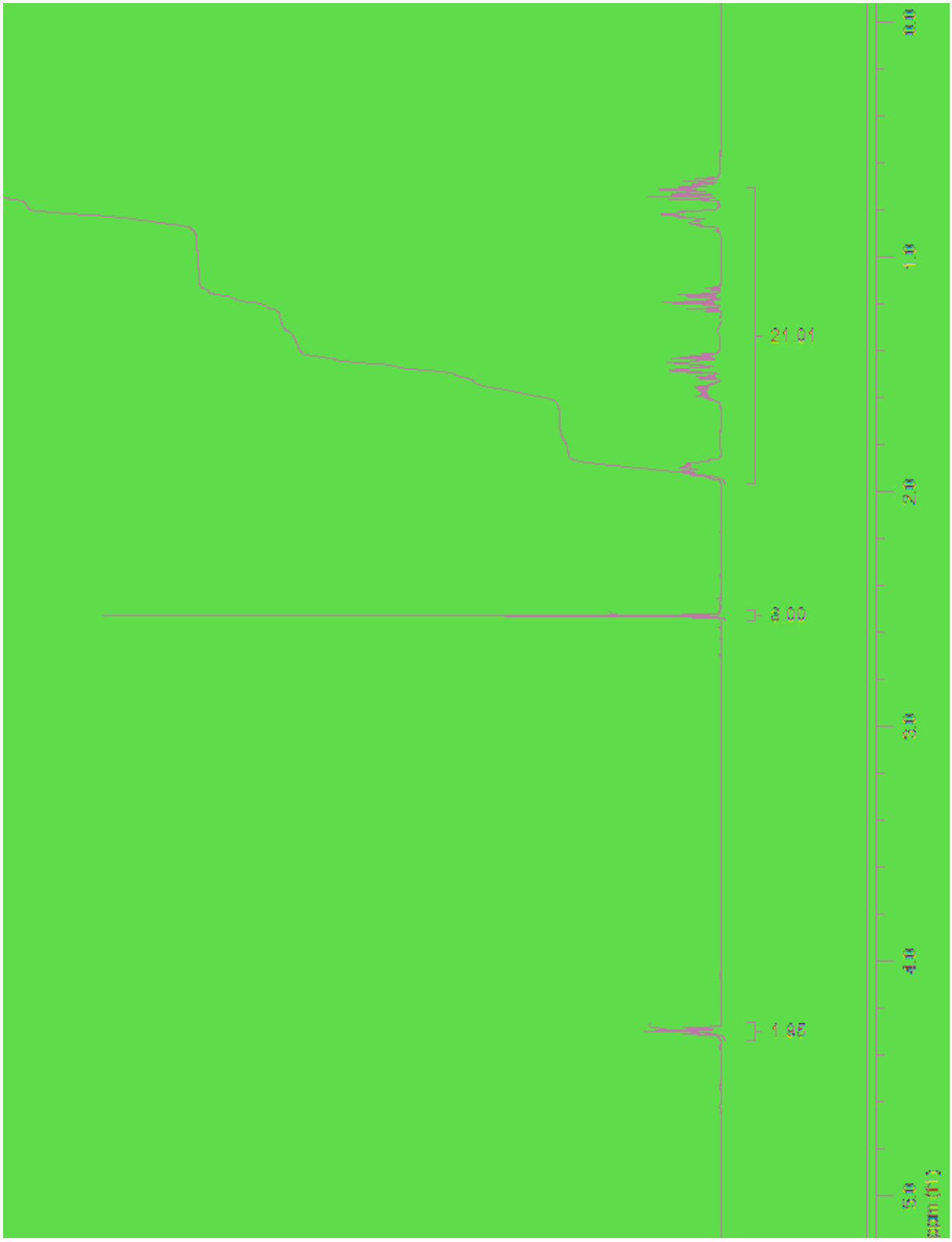

Appendix P: ^{13}C NMR spectrum of 19

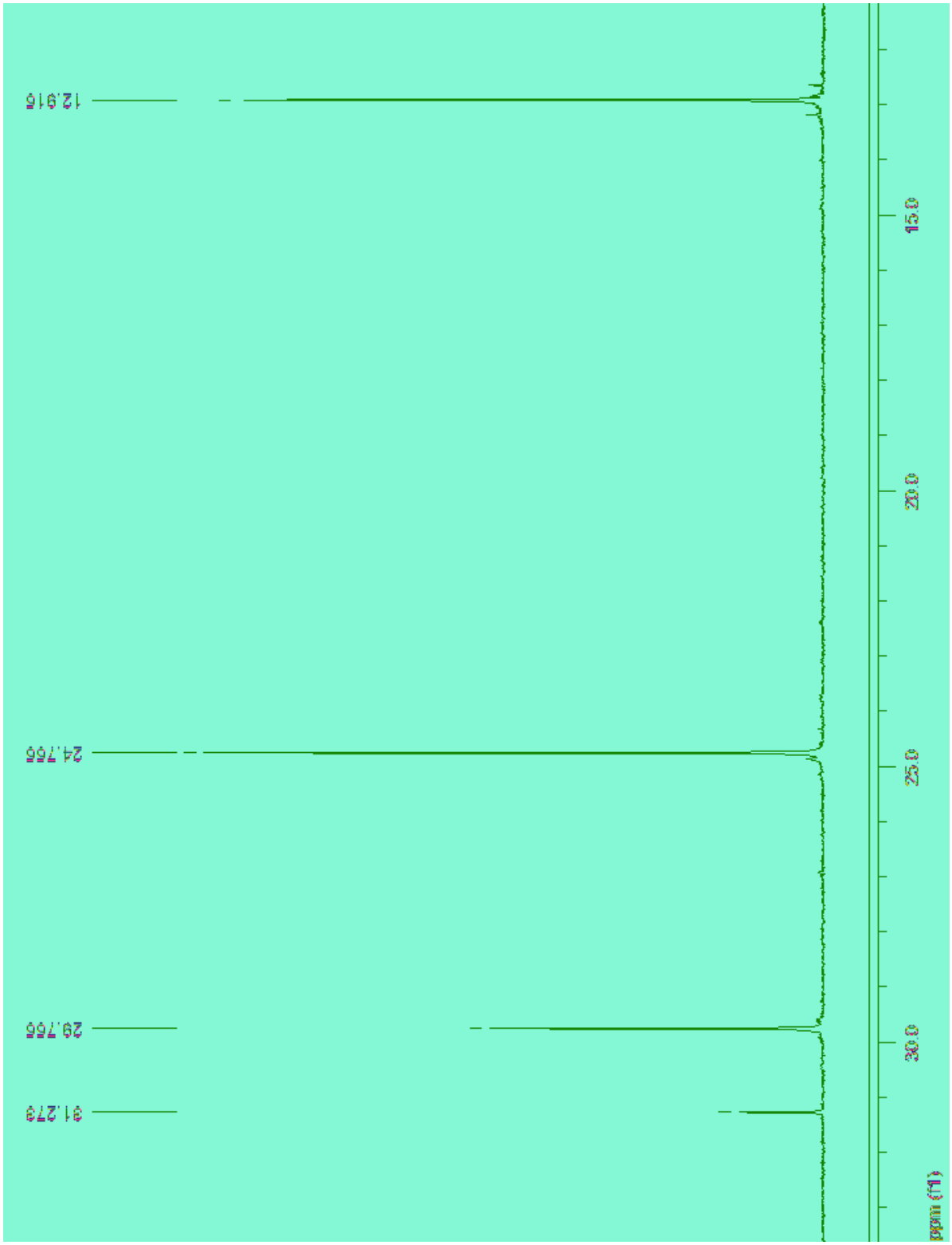

Appendix Q: ^{29}Si NMR spectrum of 19

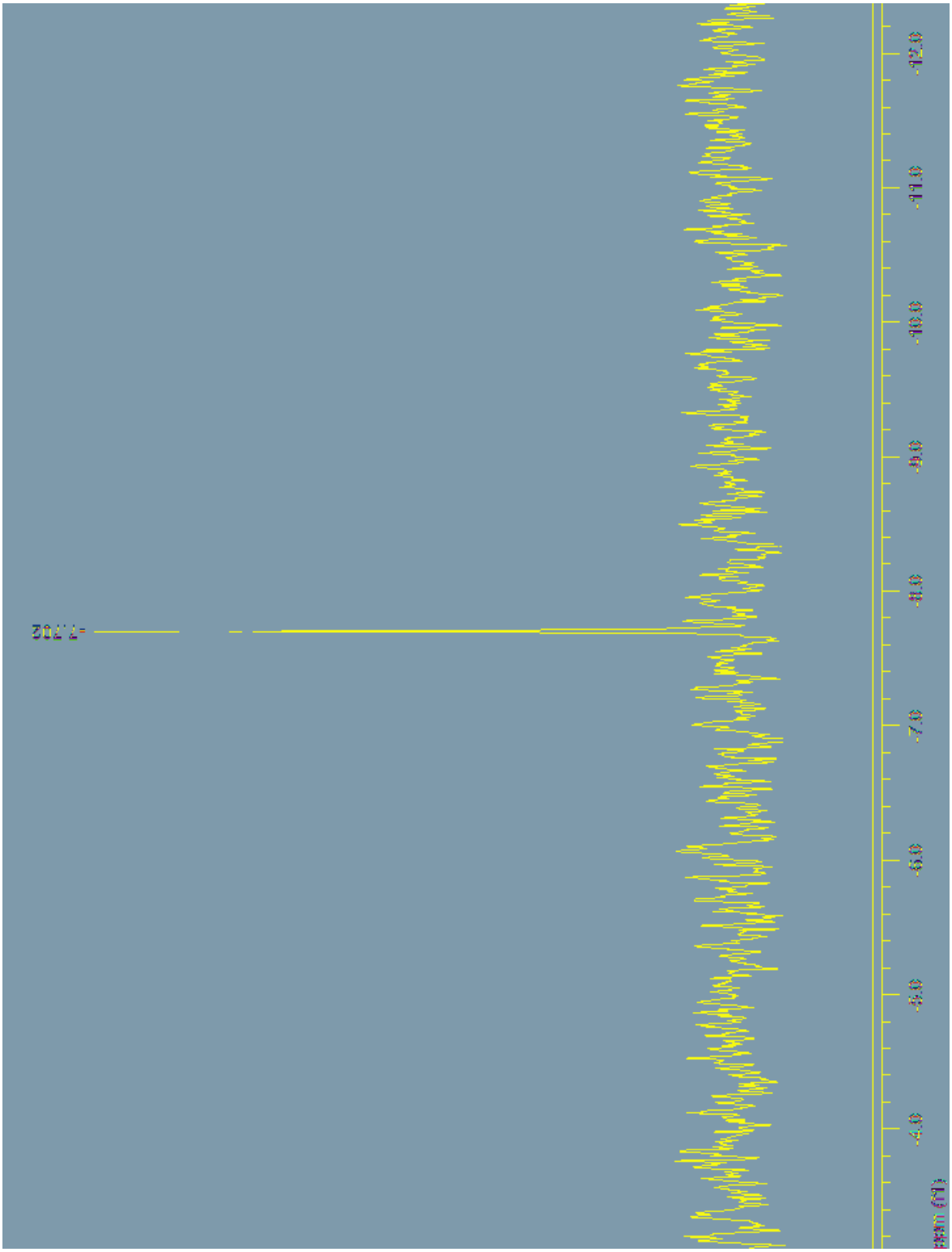

Appendix R: MS spectrum of 19

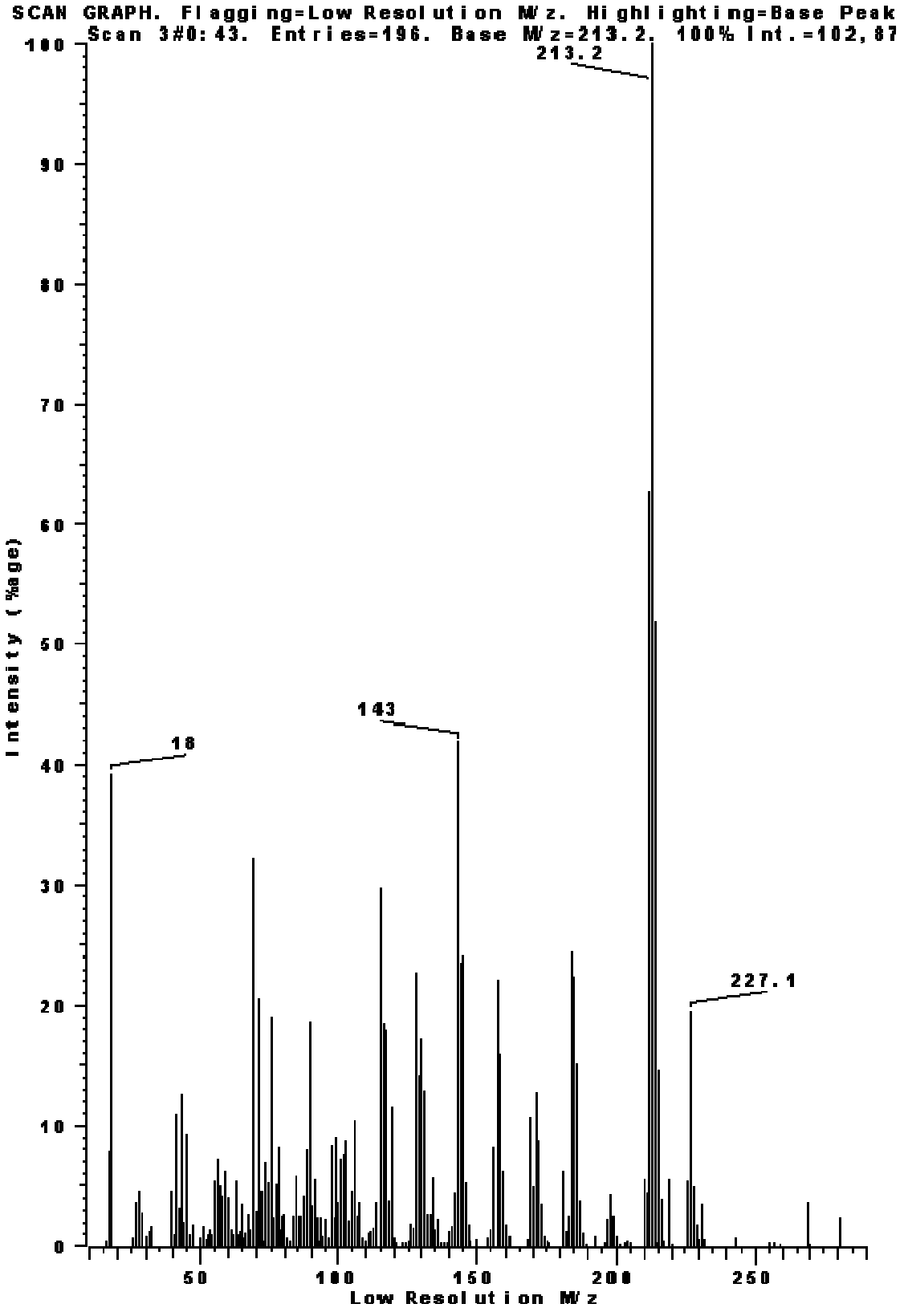

Appendix S: High Resolution MS spectrum of 19

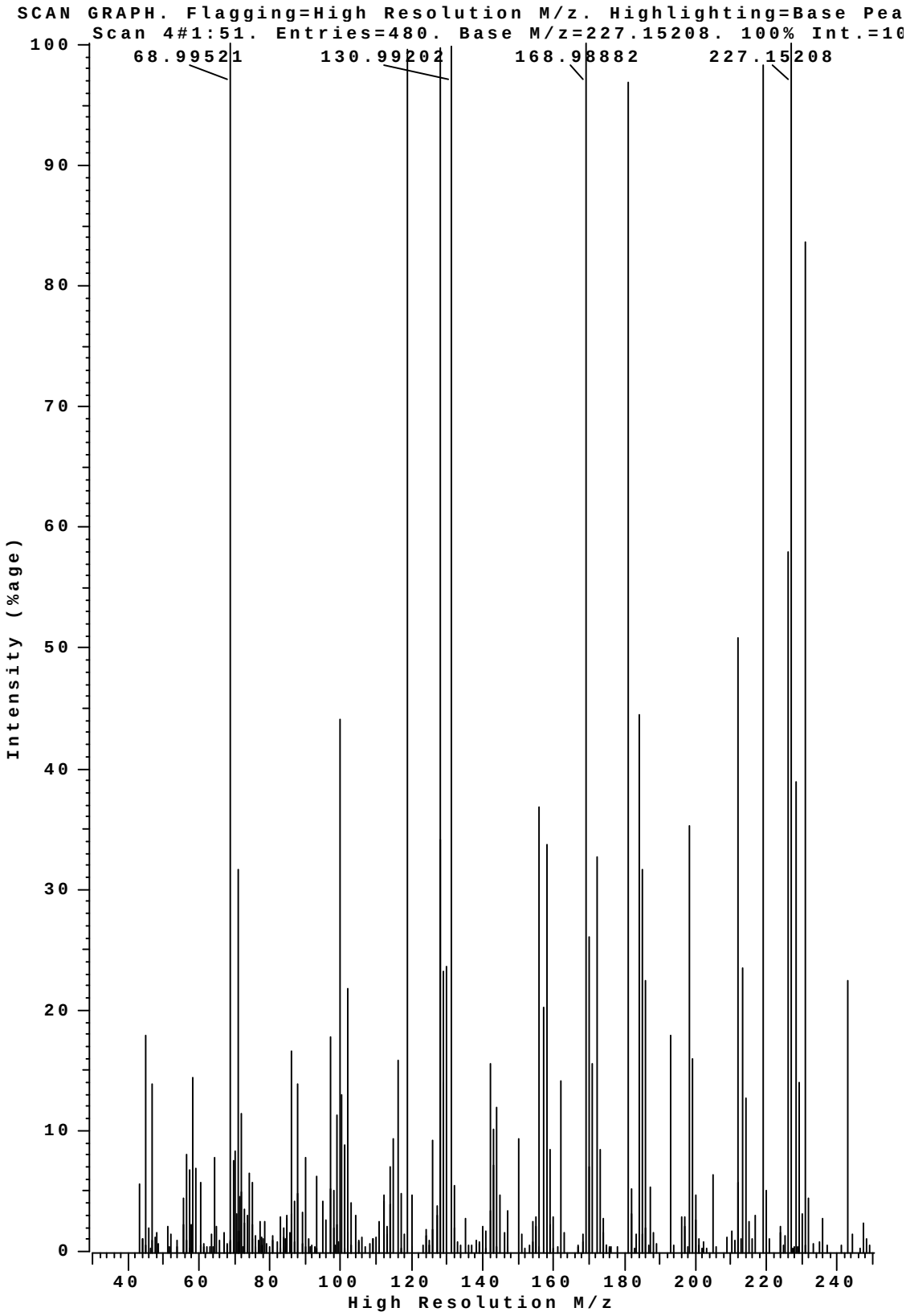

Appendix T: ^{1}H NMR spectrum of 24

Appendix U: ^{13}C NMR spectrum of 24

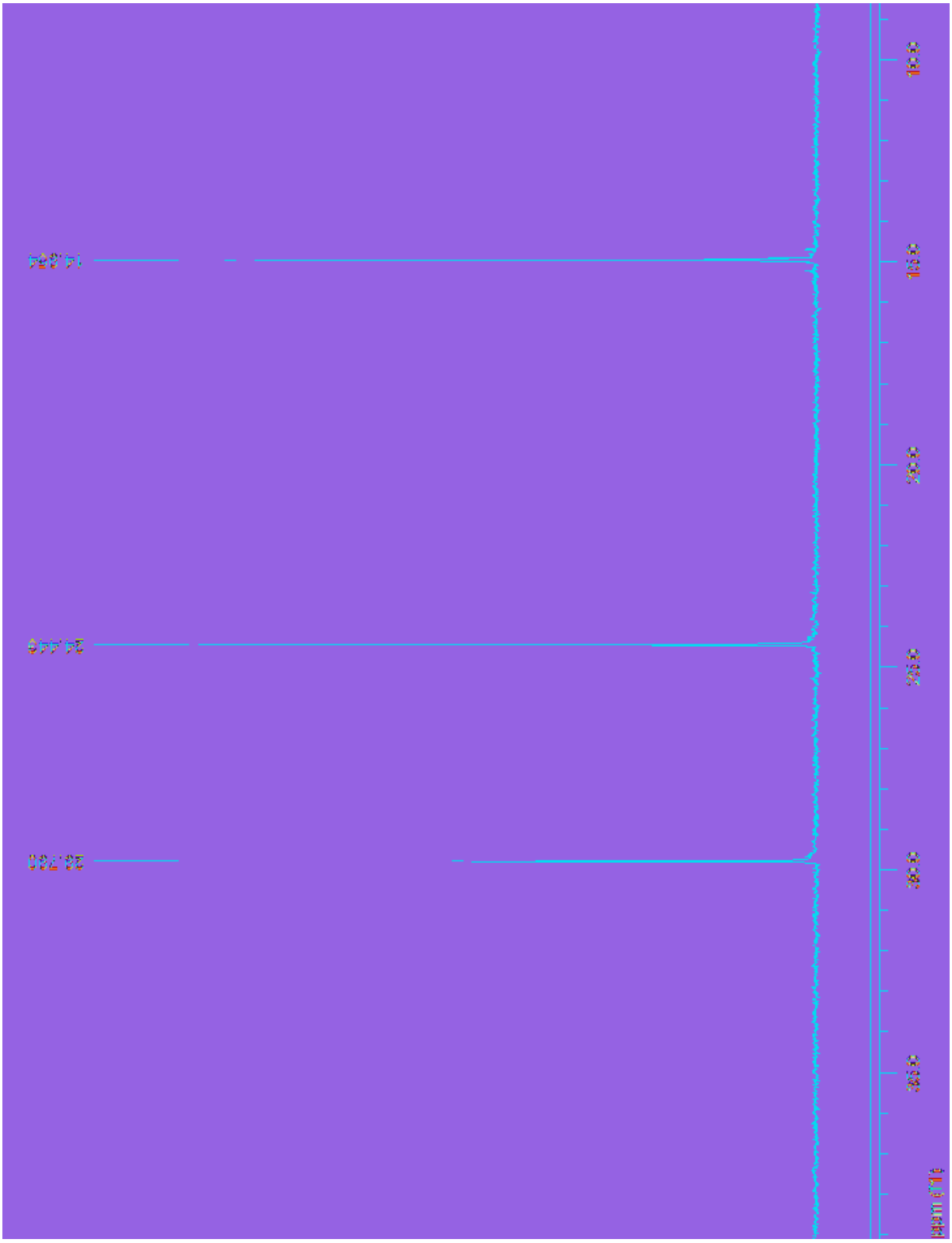

Appendix V: ^{29}Si NMR spectrum of 24

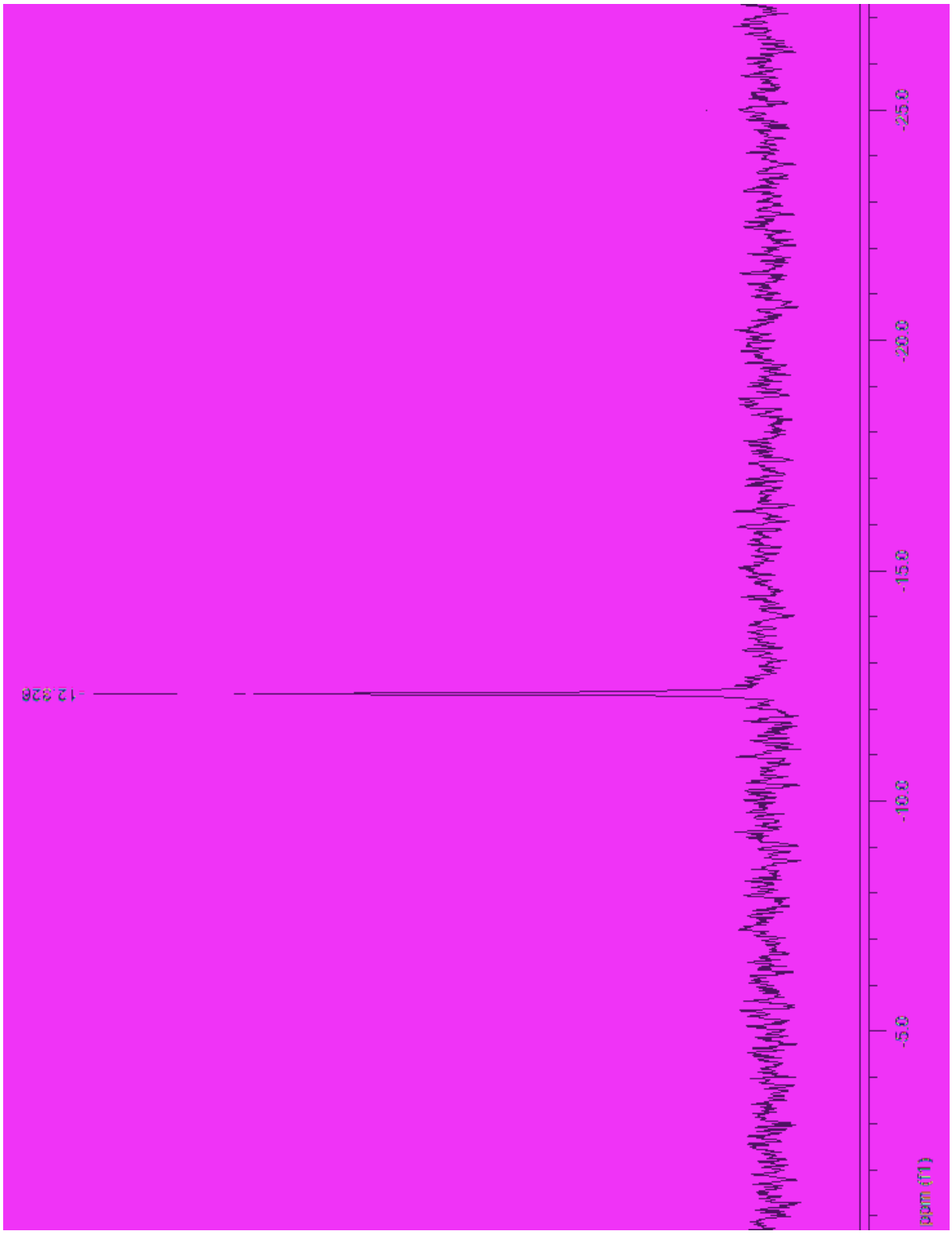

Display Report

Analysis Info

Analysis Name	SOW002.d	Acquisition Date	2/19/2008 5:03:16 PM
Method	tune_low.m	Operator	a
Sample Name	Blank	Instrument	micrOTOF-Q 67
Comment	1:30 ESI		

Acquisition Parameter

Source Type	ESI	Ion Polarity	Positive	Set Nebulizer	0.4 Bar
Focus	Active	Set Capillary	4500 V	Set Dry Heater	190 °C
Scan Begin	50 m/z	Set End Plate Offset	-500 V	Set Dry Gas	4.0 l/min
Scan End	3000 m/z	Set Collision Cell RF	150.0 Vpp	Set Divert Valve	Waste